DURBAN UNIVERSITY of TECHNOLOGY

DESIGN AND OPERATION OF A LABORATORY SCALE PHOTOBIOREACTOR FOR THE CULTIVATION OF MICROALGAE

Submitted in fulfilment of the requirements of the degree of Master of Technology: Biotechnology in the Faculty of Applied Sciences at the Durban University of Technology

Virthie Bhola

(BSc Hons: Microbiology)

June 2011

Supervisor: Prof F. Bux

DECLARATION

DESIGN AND OPERATION OF A LABORATORY SCALE PHOTOBIOREACTOR FOR THE CULTIVATION OF MICROALGAE

VIRTHIE BHOLA

I hereby declare that the dissertation represents my own work. It has not been submitted before for any diploma/degree or examination at any other Technikon/University.

Virthie Bhola	**Date**

2011

Reference Declaration in Respect of a Master's Dissertation

I, _____ (full name of student) and, _____ (full name of supervisor) do hereby declare that in respect of the following dissertation:

_____
_____

1. as far as we know and can ascertain:
   (a) no other similar dissertation exists;
   (b) the only similar dissertation(s) that exist(s) is/are referenced in my dissertation as follows:

   _____
   _____

2. all references as detailed in the dissertation are complete in terms of all personal communications engaged in and published works consulted.

_____ _____

Signature of Student **Date**

_____ _____

Signature of Supervisor **Date**

APPROVAL

I hereby approve the final submission of the following dissertation.

_____

Prof. F. Bux
Supervisor
Doctoral Degree in Technology: Biotechnology
Durban University of Technology (DUT)

This _____ day of _____, 2011, at the Durban University of Technology.

*** SUBMISSION APPROVED FOR EXAMINATION**

SUPERVISOR	**DATE**

Prof. F. Bux
Doctoral Degree in Technology: Biotechnology
Durban University of Technology

* Only when your supervisor agrees that the dissertation is ready for examining will he/she then sign the above endorsement.

* Please ensure that your supervisor's abbreviated academic qualifications are inserted after his/her name.

DEDICATION

This dissertation is dedicated to:

My father, **Mr K. Bhola**, for his endless love, support and encouragement. All of my achievements I owe to your unwavering devotion.

and

In loving memory of my mother, the late **Mrs S. Bhola**, who will live on forever in my heart. You are and always will be my eternal source of inspiration.

ABSTRACT

Due to greenhouse gas emissions from fossil fuel usage, the impending threat of global climate change has increased. The need for an alternative energy feedstock that is not in direct competition to food production has drawn the focus to microalgae. Research suggests that future advances in microalgal mass culture will require closed systems as most microalgal species of interest thrive in highly selective environments. A high lipid producing microalga, identified as *Chlorella vulgaris* was isolated from a freshwater pond. To appraise the biofuel potential of the isolated strain, the growth kinetics, pyroletic characteristics and photosynthetic efficiency of the *Chlorella* sp was evaluated *in vitro.* The optimised preliminary conditions for higher biomass yield of the selected strain were at 4% CO_2, 0.5 g l^{-1} $NaNO_3$ and 0.04 g l^{-1} PO_4, respectively. Pulse amplitude modulation results indicated that *C. vulgaris* could withstand a light intensity ranging from 150-350 µmol photons $m^{-2}s^{-1}$. The pyrolitic studies under inert atmosphere at different heating rates of 15, 30, 40 and 50 ºC min^{-1} from ambient temperature to 800 ^oC showed that the overall final weight loss recorded for the four different heating rates was in the range of 78.9 to 81%. A tubular photobioreactor was then designed and utilised for biomass and lipid optimisation. The suspension of microalgae was circulated by a pump and propelled to give a sufficiently turbulent flow periodically through the illuminated part and the dark part of the photobioreactor. Microalgal density was determined daily using a Spectrophotometer. Spectrophotometric determinations of biomass were periodically verified by dry cell weight measurements. Results suggest that the optimal $NaNO_3$ concentration for cell growth in the reactor was around 7.5 g l^{-1}, yielding maximum biomass of 2.09 g l^{-1} on day 16. This was a significant 2.2 fold increase in biomass ($p < 0.005$) when compared to results achieved at the lowest $NaNO_3$ cycle (of 3.8 g l^{-1}), which yielded a biomass value of 0.95 g l^{-1} at an OD of 1.178. Lipid accumulation experiments revealed that the microalga did not accumulate significant amounts of lipids when $NaNO_3$ concentrations in the reactor were beyond 1.5 g l^{-1} ($p > 0.005$). The largest lipid fraction occurred when the $NaNO_3$ concentration in the medium was 0.5 g l^{-1}. Results suggest that the optimal trade-off between maximising biomass and lipid content occurs at 0.9 g l^{-1} $NaNO_3$ among the tested conditions within the photobioreactor. Gas chromatograms showed that even though a greater number of known lipids were produced in Run 8, the total lipid percentage was much lower when compared to Runs 9-13. For maximal biomass and lipid from *C. vulgaris*, it is therefore crucial to optimise nutritional parameters such as $NaNO_3$.

However, suitable growth conditions for *C. vulgaris* in a tubular photobioreactor calls for innovative technological breakthroughs and therefore work is ongoing globally to address this.

PREFACE

Aspects of the work covered in the following dissertation can be found in the following accepted publication:

Bhola V., Desikan R..,Santosh S. K., Subburamu K., Sanniyasi E., Bux F. Effects of Parameters Affecting Biomass Yield and Thermal Behaviour of *Chlorella vulgaris*. Journal of Bioscience and Bioengineering. (2010). doi: 10.1016/j.jbiosc.2010.11.006.

ACKNOWLEDGMENTS

I would like to acknowledge the following people:

- God Almighty without whom none of this would have been possible. I offer my respectful obeisance's unto his lotus feet.

- My father, Mr K. Bhola, for his unwavering faith, support and love that helped make all my dreams a reality.

- My brother, Kamith, for been my constant pillar of strength.

- Prof F. Bux, for his advice, assistance and encouragement during the course of this project. His commitment to research excellence ensured that my project conformed to the highest standards.

- Dr D. Ramesh, for his devoted efforts in assisting me throughout my research and guidance in overcoming the various obstacles encountered during my study.

- Dr S. Kumari, for her valuable contribution towards the successful submission of my research article as well as supervision with molecular aspects of my study.

- Dr S. Karthy, for his insightful knowledge and experience.

- Dr R. Kumar for his constant advice, assistance and encouragement.

- Mr S Ramluckan, for assistance with Gas Chromatography studies and always going the extra mile to ensure that all my academic endeavours were successful.

- Dr A. Anandraj, for guidance with Pulse Amplitude Modulation studies.

- Mr R Bhana, for always believing in me.

- Mr I. Rawat, for his invaluable efforts and aid throughout my research project

- Mrs N. Ramdhani, for her dependable friendship and ever obliging advice and assistance with molecular work.

- Miss T. Govender, a friend I could always rely on for her patience, support and understanding.

- Staff and students at the Institute for Water and Wastewater Technology, Durban University of Technology for their analytical support and guidance.

- The National Research Foundation and Durban University of Technology for funding.

Contents

List of Figures

List of Tables

Chapter One: Introduction

1.1 Introduction

Due to diminishing crude oil reserves as well as the deleterious environmental consequences of exhaust gases from petroleum diesel, biodiesel has attracted much attention during the past few years as a renewable and environmentally friendly fuel. Since biodiesel is usually made entirely from vegetable oil or animal fats, it is renewable and biodegradable (Vasudevan and Briggs, 2008). Its chemical structure is that of fatty acid (FA) alkyl esters. This biofuel is produced by transesterification of oils with short-chain alcohols or by the esterification of FAs. The transesterification reaction consists of transforming triglycerides into FA alkyl ester, in the presence of an alcohol, such as methanol or ethanol, and a catalyst, such as an alkali or acid, with glycerol as a byproduct (Vasudevan and Briggs, 2008).

Recent studies propose that microalgae appear to be the only source of biodiesel that has the potential to completely displace fossil diesel (Borowitzka, 1997; Chisti, 2007; Chisti, 2008; Ugwu *et al*., 2008). Microalgae are of particular interest because of their rapid growth rates, tolerance to varying environmental conditions and can also fix greater amounts of CO_2 per land area than higher plants. Unlike oil crops, these organisms grow extremely rapidly and many are rich in oil. Microalgae commonly double their biomass within 24 hours, and oil content in certain strains can exceed 80% by weight of dry biomass (Chisti, 2007; 2008). The energy rich biomass is widely used as a source of fuel (liquid and gaseous), health foods, animal feed and also in producing vitamins and pigments. Processes in conversion of microalgal biomass to such useful products would indirectly decrease dependence on fossil fuels (Chisti, 2007; 2008).

Microalgae can be grown either in open culture systems (raceway ponds) or closed systems (photobioreactors). However only a few can be maintained in traditional open systems, in which contamination is controlled by using highly alkaline or saline selective environments

(Molina *et al*., 2001). The low productivity and photosynthetic efficiency of open ponds or outdoor reactors due to the long light path, and other environmental factors such as temperature and microbial contaminants has led to the design and development of enclosed indoor photobioreactors (PBRs). Photobioreactors have attracted much interest as they allow a better control of the cultivation conditions than open systems. With closed systems, higher biomass productivities may be obtained and contamination can be easily prevented (Borowitzka, 1997; Chisti, 2007; Ugwu *et al*., 2008). Future advances in microalgal mass culture will therefore, require closed systems as most microalgal species of interest thrive in highly selective environments.

In recent years there have been several major advances in the design and operation of closed photobioreactors for microalgal culture, yet only a few of them can effectively utilise solar energy for mass production of microalgae (Borowitzka, 1997; Ugwu *et al*., 2008). The critical design requirement in a photobioreactor design is the illumination surface area per unit volume (S/V ratio). An efficient photobioreactor has a high S/V ratio. A major drawback in mass production of microalgae is the lack of efficient photobioreactors. To improve microalgal productivity, a thorough understanding on photobioreactors is essential.

Each type of photobioreactor has its own distinct advantages and disadvantages in terms of potential efficiency of light utilisation, effective mass transfer of oxygen (O_2) and carbon dioxide (CO_2), ease of cleaning, as well as scalability (Molina *et al*., 2001). Of the many closed systems employed, devices with tubular solar collectors are the most promising since they are easy to use and have a high S/V ratio. It can therefore be hypothesised that the manipulation of conditions within a Tubular Photobioreactor (TPBR) could increase biomass and lipid concentrations and hence be used as a technology for biodiesel production.

This research project was divided into three stages. During the first stage the biofuel potential of an isolated *C. vulgaris* strain was appraised by establishing the growth kinetics, pyrolytic characteristics and photosynthetic efficiency of the selected strain *in vitro*. The second stage entailed designing and operating a closed reactor for cultivation of the chosen microalgal

strain. Whereas, the third and final stage incorporated a series of batch cultivations within the photobioreactor in order to optimise biomass and lipid yields of the selected strain.

1.2 Aims and Objectives

Aim:

Design and operation of a photobioreactor for the cultivation of microalgae.

Objectives:

-To select a superior lipid producing microalgal strain,

-To evaluate the biofuel potential of the selected strain,

-To design and operate a laboratory scale photobioreactor to grow microalgae,

-To optimise abiotic conditions for maximum biomass yields,

-To optimise abiotic conditions for maximum lipid yields.

Chapter Two: Literature Review

2.1 Global warming and the world energy crisis

Energy plays a significant role in the development process, not only as a domestic requirement but also as an aspect of production whose cost directly affects price of other goods and services (Amigun *et al*., 2006). In recent years, the world has been dealt with an energy crisis due to depletion of limited reserves of fossil fuels (Khan *et al*., 2009). According to British Petroleum's (BP's) annual Statistical Review of World Energy in 2008 (Anonymous, 2009), the world proven oil reserves were estimated at 1.7×10^{11} tons with a reserve-to-production ratio of 42 years. Also, the potential threat of global climate change has amplified. This has been mainly attributed to greenhouse gas (GHG) emissions from fossil fuel usage (Brennan and Owende, 2010). Conventional fossil fuels are the largest contributor of GHGs to the atmosphere (Brennan and Owende, 2010). The associated climatic change projections could have disastrous implications on nature as well as mankind. This creates insecurity regarding the sustainability of current fossil fuel use, not only in relation to the availability of the resource, but also based on the negative effects of CO_2 emissions (Brennan and Owende, 2010). Petroleum-based products are one of the leading causes of anthropogenic (CO_2) emissions to the biosphere (Vasudevan and Briggs, 2008). The transportation sector worldwide is almost totally dependent on petroleum-derived fuels. One-fifth of global CO_2 emissions are created by the transport sector which accounts for about 60% of global oil consumption (Balat and Balat, 2010).

South Africa by far is one of the largest emitters of greenhouse gases (GHGs) and amongst the top 20 most carbon intensive countries in the world. This is partly due to the high-energy usage and the dependence on coal for electricity generation. The transport sector accounts for approximately 24% of South Africa's total CO_2 emissions (Murugesan *et al.,* 2008).

Active research programs are underway worldwide to reduce the reliance on fossil fuels by the use of cleaner and sustainable alternative fuel sources, and as a result to also increase the time over which fossil fuels will still be available (Balat and Balat, 2010; Namasivayam *et*

al., 2010). Biofuels can be considered as a substitute to petroleum-based transportation fuels by reinforcing energy security and reducing the emissions of both GHGs and urban air pollutants (Balat and Balat, 2010).

Biofuels can be defined as liquid or gaseous fuels utilised by the transport sector that are predominantly produced from biomass (Balat and Balat, 2010). Biomass resources could be exploited to produce a wide variety of fuels including liquid fuels, such as bioethanol, methanol, and biodiesel as well as gaseous fuels, such as hydrogen and methane (Demirbas, 2008; Balat and Balat, 2010).

Globally Southern Africa has been recognised as an area with far-reaching biofuel potential (Smeets *et al*., 2007). Besides Southern Africa having vast amount of land that could be utilised for biofuel production, the climate in certain areas are also suited to high levels of biomass production. In contrast to fossil fuel, biofuels also create a large number of job opportunities. As a result the biofuel industry sees huge potential for biofuel production in Southern Africa, and a number of companies have, or are investigating and investing in the region (Batidzirai *et al*., 2006).

Biofuels can be defined as liquid or gaseous fuels utilised by the transport sector that are predominantly produced from biomass (Balat and Balat, 2010). Biomass resources could be exploited to produce a wide variety of fuels including liquid fuels, such as bioethanol, methanol, and biodiesel as well as gaseous fuels, such as hydrogen and methane (Demirbas, 2008; Balat and Balat, 2010).

At present, biodiesel is produced from soybean and vegetable oils, palm oil, sunflower oil, rapeseed oil as well as restaurant waste oil (Huang *et al*., 2009). However, in recent years microalgae have gained rapid attention in an attempt to produce biodiesel. Biodiesel is an attractive energy resource for several reasons. Firstly, biodiesel is a renewable and biodegradable source of energy that could be continuously supplied. Secondly, biodiesel has

many favorable environmental characteristics resulting in no net increased release of CO_2 and very low sulfur content (Antolin *et al*., 2002; Vicente *et al*., 2004). By using biodiesel as an energy source, the gas generated during combustion could be reduced, and a decrease in carbon monoxide would be seen owing to the relatively high O_2 content present in the biofuel. Moreover, biodiesel contains no aromatic compounds and other chemical substances which could be detrimental not only to humans but to the environment as well. Recent studies suggest that the use of biodiesel could decrease 90% of air toxicity and 95% of cancers compared to the common diesel source (Huang *et al*., 2010).

2.2 Microalgae

Microalgae which are primitive, unicellular, microscopic (2–200 µm) organisms that can also be classified as thallophytes have an important ecological role (Greenwell *et al*., 2009; Khan *et al*., 2009; Brennan and Owende, 2010; Mutanda *et al*., 2010). Besides the fact that they can serve as food and feed source for people and animals as they belong at the bottom of the food chain, they are the principle producers of O_2 on earth (Khan *et al*., 2009). They can either be autotrophic or heterotrophic. Autotrophic microalgae require inorganic compounds, salts and an appropriate light source for growth, were as heterotrophic microalgae have need of an external source of organic compounds as well as nutrients which are used as an energy source (Brennan and Owende, 2010; Mutanda *et al*., 2010). Microalgae are mainly categorised based on their pigmentation, life cycle and basic cellular structure. Due to novel genetic and ultrastructural material constantly emerging, the evolutionary history and taxonomy of microalgae is complex (Brennan and Owende, 2010; Mutanda *et al*., 2010). Microalgae can be classified into two prokaryotic divisions (Cyanophyta and Prochlorophyta) and nine eukaryotic divisions (Glaucophyta, Rhodophyta, Heterokontophyta, Haptophyta, Cryptophyta, Dinophyta, Euglenophyta, Chlorarachniophyta and Chlorophyta). However, diatoms, green microalgae, blue–green microalgae and golden microalgae are the most abundant (Khan *et al*., 2009; Mutanda *et al*., 2010). These organisms show much potential for the production of value added products and biofuels, as they are rich in minerals, vitamins, oils, and polyunsaturated FAs (Spolaore *et al*., 2006; Del Campo *et al*., 2007; Khan *et al*., 2009; Mutanda *et al*., 2010). Microalgae can be used as a second generation feedstock for production of biofuels, particularly biodiesel as they have the ability to synthesize

triacylglycerides (TAGs) (Khan *et al*., 2009). Of the many oil-producing sources, microalgae are considered to be the only source of renewable biodiesel capable of meeting global demand for transport fuels (Borowitzka, 1999; Miao and Wu, 2006; Chisti, 2007; Khan *et al*., 2009). This can be attributed to their rapid growth rates (cell doubling time of 1-10 days), ability to accumulate large quantities of neutral lipids [20-50% of dry cell weight (DCW)], capacity to fix greater amounts of CO_2 per hectare than higher plants, make use of non-arable land as well as non-potable water and most significantly they can be harvested daily and their production is not seasonal (Borowitzka, 1999; Khan *et al*., 2009). Also, a major advantage is that biodiesel produced from microalgae will not compromise the production of food and other products derived from crops (Huang *et al*., 2009).

The mechanism of photosynthesis in microalgae is similar to that of higher plants however, they are generally more efficient converters of solar energy to chemical energy, owing to their simple cellular structure. As the cells grow in aqueous suspension, they have more efficient access to water, CO_2, and other nutrients. Due to these reasons, microalgae are capable of producing 30 times the amount of oil per unit area of land, compared to terrestrial oilseed crops (Khan *et al*., 2009). Microalgae are said to possess a trigger response when placed into stressful environments such as nutrient deprivation- the cells are able to change the use of carbon uptake from reproduction to energy storage in the form of oils. Once a high oil content has been obtained, the oil from the microalgae can be extracted using solvents and then turned into biodiesel through a process known as transesterfication (Vasudevan and Briggs 2008).

The thought behind using microalgae as a source of biofuel is not novel, however it is now being taken seriously owing to the continuous rise in the price of petroleum due to the worldwide energy shortage crisis and, more notably, the emerging concern about global warming that is linked to the burning of fossil fuels (Khan *et al*., 2009; Huang *et al*., 2010).

Microalgae are usually identified in laboratories by means of microscope-based techniques. For species level identification, conventional light microscopy has been extended to include phase contrast microscopy, fluorescence microscopy, scanning electron microscopy (SEM)

and transmission electron microscopy (TEM). Conventional microscopy techniques, however, could often prove misleading in precise microalgal identification as they lack morphological markers. Microalgae are also known to change cell size and shape during their life cycle (Godhe *et al*., 2001; Mutanda *et al*., 2010). A proper identification is impossible as most microalgae do not survive fixation or they shrink, lose pigmentation and flagella. Identification of microalgae from field samples using microscopy also proves time consuming and requires both experience and significant taxonomic and technical skills (Godhe *et al*., 2001). Molecular-based techniques developed in recent years have led to rapid and accurate monitoring, identification and quantification of microalgal species. Commonly analysed DNA regions for phylogenetic purposes include ribosomal RNA genes (rRNA), mitochondria genes, plastid genes (rbcL), ITS (Internal Transcribed Sequences) and microsatellite DNA sequences. Of all DNA regions, ribosomal RNA's are one of the most widely used as they are exceptionally useful for the comparative analysis of organisms (Mutanda *et al*., 2010).

2.3 Sampling and screening for hyper-lipid producing microalgal strains

For microalgal biodiesel to become viable in the near future it is imperative to search, collect and identify hyper-lipid producing strains. The success of any microalgal mass culture, particularly for products such as biodiesel, depends on the selection of fast-growing, productive strains that have been optimised for the local climatic conditions (Mutanda *et al*., 2010). Harvesting costs should also be assessed at the time of choosing the species (Borowitzka, 1997; Mutanda *et al*., 2010). According to Mutanda *et al*. (2010) low-cost harvesting would entail large cell size, high specific gravity compared to the medium and reliable autoflocculation.

2.4 Microalgal cultivation

After selecting a strain and product of interest, the step to follow is appropriate cultivation of the organism. Microalgae can be grown naturally by absorbing sunlight from the

environment, assimilating CO_2 from the air and taking up nutrients from aquatic surroundings. Therefore, artificial cultivation of microalgae ought to reproduce and enhance the optimum natural growth conditions (Brennan and Owende, 2010).

Microalgae can be produced using three mechanisms: photoautotrophic, heterotrophic and mixotrophic cultivation, all of which follow natural growth processes. Photoautotrophic production requires autotrophic photosynthesis, and heterotrophic production makes use of organic substances (such as glucose) to stimulate growth. In a mixotrophic process some microalgal strains have the ability to combine both autotrophic photosynthesis and heterotrophic assimilation of organic compounds (Brennan and Owende, 2010).

To date, photoautotrophic growth seems to be the only method which is practical and economically feasible for the large-scale production of microalgal biomass (Brennan and Owende, 2010; Chisti, 2008). Two systems that have been extensively deployed are based on open pond and closed PBR technologies (Richmond and Wu, 2000; Molina *et al*., 2001; Suh and Lee, 2003; Chisti, 2008; Brennan and Owende, 2010).

2.4.1 Open raceway pond production systems

Early attempts to grow microalgae in open ponds were conceived by Germans during World War II. During this time microalgae were mainly used as food supplements (Borowitzka, 1999; Ugwu *et al*., 2008; Brennan and Owende, 2010). Today, these systems can be categorised into natural waters (lakes, lagoons, and ponds) and artificial ponds or containers (Brennan and Owende, 2010). Due to them been cost effective, raceway ponds are the most commonly used artificial growth systems (Borowitzka, 1999; Chisti, 2007; Brennan and Owende, 2010). They are typically constructed of a closed loop, oval shaped recirculation channels, generally between 0.2 and 0.5 m deep (Chisti, 2007; Brennan and Owende, 2010). Mixing and circulation which is required to stabilise microalgal growth and productivity is maintained within the pond by a paddlewheel (Borowitzka, 1999; Chisti, 2007; Brennan and Owende, 2010). The paddlewheel is a continuous operation that prevents sedimentation. Flow can be guided around bends by baffles placed in the flow channel (Chisti, 2007). Open

systems are built in concrete or compacted earth, and are usually lined with white plastic (Borowitzka, 1999; Chisti, 2007; Ugwu *et al*., 2008; Brennan and Owende, 2010).

For a continuous production cycle, microalgal broth and nutrients are introduced in front of the paddlewheel and circulated through the loop to the harvest extraction point. Broth is harvested behind the paddlewheel, on completion of the circulation loop (Chisti, 2007). In raceways, cooling is solely achieved by evaporation. Temperature fluctuates seasonally. Considerable loss of water due to evaporation can occur. Due to significant losses to the atmosphere, raceway ponds are known to use CO_2 much less efficiently than PBRs (Chisti, 2007). Microalgae present in open ponds usually obtain their CO_2 requirement from the surface air, but submerged aerators have been known to be installed to enhance CO_2 absorption (Brennan and Owende, 2010).

In 1998, Sheehan and co-workers discovered through studies of open systems for microalgal growth, that it was nearly impossible to maintain laboratory cultures owing to temperature fluctuations and invasive species. Though an open system is more economical, microalgal biomass productivity is significantly reduced when compared to closed bioreactors, as raceways are poorly mixed and cannot sustain an optically dark zone. If controlled at optimised conditions in a closed system, microalgal cultures could be maintained in the exponential phase of growth producing optimised biomass yields (Borowitzka, 1999; Chisti, 2007; Ugwu *et al*., 2008). Table 1 depicts some of the key differences between open and closed cultivation systems.

Table 1: An assessment of closed and open microalgal cultivation systems (Mata *et al*., 2010).

Culture systems for microalgae	**Closed systems (PBRs)**	**Open systems (Ponds)**
Contamination control	Easy	Difficult
Contamination risk	Reduced	High
Sterility	Achievable	None
Process control	Easy	Difficult
Species control	Easy	Difficult
Mixing	Uniform	Very Poor
Operation regime	Batch or semi-continuous	Batch or semi-continuous
Space required	A matter of productivity	PBRs Ponds
Area/volume ratio	High	Low
Population (algal cell) density	High	Low
Investment	High	Low
Operation costs	High	Low
Capital/operating costs ponds	Ponds 3–10 times lower cost	PBRs > Ponds
Light utilisation efficiency	High	Poor
Temperature control	More uniform temperature	Difficult
Productivity	3–5 times more productivity	Low
Water losses	Depends upon cooling design	PBRs < Ponds
Hydrodynamic stress on algae	Low–high	Very low
Evaporation of growth medium	Low	High
Gas transfer control	High	Low
CO_2 losses	Depends on pH, alkalinity, etc	PBRs < Ponds
O_2 inhibition	Greater problem in PBRs	PBRs < Ponds
Biomass concentration	3–5 times in PBRs	PBRs > Ponds
Scale-up	Difficult	Difficult

2.4.2 Closed photobioreactor systems

Microalgal production using closed PBR technology has been implemented to overcome some of the key problems associated with the above described open pond production systems. A major advantage of PBRs when compared to open raceway systems is that they permit culture of single species of microalgae for prolonged durations with lower risk of

contamination (Brennan and Owende, 2010). Harvesting costs may also be significantly reduced owing to the higher cell mass productivities attained (Chisti, 2007; Brennan and Owende, 2010). Despite the fact that a great deal of work has already been done to develop PBRs for microalgal cultures, more efforts are still required to improve PBR technologies and know-how of microalgal cultures. Photobioreactor design and development is perhaps one of the first major steps that should be undertaken for efficient mass cultivation of microalgae (Ugwu *et al*., 2008). Some commonly employed photobioreactor designs are briefly outlined below.

2.4.2.1'Big bag' system

One of the earliest and most widely used large-scale closed system was the 'big bag' system. These systems require large sterile plastic bags of about 0.5 m in diameter fitted with an aeration unit. Although most of these systems are operated in batch mode, semi-continuous systems have also been developed (Borowitzka, 1997). Cohen and Arad (1989) developed a variant on this system by using multiples of narrower bags. However, to date there appears to be no commercial production of this structure. One of the main problems associated with the big bag system is that the arrangement has to be operated indoors for temperature control and that the relatively large diameter of the bags and the need for artificial lighting results in light-limited cultures. The operation of these systems is also labour intensive and the cultures are generally inadequately mixed, leading to recurrent culture 'crashes' (Borowitzka, 1997).

2.4.2.2 Flat-plate photobioreactors

Work done by Milner (1953) paved way to the use of flat culture vessels for cultivation of microalgae. Over the years they have received much attention due to their large illumination surface area and high densities of photoautotrophic cells (Ugwu *et al*., 2008). The reactors are constructed of transparent materials, to allow for maximum light energy capture. A thin layer of dense culture is permitted to flow across the flat plate, which allows radiation absorbance in the first few mm of thickness (Brennan and Owende, 2010). Even though these systems are very suitable for mass culturing of microalgae owing to their high photosynthetic

efficiencies, they also offer major limitations such as: scale-up will require many compartments and support materials, there is also difficulty in controlling culture temperature, as well as some degree of wall growth and the possibility of hydrodynamic stress to some microalgal strains (Hu *et al*., 2008; Ugwu *et al*., 2008).

2.4.2.3 Column photobioreactors

When compared to other closed systems, column PBRs are low-cost, compact and easy to operate. They also possess high volumetric mass transfer rates, efficient mixing, and superior controllable growth conditions (Eriksen, 2008). The vertical columns are illuminated either internally or through transparent walls and aerated from the bottom. Their performance compares favourably with TPBRs (Brennan and Owende, 2010).

2.4.2.4 Tubular photobioreactors

Tubular Photobioreactors, which typically consist of an array of straight glass or transparent plastic tubes, are perhaps one of the most frequently deployed closed systems for microalgal growth (Molina *et al*., 2001; Ugwu *et al*., 2008). The tubular array or solar collector can be aligned horizontally, vertically, inclined or as a helix to maximise light energy capture. The tubes are generally 0.1 m or less in diameter. Tube diameter is limited since light does not penetrate too deeply in the dense culture broth that is necessary for ensuring high biomass productivity (Chisti, 2007). Microalgal cultures are re-circulated with a mechanical pump or airlift system. Agitation and mixing are imperative to promote gas exchange within the tubes (Molina *et al*., 2001; Chisti, 2007; Ugwu *et al*., 2008). Biomass sedimentation in tubes can be prevented by maintaining a highly turbulent flow (Chisti, 2007). Owing to their high productivity, TPBRs are likely to be used in producing much of the microalgal biomass required for making biodiesel when compared to other closed units, as they provide a controlled environment that can be tailored to the specific demands of highly productive microalgae to attain a consistently good annual yield of oil (Ugwu *et al*., 2008).

Table 2: Properties of various closed culture systems (Borowitzka, 1999).

Reactor type	Mixing	Light utilisation efficiency	Temperature control	Gas transfer	Hydrodynamic stress on microalgae	Species control	Sterility	Scale up
Stirred Tank	Largely uniform	Fair–good	Excellent	Low–high	High	Easy	Easily achievable	Difficult
Air-Lift reactor	Generally uniform	Good	Excellent	High	Low	Easy	Easily achievable	Difficult
Bag Culture	Variable	Fair-good	Good (indoors)	Low-high	Low	easy	Easily achievable	Difficult
Flat-Plate reactor	Uniform	Excellent	Excellent	High	Low-high	Easy	Achievable	difficult
Tubular reactor	Uniform	Excellent	Excellent	Low-high	Low-high	Easy	Achievable	Reason-able

2.5 Microalgal lipid productivity and triglyceride biosynthesis

Microalgae are able to synthesise FAs as building blocks for the formation of different lipids which are used by the cell for synthesis of cellular components and sources of energy (Guy, 1996). Fatty acids can either be saturated or unsaturated. Unsaturated FAs may vary in the number and position of double bonds on the carbon chains. Saturated FAs have all the hydrogen that the carbon atoms can hold, and therefore, have no double bonds between the carbons. Monounsaturated FAs have only one double bond. Polyunsaturated FAs contain 2 or more double bonds. Microalgal oils differ from most vegetable oils as they are quite rich in polyunsaturated FAs with four or more double bonds. The most regularly synthesized FAs have chain lengths that range from C16 and C18. (Hu *et al*., 2008). These non- or mono-unsaturated FAs are preferable sources to use for the production of biodiesel.

The lipid and FA content of microalgae vary depending on culture conditions and strain. Lipid classes are essentially divided into neutral lipids (e.g., triglycerides, cholesterol) and polar lipids (e.g., phospholipids, galactolipids). It has been found that in some cases, lipid accumulation and composition could be enhanced by various growth conditions such as nitrogen starvation, silicon deficiency, phosphate limitations, high salinity and heavy metal stress (Chisti, 2007; Liu *et al*., 2008 a). Increased oil production under stress occurs during the cessation of cell division. However, the increased oil content of the microalgae does not

necessary lead to increased overall productivity of oil, since the rate of production of all cell components is lower under nutrient starvation (Guy, 1996). Under these unfavourable environmental conditions many microalgae change their lipid biosynthetic pathways towards the formation and accumulation of neutral lipids, mainly in the form of Triacylglycerols (TAGs). Triacylglycerols serve primarily as a storage form of carbon and energy. Triglycerides as neutral lipids are the key resources in the production of biodiesel. The synthesis routes of triglycerides in microalgae consist of three basic steps (Huang *et al*., 2009):

(a) The formation of acetyl coenzyme A (acetyl-coA) in the cytoplasm

(b) The elongation and desaturation of carbon chain of FAs

(c) The biosynthesis of triglycerides in microalgae

Figure 1 illustrates the reaction steps that are involved in the biosynthesis of triglycerides in microalgae and Table 2 summarises the percentage of oils produced by common microalgae.

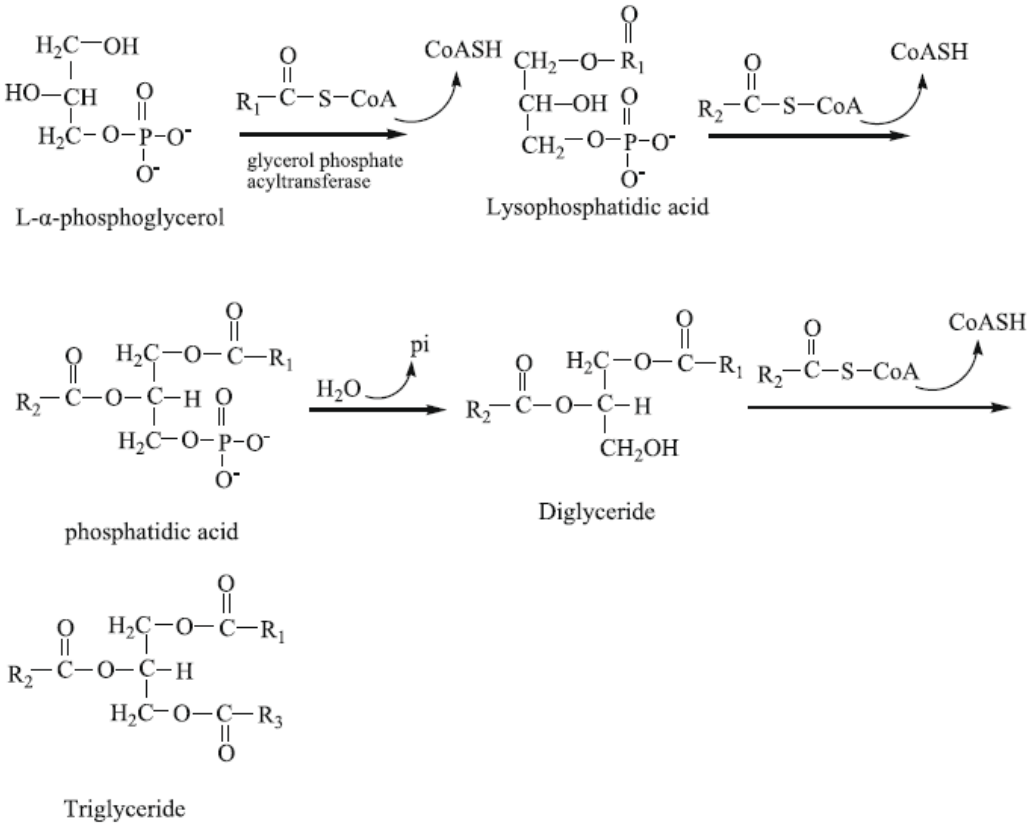

Figure 1: Reaction steps involved in the biosynthesis of triacylglycerides in microalgae (Huang *et al*., 2009).

Table 3: Percentage oil yield produced from common microalgae (Chisti, 2007).

Microalgae	Oil yield (% dry weight)
Botrycoccus braunii	25-75
Chlorella sp.	28-32
Crypthecodinium cohnii	20
Duneliella primolecta	23
Isochrysis sp.	25-33
Nannochloris sp.	20-35
Nannochloropsis sp.	31-68
Neochloris oleoabundans	35-54
Nitzschia sp.	45-47
Schizochytrium sp.	50-77

2.5.1 Lipid determination and analysis

Conventional methods for lipid determination involves solvent extraction and gravimetric determination (Bligh and Dyer, 1959). Further analysis and characterization of FAs are performed by Gas Chromatography (GC), High Performance Liquid Chromatography and Thin Layer Chromatography (Elsey *et al*., 2007). Traditional gravimetric methods are often time consuming, require relatively large amounts of biomass, labour-intensive and has a low throughput screening rate (Gao *et al*., 2008; Mutanda *et al*., 2010). Consequently, there is greater attention on a rapid in situ measurement of the lipid content. In recent years, Nile Red (NR), a lipid-soluble fluorescent dye, has been commonly used to evaluate the lipid content of microalgae. Besides NR been relatively straightforward and rapid, it also possesses several characteristic advantages to *in situ* screening. It is fairly photostable, and extremely fluorescent in organic solvents and hydrophobic environments (Elsey *et al*., 2007; Mutanda *et al*., 2010). As the polarity of the medium decreases, the emission maximum of NR is blue-shifted which allows one to differentiate between neutral and polar lipids at the excitation and emission wavelengths (Greenspan and Fowler, 1985; Mutanda *et al*., 2010). The Olympus image software, version 5.0, can further be used to qualitatively determine the lipid percentage present, by microscopic area measurements of the lipid relative to the cell area.

2.6 Harvesting

Biomass recovery poses a challenge in microalgal biomass production processes. This phase generally requires one or more solid–liquid separation steps and usually accounts for 20–30% of the total costs of production (Wang *et al*., 2008; Brennan and Owende, 2010). Common harvesting practices include flocculation, filtration, flotation, and centrifugal sedimentation. Some of these procedures can be highly energy intensive. The small size of some microalgal cells (typically in the range of 2-40 μm) and low cell densities (typically in the range of 0.3 to 5 g l^{-1}) as a result of limited light penetration make the recovery of biomass difficult (Brennan and Owende, 2010). Selecting an appropriate harvesting technology during microalgal cultivation is crucial to economic production of microalgal biomass (Schenk *et al*., 2008; Brennan and Owende, 2010).

The choice of harvesting technique is dependent on microalgae characteristics such as, size, density, and the value of the target products. Strain selection is an important factor to take into consideration since certain species are much easier to harvest when compared to others (Brennan and Owende, 2010). According to Brennan and Owende (2010), microalgae harvesting is a two stage process, involving bulk harvesting and thickening. Bulk harvesting aims at separating biomass from the bulk suspension. The concentration factors for this procedure are generally 100–800 times to reach 2–7% total solid matter. This is dependent on the initial biomass concentration and technologies employed (including flocculation, flotation or gravity sedimentation). Thickening is generally a more energy intensive step as it involves concentrating the slurry through techniques such as centrifugation, filtration and ultrasonic aggregation.

2.7 Dehydration procedures

Following harvesting, the biomass slurry must be processed rapidly as it is perishable. Dehydration or drying techniques are commonly used to extend the viability depending on the final product required. Commonly employed methods include sun drying, low-pressure

shelf drying, spray drying and freeze drying (Brennan and Owende, 2010). Even though sun drying is the cheapest form of dehydration, it poses many disadvantages such as long drying times, the requirement for large drying surfaces, and the risk of material loss. Spray drying is relatively expensive and can cause significant deterioration of some microalgal pigments, therefore it is commonly reserved for extraction of certain high value products (Desmorieux and Decaen, 2006; Brennan and Owende, 2010). Freeze drying is equally expensive, especially for large scale operations, but it enables easy extraction of oils. Intracellular elements such as oils are difficult to extract from wet biomass using solvents without cell disruption however, they are readily extracted from freeze dried biomass (Brennan and Owende, 2010).

2.7.1 Extraction of microalgal oils

Cell disruption is often utilised for recovering intracellular products from microalgae. This process is used due to the thick cell walls of certain microalgae that make penetration of solvents difficult. Cell disruption methods that have been used successfully include high-pressure homogenisers, autoclaving, sonication, and addition of HCl, sodium hydroxide, or alkaline lysis (Brennan and Owende, 2010).

2.7.1.1 Transesterification of triglycerides to biodiesel

Microalgal oils generally have a higher viscosity than that of diesel oils. Thus, they cannot be applied to engines directly. Therefore, transesterification is necessary to reduce the original viscosity and increase the fluidity (Huang *et al*., 2009). Transesterification can be defined as the reversible reaction of a fat or oil with an alcohol (methanol or ethanol) to form FA alkyl esters and glycerol (Figure 2). In this reaction TAGs are converted to diglycerides. Following that, diglycerides are converted to monoglycerides, and monoglycerides are then converted to esters (biodiesel) and glycerol (by-product) (Marchetti *et al*., 2007; Hu *et al*., 2008; Mata *et al*., 2010).

Transesterification reactions may be alkali, acid, or enzyme-catalysed. The majority of commercialised technology however, uses alkali-catalysed reactions as they have a higher reaction rate and conversion when compared to acid catalysts (Huang *et al*., 2009). The transesterification reaction proceeds with or without a catalyst by using primary or secondary monohydric aliphatic alcohols having 1 to 8 carbon atoms. Transesterification can be seen as an equilibrium reaction. In this reaction a larger amount of alcohol is used to shift the reaction equilibrium to the right side (as shown in Figures 1 and 2) and produce more methyl esters as a proposed product (Demirbas, 2008; Balat and Balat, 2010). Ethanol is a preferred source of alcohol when compared to methanol as it is derived from agricultural products and is renewable and biologically less objectionable in the environment. Methanol however, is used most often because of its physical and chemical advantages (polar and shortest chain alcohol) and low cost (Balat and Balat, 2010).

The reaction takes place at pressures around 2 atm and a temperature of 65 °C. Biodiesel can be further purified by washing followed by evaporation to remove any remaining alcohol. The oil (87%), alcohol (9%), and catalyst (1%) are the inputs and biodiesel (86%) is the main output (Balat and Balat, 2010). If the reaction is carried out under high pressure (9000 kPa) and high temperature (240 °C), then pretreatment is not required as simultaneous esterification and transesterification take place with maximum yield obtained at temperatures ranging from 60 to 80 °C at a molar ratio of 6:1 (Balat and Balat, 2010).

The key factors that affect transesterification reactions are the molar ratio of glycerides to alcohol, catalyst, reaction temperature and pressure, reaction time, the contents of free FAs and the presence of water in oils. For an entire reaction to occur a free FA value of lower than 3% is required and the other materials should be considerably anhydrous. The presence of water leads to hydrolysis of some of the produced ester, resulting in soap formation. Soap formation reduces catalyst efficiency, causes an increase in viscosity, leads to gel formation and makes the separation of glycerol difficult (Balat and Balat, 2010).

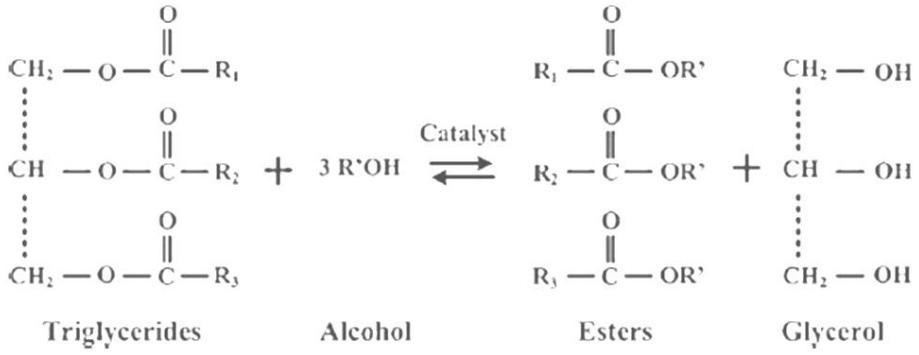

Figure 2: Overall transesterification reaction of triacylglycerides (Mata *et al*., 2010).

2.8 Direct microalgal biomass conversion

Two basic categories of conversion technologies for utilising microalgae biomass exist: thermochemical and biochemical conversion. Factors such as the type and quantity of biomass feedstock, the desired form of the energy, economic consideration, and the desired end form of the product influence the choice of conversion process. Thermochemical conversion involves the thermal decomposition of organic components in biomass to yield fuel products, and can be achieved by different methods such as direct combustion, gasification and thermochemical liquefaction. Biochemical conversion is a biological process which involves energy conversion of biomass into other fuels. This technology includes anaerobic digestion, alcoholic fermentation and photobiological hydrogen production (Brennan and Owende, 2010).

Problems with substituting triglycerides for diesel fuels often arise due to their high viscosities, low volatilities and polyunsaturated character. Dilution/blending, micro emulsification, pyrolysis, and transesterification are four techniques that are routinely applied to solve the problems encountered with the high fuel viscosity. From all these techniques, transesterification, a thermochemical process proves to be the best option, as the physical characteristics of FA esters are very close to those of diesel fuel and the process is relatively simple (Balat and Balat, 2010; Brennan and Owende, 2010).

Due to the increasing global demand for renewable liquid fuels, the need for developing suitable technology to meet this demand is crucial. Comparative analysis of producing bio-oil from crop and microalgae based biomass show the latter to be more advantageous on various aspects (Mutanda *et al*., 2010). Thus the overall objective of the study was to manipulate conditions within a closed system in an attempt to increase biomass and lipid concentrations, of the selected *C.vulgaris* strain, which could potentially be used as a technology for biodiesel production.

Chapter Three: Evaluation of the Lipid Potential of a *Chlorella* sp.

3.1 Introduction

South Africa by far is one of the largest emitters of GHGs and amongst the top 20 most carbon intensive countries in the world (Murugesan *et al*., 2008). Due to rising oil prices, the need to diversify energy supply and reduction of GHGs, biofuels have attracted much attention as it is both renewable and biodegradable.

It does not appear possible to meet the increased production capacity and mandated demand with traditional sources of biodiesel (soybeans, rapeseed/canola, palm, various greases and used cooking oils). Therefore, a rapid increase in biodiesel production capacity and governmental mandates for alternative fuel usage around the world in the last several years has necessitated the development of alternative biodiesel feedstocks (Huang *et al*., 2009; Balat and Balat, 2010; Mata *et al*., 2010). Recent research initiatives have established that microalgal biomass appear to be the only source of renewable biodiesel capable of meeting global demand for transport fuels (Borowitzka, 1999; Chisti, 2007; Khan *et al*., 2009; Brennan and Owende, 2010; Mata *et al*., 2010). Desirable characteristic features of microalgal oil as alternative fuel when compared to other feedstocks includes adaptability to local growing conditions (rainfall, soil type, latitude, etc.), regional availability, rapid growth rates and high oil content, favorable FA composition, low agricultural inputs, and the ability to grow in agriculturally undesirable lands (Huang *et al*., 2009; Balat and Balat, 2010; Mata *et al*., 2010). A study revealed that approximately 10.8 million square miles of farmland with the highest yielding biofuel crops will be needed to replace the worldwide petroleum use with biofuel, unfortunately though there are only 5.8 million square miles of farmland on earth (Khan *et al*., 2009). It is thus evident that oil crops cannot contribute considerably to replacing petroleum derived liquid fuels in the near future (Chisti, 2007). The use of microalgae to produce biodiesel will therefore, not compromise production of food, fodder and other products derived from crops (Khan *et al*., 2009).

More than 40,000 different species of microalgae have been identified so far, most of which have a high content of lipids, accounting for between 20 and 50% of their total biomass (Miao and Wu, 2006). Microscope-based techniques including conventional light

microscopy, transmission electron microscopy and scanning electron microscopy are usually the standard procedures used in laboratories for the screening of microalgal samples. However, the application of Polymerase Chain Reaction-based methods using species-specific molecular probes would be powerful technologies for rapid screening and identification of microalgal species (Godhe *et al*., 2001; Morgan-Kiss *et al*., 2008). Commonly used DNA regions for phylogenetic purposes includes ribosomal RNA genes, mitochondria genes, plastid genes, photosynthetic genes, actin genes, internal transcribed sequences and microsatellite DNA sequences (Coleman, 2003; Feliner and Rossello, 2007). Numerous studies have suggested that the quantity and quality of biomass as well as lipids can vary as a result of changes in nutrient media characteristics; which include CO_2 concentration, nitrogen, and phosphates (Illman *et al*., 2000; Liu *et al*., 2008 b).

Pulse amplitude modulation (PAM) fluorometry is a non-invasive technique that is based on chlorophyll *a* fluorescence quenching analysis and allows for measurement of photosynthetic processes and parameters in benthic microalgae (Ralph and Gademann, 2003). This technique has been used to estimate photosynthetic rates based on a linear relationship, between the ratio of variable to maximum fluorescence (Fv/Fm) and the effective quantum yield of photosystem II (PSII) (Genty, 1989). Rapid light curves could provide detailed information on the saturation characteristics of electron transport (ET), as well as the overall photosynthetic performance of microalgae (Genty, 1989; Ralph and Gademann, 2003).

Microalgal biomass can be converted into energy fuels by using thermo chemical conversion systems. Among the various conversion systems for biomass, pyrolysis produces energy fuels with high fuel-to-feed ratio, making it the most efficient process for biomass conversion. In recent years, the pyrolysis process for microalgae biomass has attracted a great deal of attention. Miao *et al*. (2006) have reported that a bio-oil product from the fast pyrolysis of autotrophic microalgae, *Chlorella protothecoides* and *Microcystis aeruginosa*, is characterized by low O_2 content, a high heating value of 29 MJ kg^{-1}, and a low viscosity of 0.10 Pa/s. Bio-oil produced from microalgae makes it more suitable for fuel usage than oils by fast pyrolysis from lignocellulosic materials. This process represents a valuable contribution to creating an industrial system that produces liquid fuel from microalgae. In thermogravimetric analysis (TGA), the sample is programmed through a predetermined

temperature regime in an inert atmosphere. Thermogravimetric analysis is used to reveal degradation, oxidation or reduction reactions, evaporation, sublimation, and other heat-related changes that occur in biomass (Peng *et al*., 2000; Grierson *et al*., 2008; Bahng *et al*., 2010). The study of the thermal behavior of the decomposition and volatile emission of biomass is of interest for its use in the determination of residence times of these materials in high temperature processes such as pyrolysis, gasification or combustion (Miao *et al*., 2006). One of the first issues that can be encountered when implementing these processes in a commercial reactor is knowledge of the thermal degradation behavior under different conditions (Goyal *et al*., 2008; Grierson *et al*., 2008; Bahng *et al*., 2010). Thermogravimetric analysis results will yield basic information about thermal behaviour and pyrolytic kinetic parameters of reactions. This information could therefore, help in design of pyrolysis systems for converting the biomass into renewable fuels.

The screening of microalgae biomass is necessary to choose the best one(s) in terms of quantity and quality as an oil source for biofuel production. Thus the objective of this part of the study was to identify and to determine the biofuel potential of a selected microalgal strain by subjecting it to variations in CO_2 and nutrient concentrations, and to study the thermal behaviour of microalgal biomass during pyrolysis using TGA. An attempt to determine the best range of light intensity required for optimal biomass production was also conducted using a PAM technique.

3.2 Materials and Methods

3.2.1 Microalgal strain, growth medium and culture conditions

The autotrophic microalgal strain was selected after preliminary screening of a variety of different microalgal species. These green microalgae were originally isolated from a turbid, open pond in KwaZulu-Natal, South Africa. The strain was grown and maintained in the complete BG11 medium according to Watanabe *et al*. (2000) and was exposed to an irradiance of 80 µmol photons $m^{-2}s^{-1}$, a light/dark-cycle of 16/8 h and a temperature of 25$\pm$1 °C on an orbital shaker at 80 rpm.

3.2.2 Strain identification

DNA was extracted using a modification of the boiling method described by Sepp *et al*. (1994). Two millilitres of sample was centrifuged at 7826 x g for 5 min. The supernatant was decanted and the pellet was re-suspended in 500 µl of sterile distilled water. This was boiled at 80 ºC for 10 min and was stored at -20 ºC for further analysis. The extracted DNA was subjected to PCR amplification with a Veriti (Applied Biosystems) 96 well thermal cycler. The reaction mixture consisted of Taq buffer (10X), 200 µM dNTPs, 50 pM of each primers, (DIR, 5'CCTTGGTCCGTGTTTCAAGA3'/D2C, 5'ACCCGTGATTTTAAGCATA3'), 1U Taq enzyme and 1 µl of genomic DNA (Lenaers *et al*., 1989). A total working volume of 25 µl was used for the microalgal strain identification. Polymerase Chain Reaction was performed under the following conditions: Denaturation step at 95 ºC for 5 min followed by 45 ºC for 1 min; 39 cycles of 95 ºC for 1 min, 52 ºC for 1.5 min, 72 ºC for 1 min, and a final extension step at 72 ºC for 5 min. All PCR products were run on an agarose gel (1%) at 80 volts for 60 min (Bio-Rad Power Pac 300, South Africa). The gel was viewed using a gel documentation system (Vacutec G: Box, South Africa). Sequencing of PCR amplified 28S ribosomal DNA was done at a commercial lab, Inqaba Biotechnical Industries, Pty Ltd, South Africa. Sequences were aligned using FinchTV (Geospiza). Sequences were then compared to the National Centre for Biotechnology Information (NCBI) database (http://www.ncbi.nlm.nih.gov/blast/Blast.cgi) using the Basic Local Alignment Search Tool (BLAST) to determine phylogenetic affiliations (Altschul *et al*., 1990). The sequence was then aligned with selected GenBank sequences using multiple alignments programme (CLUSTAL_X) and Maximum likelihood analysis was performed using CLC Bio DNA Workbench version 5.6.1.

3.2.3 Measurements of fluorescence induction

Non invasive fluorescence measurements were obtained using a Dual-PAM 100 Chlorophyll Fluorometer (Heinz Walz Gmbh, Effeltrich, Germany). Samples (3 ml) were incubated in a quartz glass cuvette. Rapid photosynthetic light curves were generated by applying a sequence of increasing actinic irradiance in 15 discrete increments. Each period of actinic

light lasted for 10 s before a saturation pulse of blue light (0.6 s at 10000 µmol photons $m^{-2}s^{-1}$) was applied to determine the ET rate for each irradiance level. Photon irradiance (400 to 700 nm) incident on the sample surface was measured continuously using a PAR micro-sensor (Spherical MicroQuantum Sensor US-SqS/W, Waltz) connected to the PAM fluorometer control unit. Variable fluorescence was measured by a saturating pulse (0.8 s; 2000 µmol $m^{-2}s^{-1}$). The quantum efficiency of PSII charge separation (Fv/Fm) is calculated as (Genty *et al*., 1989):

$$Fv/Fm\ (dimensionless) = (Fm - F0) / Fm \quad (1)$$

Where F0 is the minimum and Fm is the maximum fluorescence yields of a 30 min dark adapted sample. Subsequent to a saturating pulse, the undisturbed sediment samples were maintained in the dark for 10 min, thereafter exposed to actinic light for 5 min at an irradiance corresponding to the in situ PAR level at the sediment surface, for that period and station from which the intact core was collected. F0′ and Fm′ values were subsequently recorded. DualPAM software v 1.9 was used to record all data and to generate the rapid light curves. The DualPAM measured ETR as:

$$ETR = F'q/F'm \times PPFD \times aL \times (PSII/PSI) \quad (2)$$

Where F'q = (F'm – F'), the default adsorptance factor (aL) of 0.84 and the default value of 0.5 for the estimated light absorption by PSI and PSII (PSII/PSI) were used.

3.2.4 CO_2 concentration

The microalgal strain was grown in 100 ml of BG11 medium (Appendix A) in air-tight 500 ml bottles. Based on preliminary research by Chinnasamy *et al*. (2009) the CO_2 content in air was assumed to be approximately 0.03%. The headspace atmosphere was transformed with

graded concentrations of CO_2 ranging from 0.03 to 15%. This was achieved by withdrawing the air. Thereafter, appropriate quantities of CO_2 were injected into the bottles daily using commercial grade CO_2 (99.97% v/v with less than 10 µl l^{-1} CO) as described by Chinnasamy *et al*. (2009). Incubation vessels were tightly sealed with rubber stoppers to prevent leakage.

3.2.5 Nutrient concentrations

For the nutrient studies the complete BG11 medium was modified with varying $NaNO_3$ (0, 1, 1.5, 2, 5 and 10 g l^{-1}) and $K_2HPO_4.3H_2O$ (0, 0.01, 0.04, 0.08 and 0.1 g l^{-1}) concentrations. A 10% v/v exponentially growing culture (growth curve was pre-determined) was used. Other conditions of incubation such as temperature, light intensity, and the light:dark cycle were the same as the corresponding growth condition.

3.2.6 Analytical methods

The microalgal density was determined daily by Optical Density (OD) measurements at 686 nm using a Spectrophotometer (SpectroquantR Pharo 300, Merck USA). A wavelength spectrum (400 to 700 nm) was performed to determine the absorbance maxima (λ_{max}) of the microalgal culture. Spectrophotometric determinations of biomass were periodically verified by DCW measurements. A 50 ml sample was centrifuged (Heraeus multifuge centrifuge 4KR, USA) at 1509 x g for 15 min at 4 ^oC. The supernatant was discarded and the pellet was washed with 0.05 M HCl and distilled water to remove non-biological adhering materials such as mineral precipitates, and dried at 60 ^oC for 24 h. Growth kinetics was determined using spectrophotometeric data and biomass yields. Soxhlet extraction was used to determine the lipid content of the microalgae according to the protocol described by Bligh and Dyer (1959).

Experimentation was carried out in triplicate and the data were statistically analysed using the SPSS version 15.0 software. Individual effects of CO_2, $NaNO_3$, and $K_2HPO_4.3H_2O$ were analysed and the difference between the means was determined after analysis of variance.

3.2.7 Proximate and elemental analysis of microalgal biomass

The elemental composition of the microalgae was established using a CHNS 9302 Leco analyser. Moisture content, volatile matter, fixed carbon and ash content were determined as described by ASTM D3172-89. The calorific value of microalgal biomass was calculated using the equation developed by Changdong and Azevedo (2005). The carbon fixation rate was calculated from the elemental analysis of the biomass according to the equation described by Lopes *et al*. (2007):

$$R_c = C_c \times \left(\frac{X_m - X_0}{t - t_0} \right) \times \left(\frac{M_{CO_2}}{M_c} \right) \quad (3)$$

Where, maximum cell concentration (Xm, mgL^{-1}), maximum specific growth rate (μmax, h^{-1}) and generation time (tg, h).

3.2.8 Pyrolytic characteristics of microalgal biomass

Two milligrams freeze-dried microalgal cells were subjected to thermo gravimetric analysis in a nitrogen atmosphere at different heating rates of 15, 30, 40 and 50 ºC min^{-1} from ambient temperature to 800 ºC min^{-1} in a SDT Q600 Thermal Analyzer (TA Instruments, USA). A high-purity nitrogen gas (99.99%) was used as an inert purge gas to displace air in the pyrolysis zone, which was fed at a constant flow rate of 60 ml min^{-1}, thereby avoiding unwanted oxidation of the sample. The continuous online records of weight loss and temperature were obtained. This data was used to plot the TGA curve and the Derivative Thermo Gravimetric analysis (DTG) curve (Peng *et al*., 2000).

3.3 Results

Approximately 700bp of the large subunit rDNA were amplified by PCR using primers targeting towards conserved positions 24-43 (DIR, 5'CCTTGGTCCGTGTTTCAAGA3', forward primer) and 733-714 (D2C, 5'ACCCGTGATTTTAAGCATA3', reverse primer). Sequence results from BLAST searches into the Gen-Bank databases confirmed that obtained sequences were homologous to ribosomal genes of *Chlorella vulgaris* with 99% similarity (Figure 3). The sequence obtained were deposited to Gen-Bank with the accession number HM046832.

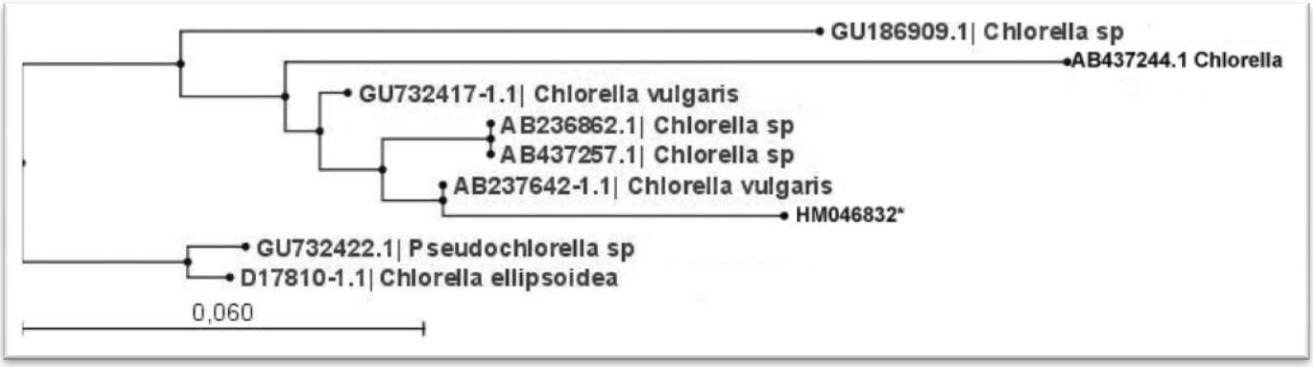

Figure 3: Phylogeny tree generated using maximum likelihood method.

Plotting relative Electron Transport Rate (rETR) as a function of irradiance in the current study showed the classical shape of a P–E curve (Figure 4 and 5), were the ETR of *C. vulgaris* increases rapidly with an increase in light intensity (Figure 4 and 5). A linear rise was observed where light was limiting followed by a plateau, where the photosynthetic pathway became limited. At a high light intensity of 369.33 µmol photons $m^{-2}s^{-1}$ rETR was found to decline after saturation, which could be attributed to photo inhibitory damage (Figure 4 and 5). The light curve indicated that *C. vulgaris* was able to perform well at light intensities between the range of 150-350 µmol photons $m^{-2}s^{-1}$.

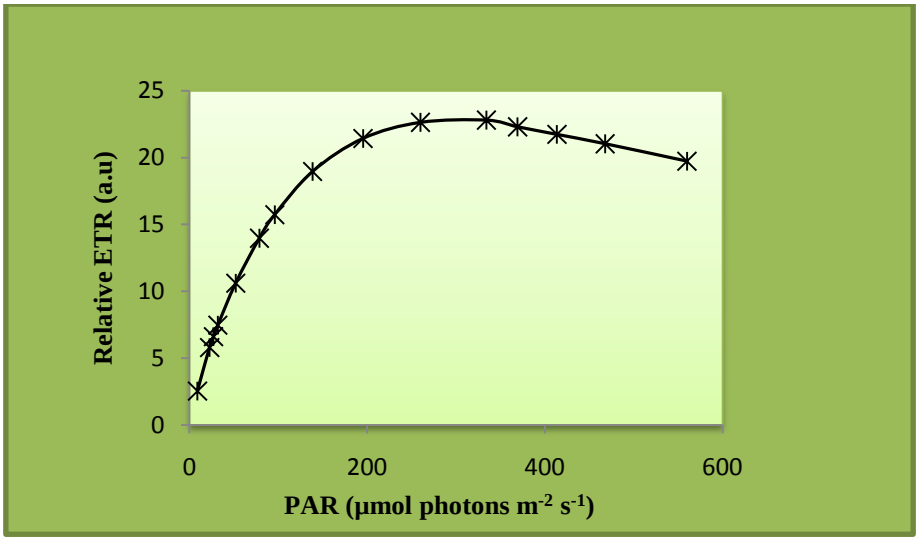

Figure 4: Effect of actinic irradiance on the light curve of *C.vulgaris.*

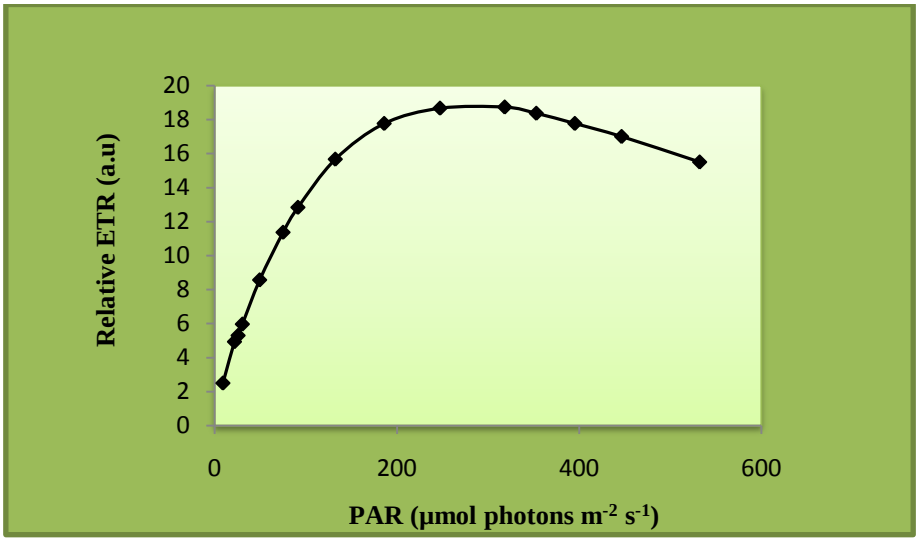

Figure 5: Effect of actinic irradiance on the dark curve of *C.vulgaris.*

The growth of the microalgal strain under varying concentrations of CO_2 is shown (Figure 6). A rapid increase in biomass production at both ambient (0.03%) and elevated (0.1-4%) CO_2 levels were observed over a duration of 15 days. A significant increase in biomass content (1.22 g l^{-1}) was recorded at 4% CO_2 level on day 15, with a corresponding OD value of 1.805. This was a 5 fold increase in biomass when compared to ambient conditions, where 0.226 g l^{-1} of biomass was produced. At this CO_2 level, a pH value of 6.5 was noted. An increase in pH

values above 6.5 were observed at lower CO_2 values of 0.1-1%. Further increases in the CO_2 concentration (6-15%) led to a decline in biomass yield. At a 15% CO_2 concentration, biomass levels doubled when compared to ambient conditions. However, at 15% CO_2 concentration there is a 3 fold decline in biomass yield when compared to the yield produced at a 4% CO_2 concentration. This suggests that the strain under study could possibly not endure CO_2 concentrations greater than 4%.

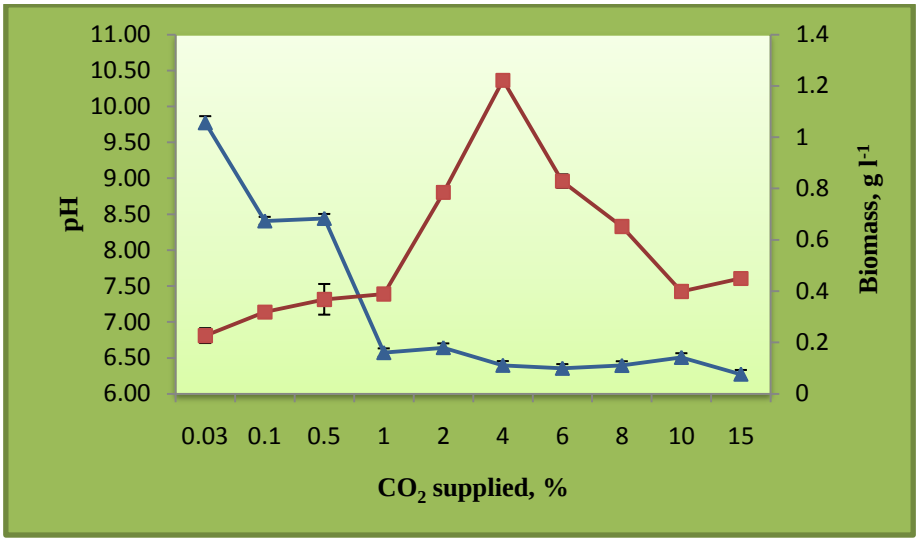

Figure 6: Biomass (red) and pH (blue) trends when the microalga was subjected to diverse CO_2 concentrations over a 15 day period.

A gradual increase in growth at the different $NaNO_3$ concentrations were noted from days 1 to 15 (Figure 7), thereafter a substantial reduction in microbial growth occurred between day 15 and 16. A $NaNO_3$ concentration of 5 g l^{-1} facilitated maximum growth, enabling the microalga to reach an OD of 0.69 on day 15, and a biomass concentration of 0.46 g l^{-1}. This was a 1.2 fold increase in growth when compared to the control in which $NaNO_3$ was absent. The lowest growth rate of 0.37 g l^{-1} at an OD of 0.54 was observed in the absence of $NaNO_3$. A similar growth pattern was observed with the $K_2HPO_4.3H_2O$ study. A gradual increase in $K_2HPO_4.3H_2O$ concentration (0-0.04 g l^{-1}) encouraged the growth of *C. vulgaris* (Figure 8). The microalgae entered stationary phase around day 11, and maintained this state up to day 14, thereafter leading to a decline in growth. A $K_2HPO_4.3H_2O$ concentration of 0.04 g l^{-1}

proved most effective in promoting growth of *C. vulgaris*, generating a biomass concentration of 1.21 g l^{-1} at an OD of 1.780 on day 14. (Figure 8). This was a 1.3 fold increase in growth when compared to the control which lacked $K_2HPO_4.3H_2O$.

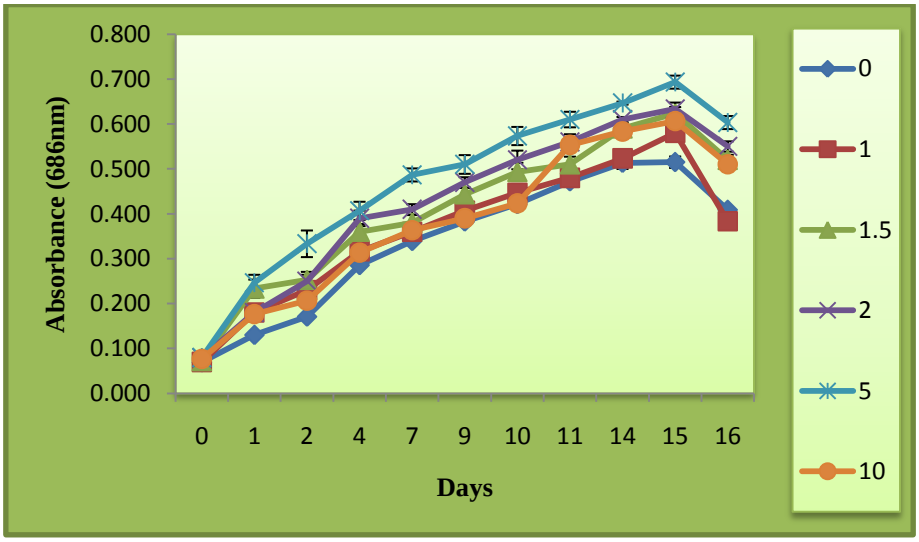

Figure 7: Effects of varying $NaNO_3$ concentrations (in g l^{-1}) on the growth of *C. vulgaris* over a 16 day duration

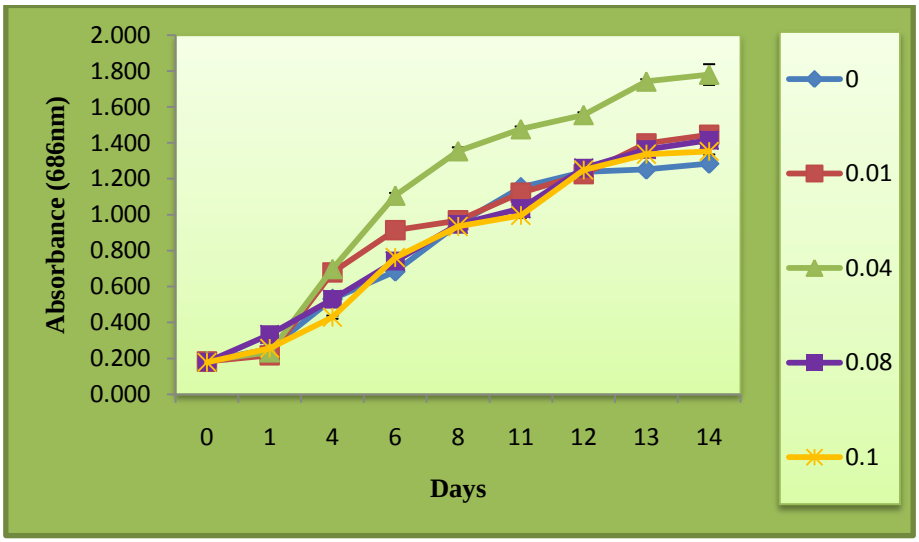

Figure 8: Growth of *C. vulgaris* in response to assorted $K_2HPO_4.3H_2O$ concentrations (in g l^{-1}) over a 14 day period

Table 4: Proximate analysis values of *C. vulgaris.*

S. No.	Particulars	Composition
1	CO_2 fixation rate, mg l^{-1} h^{-1}	6.17
2	Lipid content, %	21

*value calculated by difference

The carbon fixation rate of the selected microalgal strain at optimum CO_2 and nutrient concentrations was found to be 6.17 mg l^{-1} h^{-1} (Table 3), and the lipid content was found to be 21% dry weight prior to subjecting it to stressed conditions (Table 3).

Table 5: Three stages of thermal decomposition of microalgae biomass during pyrolysis.

^{o}C min^{-1}	Stage I	Stage II	Stage III	^{o}C
15	<231	231 - 352	352 - 800	281
30	<254	254 - 371	371 - 800	298
40	<258	258 - 377	377 - 800	303
50	<262	262 - 376	376 - 800	303

The TGA and DTG curves of the microalgae at diverse heating rates of 15, 30, 40, and 50 ºC min^{-1} in nitrogen revealed that three stages of thermal decomposition existed (Figures 9 and 10). In the DTG curve, the first peak represents the weight loss due to release of moisture, whereas the second peak depicts the pyrolytic reaction of the microalgal biomass (Figure 10). The first stage (Stage I) occurred from the starting temperature to the temperature of initial devolatilization (T_i). The temperature ranges for this initial volatilization stage is less than 230 ºC. The second stage (Stage II) was from T_i to the end of the main devolatilization (T_e). The reaction then proceeded at a high rate and led to the formation of the pyrolysis products. Maximum rate of weight loss (DTGmax) was 0.39, 0.41, 0.42 and 0.46% at 281, 298, 303 and 303 ºC respectively (Table 4). The third stage (Stage III) was from T_e to the final

temperature (350–800 ºC) (Table 4). An overall final weight loss recorded for the four different heating rates were in the range of 78.9-81%. From this study it can be seen that the optimal pyrolytic reaction occurred in temperatures ranging from 230 to 400 ºC.

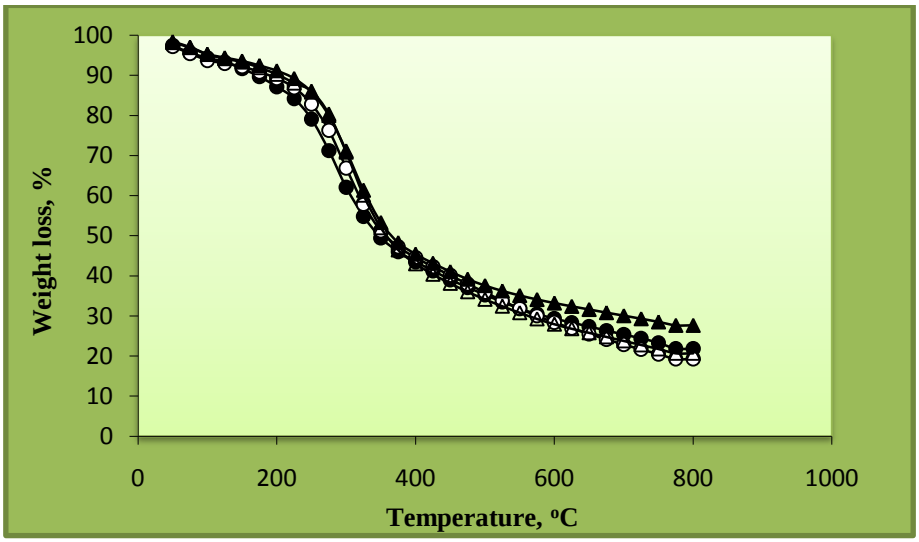

Figure 9: Thermo gravimetric curve of *C. vulgaris* depicting the weight loss of the microalgal biomass under different heating rates. Closed circle, open circle, closed inverted triangle, and open triangle represent heating rates of 15, 30, 40 and 50 ºC min^{-1} respectively

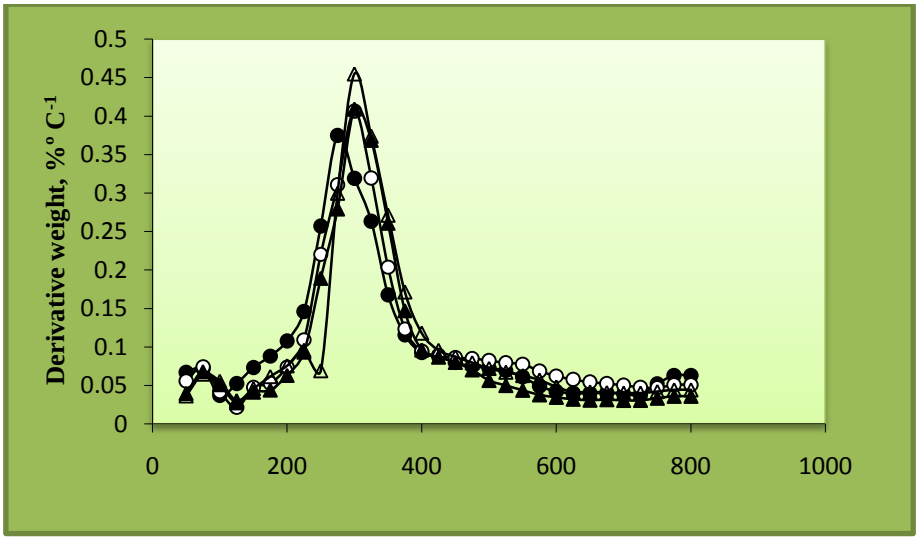

Figure 10: Derivative thermo gravimetric curves of *C.vulgaris* depicting the derivative weight as well as the pyrolytic reaction of the microalgal biomass under different heating rates. Closed circle, open circle, closed inverted triangle, and open triangle represent heating rates of 15, 30, 40 and 50 ºC min^{-1} respectively.

3.4 Discussion

BG-11 media (Appendix A) was used as the growth medium for cultivation of the selected strain (Chinnasamy *et al*., 2009; Feng *et al*., 2011).

Light intensity is an important parameter for microalgal cultivation, since low illumination decreases growth rate but excessive illumination exceeding the photoadaptive potential of the microalga readily causes photooxidative damage to the culture. Initially the culture under study was exposed to an irradiance of 80 µmol photons $m^{-2}s^{-1}$. A rapid light curve (Figures 4 and 5) was established to determine the minimum amount of light required to induce photosynthesis as well as the maximum photosynthetic rate of the organism (Genty, 1989; Ralph and Gademann, 2003). This information would be useful in the design of the PBR as it gives an idea on the optimum light range required by the organism. From the light curve it can be seen that growing the microalgal strain at 80 µmol photons $m^{-2}s^{-1}$was suboptimal, as the optimum photosynthetic rate was recorded at 150 to 350 µmol photons $m^{-2}s^{-1}$. If the strain continued to grow under suboptimal light conditions, its biomass production would be retarded. This would lead to a significant loss in terms of biomass productivity. By determining the optimum light range (150 to 350 µmol photons $m^{-2}s^{-1}$) of the culture it led to an overall increase in biomass productivity. Any further increases in light intensity beyond 369.33 µmol photons $m^{-2}s^{-1}$ would negatively affect the photosynthetic apparatus within the microalgal cells. This in turn would suppress biomass production. Therefore to support maximum biomass production, it is imperative that the microalgal cells do not receive 'too much' or 'too little' light. Results obtained in the present study correlated with work done by Ralph and Gademann (2003).

Photosynthetic organisms, such as microalgae play a key role in the biogeochemical cycling of carbon. Even though many microalgae are able to utilise different sources of organic carbon for their growth, CO_2 still remains the main source of carbon for the majority of them under illuminated conditions (Chinnasamy *et al*., 2009; Widjaja *et al*., 2009). Therefore, varying concentrations of CO_2 were studied to determine the optimal level required by *C. vulgaris* to promote growth. *Chlorella vulgaris* used in the present study grew extremely well and showed considerable improvement in biomass concentrations up to 4% CO_2 level, (Figure 6). Above 5%, toxic effects could become evident (Lopes *et al*., 2007). This could

explain the decline in biomass level above CO_2 concentrations of 4%. Elevated concentrations of CO_2 could possibly result in decreases in pH due to unutilised CO_2 that will be converted to H_2CO_3 (Sorensen *et al*., 1996; Changdong and Azevedo, 2005). A pH value of 6.5 was recorded at 4% CO_2 level on day 14. *Chlorella* sp. grow optimally at pH values that range from 7.5-8.0 **(**Rachlin and Grosso, 1991). Acidic (3.0-6.2) and alkaline (8.3-9.0) values are known to retard the growth of this microalgae **(**Rachlin and Grosso, 1991). At the start of experimentation the pH value recorded for the BG11 medium was 7.5. However, after a 14 day growth period an inverse relationship was observed where an increase in CO_2 consequently resulted in a decrease in pH. If there is not enough CO_2 gas supply, microalgae will utilise carbonate to maintain its growth. Since microalgae use CO_2 (aq) from bicarbonate as a compensation of lacking enough CO_2 from gas supply, this will result in an increase in pH (Zhang *et al*., 2002; Celekli *et al*., 2009; Widjaja *et al*., 2009), and this was noted in our present study. At low CO_2 values of 0.1 to 1% an increase in pH values above 6.5 were observed. A study by Chinnasamy *et al*. (2009) showed the highest biomass concentration (0.21 g l^{-1}) was recorded at 6% CO_2 level, which was a 20 fold increase in biomass when compared to ambient results. A difference in results between the biomass content obtained in the present study and the study conducted by Chinnasamy *et al*. (2009) could be due to the diverse CO_2 concentrations utilised as well as temperature. Temperature can regulate various metabolic processes therefore; the interaction between CO_2 concentration and temperature is bound to reflect in growth and biomass production by microalgae. Kodama *et al*. (1993) reported that *Chlorella littorale,* a marine microalgae performed better at a CO_2 concentration of 20% and a pH value of 4.

Nitrate and phosphate are known to have a central role in cell physiology and growth. Increases in nitrate and phosphate concentrations are known to enhance the growth rate of microalgal cultures (Sorensen *et al*., 1996; Martin-Jezequel *et al*., 2000; Changdong and Azevedo, 2005). This was evident as the gradual increase in $NaNO_3$ concentrations supported a steady increase in cell growth (Figure 7). A $NaNO_3$ rich medium (5 g l^{-1}) stimulated maximum growth of *C. vulgaris* (Figure 7). In the absence of $NaNO_3$, growth rate and biomass concentration of the strain was reduced. This further served to prove the important effect nitrate has on cell physiology and growth. On the other hand, it must be noted that a

further increase in $NaNO_3$ to 10 g l^{-1}seems to be inhibitive to cell growth. Studies by Goleuke *et al*. (1967) established that an excess of nitrate could prove toxic, leading to a decline in microalgal population. Studies suggest that, to effectively produce biofuel from microalgae, the optimum compromise between a slowdown in growth and the increase in the lipid fraction has to be achieved (Chisti, 2007). Under $K_2HPO_4.3H_2O$ limitation (0 to 0.01 g l^{-1}) cell division was retarded, which suggested that intracellular PO_4 was sufficient for only a few cell divisions (Figure 8). The nitrogen content of microalgae varies but is usually between 4-8% of the cells (dry weight basis) depending on physiological state and nutrient limitation.

The carbon fixation rate was within the range reported by Lopes *et al*. (2007), whose findings varied from 3.45 to 45.78 mg l^{-1} h^{-1} under different culture conditions. Kajiwara *et al*. (1997) reported carbon fixation rates of 25 mg l^{-1} h^{-1} when cultivating the cyanobacterium *Synechoccus* (PCC 7942) in PBRs. A difference in results reflects the adaptation of different microorganisms to the experimental conditions.

A lipid content of 21% was obtained, however, it can reach 46% (dry weight) under conditions of stress (Lopes *et al*., 2007; Huang *et al*., 2009) and 55% (dry weight) when grown heterotrophically (Miao and Wu, 2006). The calorific value of *C. vulgaris* biomass was found to be 17.44 kJ g^{-1}, and this value is in close agreement with Illman *et al*. (2000). Microalgae grown under normal conditions have been shown to have calorific values between 18 and 21 KJ g^{-1} (Illman *et al*., 2000). Several studies show that the calorific value of *C. vulgaris* biomass can be increased by growing them under low nitrogen conditions (Illman *et al*., 2000, Scragg *et al*., 2002; Hu *et al*., 2008; Wang *et al*., 2008).

Pyrolysis can be defined as the degradation of macromolecular materials in the absence of O_2 using solely heat (Peng *et al*., 2000; Grierson *et al*., 2008; Bahng *et al*., 2010). Trend lines of TGA and DTG curves followed a similar pattern. Stage I was characterised by a slight weight loss ranging from 3.81 to 4.5% (Figure 9). This weight loss could have occured due to

elimination of water in the cells and external water bound by surface tension (Peng *et al*., 2000). Stage II corresponded to the main pyrolysis process and was characterised by a major weight loss of 57.5% at a heating rate of 50 ºC min^{-1}. During this stage, the weight loss was recorded as the maximum for all selected heating rates (53.3 to 57.5%). Most of the volatile matter present in the microalgal biomass were released during this stage. The reaction then proceeded at a high rate and led to the formation of the pyrolysis products (Rachlin and Grosso, 1991). Peng *et al*. (2000) showed that the maximum rate of weight loss (DTGmax) for *C. protothecoides* was 0.45% at a temperature of 340 ºC. Variation in results is possibly due to the difference in classification and cellular composition of the microalgae. Data obtained from the current study indicates that an increase in the heating rate led to changing of position of the DTG peak to the higher temperatures. A slow continued loss of weight in Stage III revealed that the carbonaceous matter in the microalgal biomass continuously decomposed at a gradual pace and the solid residue reached a constant residual value. During this step, some internal rearrangement such as water elimination, bond breakage, appearance of free radicals, and formation of carbonyl, carboxyl, and hydroperoxide groups took place (Shafizadeh, 1982; Demirbas, 2008). The overall final weight loss recorded for the four different heating rates were in the range of 78.9 to 81%. The present study indicates that increased heating rates resulted in increases in the total volatile matter and shifting of T_{max} to higher temperatures. The peak position and height in the DTG evolution profiles represent the reactivity of the samples i.e. the temperature corresponding to peak height is inversely proportional to reactivity while the peak height is directly proportional to the reactivity (Vamvuka *et al*., 2003). The height of the peak position (T_{max}) increased with increased heating rates and it clearly showed that reactivity accelerated due to higher temperatures. Maiti *et al*. (2007) reported that lower heating rates results in longer residence times inside the reactor and favor secondary reactions such as cracking, re-polymerization and re-condensation, which ultimately lead to the formation of the solid char. At lower heating rates, the heating of biomass particles occurred more gradually leading to an improved and more effective heat transfer to the inner portions of the particles (Biagini *et al*., 2006). Therefore cracking was more effective which caused more weight loss in the form of volatile components. As the heating rate decreases, the residue at the end of the pyrolysis reactions also decreases. The reason for T_{max} temperature shifting to higher temperatures is due to the fact that less heat is required for the cracking of the solid fuel particles into end products. The T_{max}, which is the point at which maximum weight loss takes place, shifts to higher values

with an increase in the heating rates. These shifts have been reported by microalgal biomass researchers (Peng *et al*., 2000; Shuping *et al*., 2010). The optimal pyrolytic reaction occurred at temperatures ranging from 230 to 400 ºC. The result of the present pyrolytic study provides basic information for designing of larger scale pyrolytic reactors for the conversion of *Chlorella* microalgae biomass into energy fuels.

These various experiments were performed for an integral part of the feasibility of using microalgal biomass for production of biofuels by thermal decomposition. Optimisation of biomass production and lipid content is essential to the production of high yields of pyrolysis products. The TGA results put the optimal reaction temperature in the range required for slow pyrolysis. The typically expected results for slow pyrolysis is 30% liquid fuels (Bio-oil), 35% syngas and 35% char (Biagini *et al*., 2006; Brennan and Owende, 2010; Ross *et al.*, 2010; Shuping *et al*., 2010). The high lipid is favourable in pyrolytic reactions as high lipid content improves the heat balance as compared to non lipid containing biomass, thus reducing the level of bio-oil upgrading required when using bio-oil as a liquid fuel (Shuping *et al*., 2010). Char produced may subsequently be upgraded for use as activated charcoal, improving the process economics. Flash pyrolysis (500 °C for 1-5 s) has shown promising results for commercial production of liquid fuel from biomass giving 95.5% feed to fuel conversion (Brennan and Owende, 2010). The pyrolytic route to production of bio-oil and syngas is favoured over extraction of oil and transesterification as it is 'zero waste' process and negates the need for use of extraction process that are still a global challenge. The optimal pyrolytic reaction range for *C. vulgaris* was found to be close to that required for flash pyrolysis, thus further investigation is warranted in this regard (Biagini *et al*., 2006; Ross *et al.*, 2010; Shuping *et al*., 2010). The result of the present pyrolytic study provides basic information for designing of larger scale pyrolytic reactors for the conversion of *Chlorella* microalgal biomass into energy fuels. Mass culture of the *Chlorella* sp. was further investigated using a closed PBR with controlled CO_2 and nutrient conditions. This will be discussed in Chapters 4 and 5.

Chapter Four: Design and Operation of a Laboratory Scale Photobioreactor for Microalgal Cultivation

4.1 Introduction

Up until recently, only about 100 tons per year, which is approximately 10% of microalgal biomass, is derived from closed PBRs, while the biggest part of a few thousand tons per annum is cultivated in open ponds (Pulz and Gross, 2004; Lehr and Posten, 2009;). Despite the success of open systems, research suggests that future advances in microalgal mass culture will require closed systems as most microalgal species of interest thrive in highly selective environments (Chisti, 2008; Ugwu *et al*., 2008). Furthermore, many microalgal products must be grown free of potential contaminants such as heavy metals and micro-organisms (Borowitzka, 1999). Closed systems have been around for many years, however, their high production cost has largely precluded their commercial application until recently (Pirt *et al*., 1983; Borowitzka, 1999; Grima *et al*., 2003; Chisti, 2008). Besides saving water, energy and chemicals, closed systems possess numerous other advantages (as mentioned above), which are increasingly making them the reactor of choice for biofuel production, as operating costs can be minimised in the long run (Schenk *et al.*, 2008).

Closed systems could be tubes, plates or bags made of plastics, glass or other transparent materials, in which microalgae are supplied with nutrients, light, and CO_2 (Lehr and Posten, 2009). Over the years, there have been several major advances in the design and operation of closed PBRs for microalgal cultures based on new reactor geometries as well as optimised aeration and mixing strategies. Yet even with current advances only a few designs can effectively utilise light energy for the mass production of microalgae (Borowitzka, 1999; Chisti, 2008; Ugwu *et al*., 2008; Lehr and Posten, 2009).

One of the most important factors that control cell growth in a PBR is light availability (Wu and Merchuk, 2004). The critical design requirement in a PBR is the illumination surface area per unit volume. An efficient PBR has a high S/V ratio. Microalgal culture systems can be illuminated by artificial light, solar light or a combination of both. Laboratory-scale PBRs

are generally artificially illuminated using fluorescent lamps or other light distributors (Ugwu *et al*., 2008). According to Lambert–Beer's Law, 'light intensity decays exponentially as it penetrates into an optically dense culture. In highly dense cultures, while the region close to the light source receives plenty of light, some zones in the reactor may remain in the dark as a result of optical absorption and self-shading of the cells. In this region, the light intensity is too weak to maintain positive growth of cells; hence the net biomass production would be negative' (Wu and Merchuk, 2004).

Besides light availability, a thorough understanding on hydrodynamic and mass transfer of PBRs is also essential to improve microalgal productivity. Growth of microalgae in closed reactors is largely dependent on suitable mass transfer of CO_2 and O_2. In addition, good mixing significantly helps to prevent the cells from staying too long in dark or bright zones of the reactor (Lehr and Posten, 2009). Ordered mixing is generally recommended as it compels the cells to experience periodical light/dark cycles. A periodical light/dark cycle is known to enhance growth rates (Wu and Merchuk, 2004).

Each type of PBR has its own distinct advantages and disadvantages in terms of potential efficiency of light utilisation, effective mass transfer of CO_2 and O_2, ease of cleaning, as well as scalability. Table 5 shown below, depicts some inherent properties of commonly used PBRs for microalgal mass culture.

The majority of closed PBRs are designed as tubular, plate or bubble column reactors (Pulz, 2001; Ugwu *et al*., 2008). The most common type of closed bioreactor however, is the TPBR, owing to its high S/V ratio (Molina *et al.*, 2001; Ugwu *et al*., 2008). Tubular Photobioreactors offer several other advantages over other bioreactors and conventional ponds, as they can be erected over any open space, can operate at high biomass concentration and keep out atmosphere contaminants. They also seem to be most satisfactory for producing microalgal biomass on the scale needed for biodiesel production.

Despite the fact that a great deal of work has already been done to develop PBRs for microalgal cultures, more efforts are still required to improve PBR technologies and know-

how of microalgal cultures. Photobioreactor design and development is perhaps, one of the first major steps that should be undertaken for efficient mass cultivation of microalgae (Ugwu *et al*., 2008). In view of their much greater productivity than raceways, PBRs are likely to be used in producing much of the microalgal biomass required for making biodiesel (Ugwu *et al*., 2008). Photobioreactors provide a controlled environment that can be tailored to the specific demands of highly productive microalgae to attain a consistently good annual yield of biomass and lipids (Ugwu *et al*., 2008). Hence the current part of the study focuses on the design and operation of a laboratory scale TPBR that could be utilised for microalgal cultivation.

4.2 Materials and Methods

4.2.1 The photobioreactor system

A pilot-scale TPBR was designed, developed and used for this study (Figure 11, 12 and 13). It consists of a retention tank with a holding capacity of 60 L and the photo array, or the solar collector. The solar collector consists of an array of straight horizontal tubes joined together using 180º bends, and both the inlet and outlet of the solar collector is connected to the retention tank. The solar collector is illuminated by artificial light sources to support microalgal growth and is where the light required for photosynthesis is captured. Both the tank and tubes were constructed using Polyvinyl Chloride (PVC). The retention tank and horizontal tubes are connected using rubber tubing to create a circuit within which the microalgae circulate. The circulation is facilitated by a mechanical pump which propels the microalgae suspension through the array of horizontal tubes and back to the tank at an optimised flow rate of 1.7 m^3/hr. The suspension of microalgae was circulated and propelled periodically through the illuminated part of the PBR (solar collector) and the dark part (retention tank, pump, non-transparent tubes) (Chisti, 2007; Molina *et al.,* 2001). The tubular PBR was operated at ambient temperature (± 25 °C) under 150 µmol $m^{-2}s^{-1}$ light intensity using a 16/8 h photoperiod (light:dark cycle) in a semi-continuous mode. The operational parameters such as pH, Total Dissolved Solids (TDS), temperature, and Dissolved Oxygen (DO) were monitored daily using the YSI 556 multi probe system (YSI Incorporated, Yellow Springs, USA).

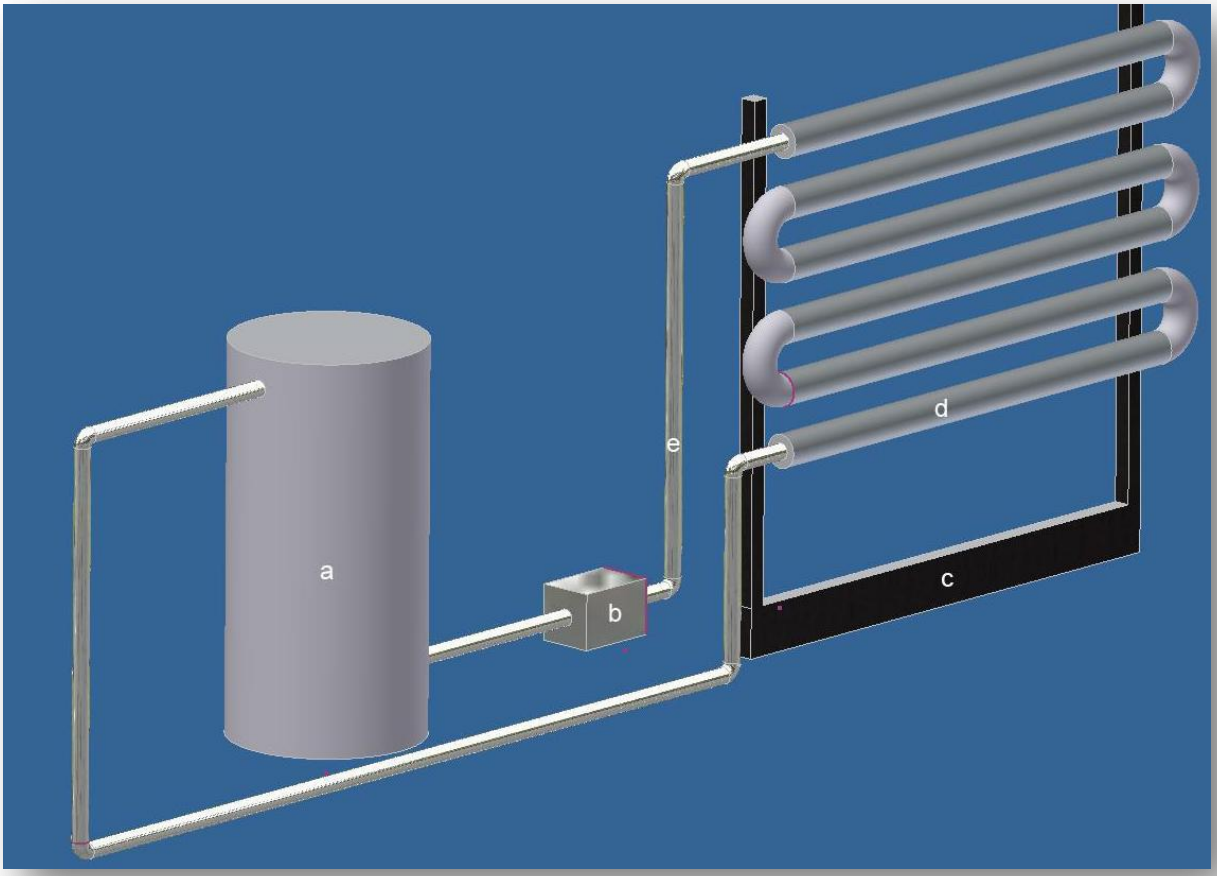

a - Retention tank, b - Mechanical pump, c – Stand for holding photo array,
d- Transparent horizontal tubes, e – Connecting tubes for pump, tank and photo array

Figure 11: Schematic diagram of Tubular Photobioreactor system.

4.2.2 Retention tank

The retention tank (denoted by *a* in Figure 11) has a height of 0.7 m and a diameter of 0.35 m. The output feed is located at 0.05 m from the bottom of the tank whilst the return feed is positioned at 0.05 m from the top of the tank. Before the TPBR commences its continuous cycle the tank serves as the initial store into which the microalgae along with the required nutrients can be added. During a continuous cycle the tank becomes a reservoir, holding a quantity of microalgal broth while it awaits further circulation through the photo array. Oxygen produced by photosynthesis accumulates in the broth and is released from a one-way

outlet fitted on the top of the retention tank. Culture pH was maintained daily by controlled supplementation of CO_2 gas to the retention tank. After a growth cycle has been completed (± 20 days), the tank serves as the harvesting point. Microalgal biomass was harvested by centrifugation (Heraeus Mulitfuge Centrifuge 4KR) at 3000 rpm for 15 min at 4 °C.

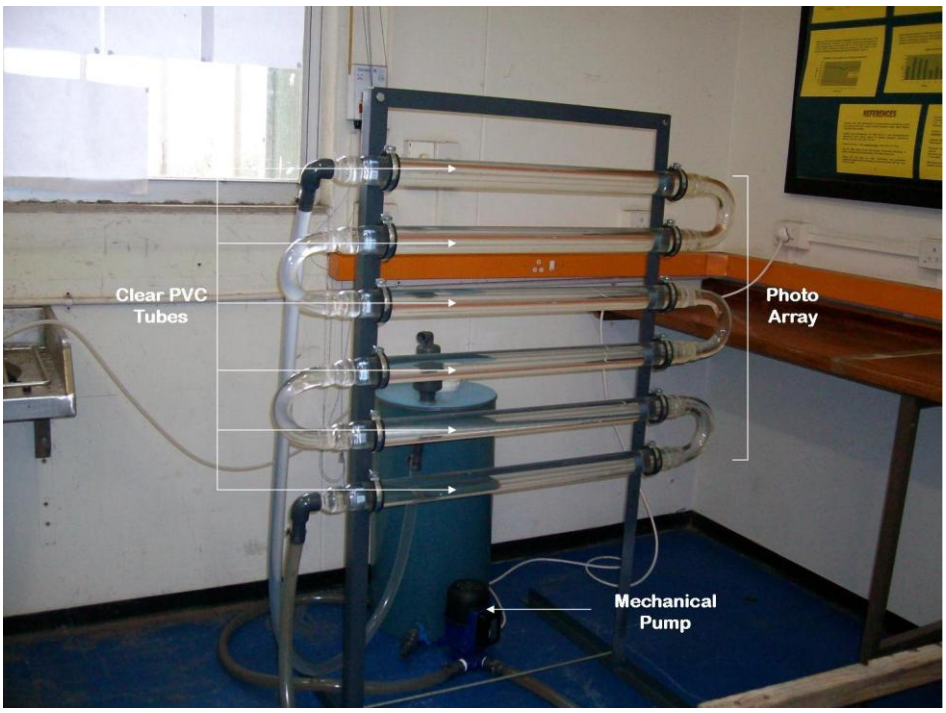

Figure 12: Picture of Tubular Photobioreactor prior to trial runs.

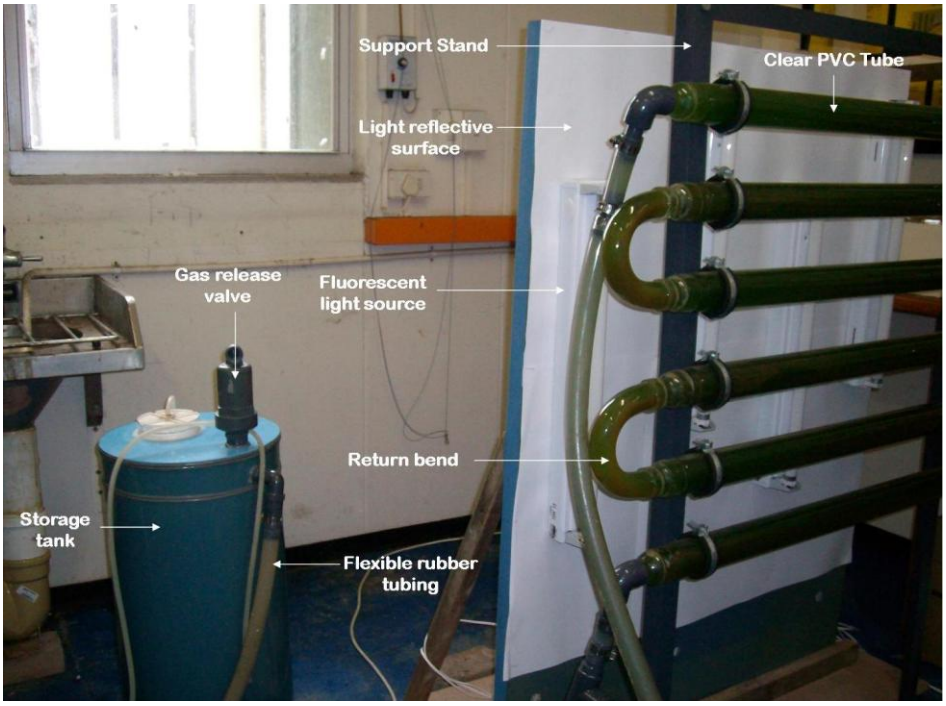

Figure 13: Picture of Tubular Photobioreactor during a trial run.

4.2.3 The solar collector

The solar collector (denoted as *d* in Figure 11) is perhaps the most critical design consideration within the tubular reactor system. The tubes and bends of the solar collector are made of transparent PVC materials, which are permeable to light. A vertical orientation was adopted for the solar collector where the tubes and bends were attached to a support stand (denoted as *c* in Figure 11). Each PVC tube has an outer diameter of 0.06 m and is 0.95 m in length. The 180^{o} bend tubes had an outer diameter of 0.04 m. Collectively the solar collector comprised of six tubes and five 180^{o} bends with total effective surface area and volume being 1.45 m^2 and 0.02 m^3, respectively. This consequently gives the reactor a 72.5 m surface to volume ratio. The distance between two adjacent horizontal tubes were 0.08 m. Sylvania Plant Grow lights were used as light sources as they proved to be the best source of illumination. Eight such lights were utilised, four placed equidistant to each other on either side of the solar collector, providing a light intensity of between 150 to 350 μmols.

4.2.4 Flow characteristics

Flow of the microalgal suspension was induced to be turbulent by the mechanical pump which accelerated fluid flow from the retention tank to a velocity of 0.472 m/sec within the horizontal tubes of the solar collector system. Design parameters such as tube diameter and volumetric flow rate were selected using Reynold's (Re) number in order to ensure a turbulent flow. The dimensionless Reynold's number for this system was calculated using the following equation (Pirt *et al*., 1983):

$$\mathrm{Re} = \frac{D_t \times \rho \times V}{\mu} \qquad (4)$$

Where D_t = diameter of tubes (m), ρ = density of fluid at 25 ^{o}C (kg/m^{3}), V = fluid velocity (m/sec), μ = fluid viscosity at 25 ^{o}C (Pa/s).

4.3 Results and Discussion

Due to the nature of this chapter the results and discussion will be presented together, to improve flow and readability.

The design of this particular TPBR system placed high emphasis on optimisation of culture growth conditions as well as practicality. The type of material used for the photo-stage is of fundamental importance as it must lack toxicity, have high transparency, high mechanical strength, high durability, chemical stability and low cost (Molina *et al.*, 2001). The use of transparent PVC tubes provided the system with an effective yet durable option as it is permeable to light and has a high strength to weight ratio. The retention tank outlet was devised to be at the bottom of the tank to create a pressure difference to initialise fluid flow; whereas the tank inlet at the top ensured that fluid that entered the tank first would be

circulated through the solar collector to ensure cells are exposed to similar photoperiods as well as to ensure that agitation inside the tank enables the microalgae to always remain in suspension. The inclusion of an outlet for O_2 was critical to ensure that O_2 liberated during photosynthetic processes did not reach inhibitory levels. A combination of high O_2 concentration and high light intensity may lead to damage of the cells due to photo-oxidation (Molina *et al.*, 2001). The radius of the tubes had to be selected as a compromise between two conflicting factors; (a) the greater the radius the greater the volume and surface area exposed to light and thus potentially greater biomass yields, (b) light intensity drops to growth limiting levels at a certain depth. In otherwise constant conditions, there is a significant drop in culture productivity as tube diameter is increased (Kobayashi and Fujita, 1997). Hence a radius of 0.06 m was selected as this resulted in a relatively high surface to volume ratio of 72.5 m plus allowing for light to penetrate to almost its entire radial depth. The smaller radius of 0.04 m for the 180^o bend tubes brought about higher fluid velocities to reduce settling on these surfaces due to the higher frictional forces present at these bends. The space of 0.08 m between two adjacent tubes was small enough to ensure a compact solar collector whilst simultaneously large enough to ensure light could be received throughout the tube surface. The tubes of the solar array are arranged horizontally, relative to the light source, as light level is always greater in relatively thin horizontal tubes than they are to their vertical column counterparts. The solar array of the tubular system was orientated vertically which yielded various advantages such as occupation of less ground space by the collector, reduction of photo-inhibition due to exposure to high light intensities and better capture of reflected light under low light intensities (Camacho *et al.*, 1999).

The microalgal broth was circulated turbulently through the reactor system as a turbulent flow has been shown to ensure good mixing which consequently encourages growth of microalgae in tubular bioreactor systems (Scragg *et al.*, 2002). A turbulent flow continuously shuffles cells from less illuminated areas within the tube to better illuminated areas close to the surface ensuring that cells are not deprived of light for prolonged periods of time (Molina *et al.*, 2001). A common problem affecting TPBRs is fouling, where microalgae settle on light permeable surfaces and reduce the amount of light which can penetrate the surface. A turbulent flow regime is sought after as it provides several benefits such as facilitating effective and rapid mixing of the broth which significantly reduces the chance of microalgae

settling on the tube walls and prevents microalgal cells from stagnating in areas of the pipe with little or no light penetration (Molina *et al.*, 2001). The yield of *Chlorella* sp. is known to improve significantly when the flow pattern is shifted from laminar to turbulent (Pirt *et al*., 1983). Fluid in a pipe is assumed to achieve turbulence when the Reynolds number exceeds the value of 2000 (Pirt *et al*., 1983). The Reynold's number for fluid flow within the tubes was calculated to be 10855 using equation (3) with ρ 1000 kg/m^3 and μ = 0.001 Pa/s. A velocity of 0.97 m/sec however causes damage to the culture and reduces biomass productivity (Molina *et al.*, 2001). The Reynold's number for the destructive velocity of 0.97 m/sec for this particular system is 63050. Thus the TPBR's Reynold's number of 10020 is sufficiently turbulent enough for our purposes whilst ensuring there is no damage to the culture.

Microalgal biomass production performance is often restricted by the light energy supplied (Chen *et al*., 2010). As mentioned in chapter three, a light curve was developed by using a Dual-PAM-100 chlorophyll fluorometer. Electron transport rate was then used as an indicator of photosynthetic rates. The photosynthetic rate of the organism under study was recorded at 150 to 350 μmol photons $m^{-2}s^{-1}$. At mid-day, sunlight provides the highest light intensity of ± 5027 μmol photons $m^{-2}s^{-1}$ (Chen *et al*., 2010). This far exceeds the intensity required for efficient growth of the strain under study. Hence, if the *Chlorella* sp. under study was cultivated in an open pond system, photo inhibition would occur due to the excessive amount of light the organism would receive. Hence the organism would not function at its optimal. A closed reactor with artificial lighting therefore, provided the ideal set up for cultivation of this organism, as conditions were controlled, keeping the light intensity between 150 to 350 μmol photons $m^{-2}s^{-1}$. Light intensity within this range was provided by Sylvania Plant Grow fluorescent lights. Fluorescent lamps have been found to distribute light more or less uniformly along the length of the lamp (Kemka *et al.*, 2007). Furthermore, according to Chen *et al*. (2010), the light intensity would decrease exponentially with distance from a reactor wall as the concentrations of both cell and product increase. Hence, the light intensity is likely to decrease rapidly due to light shading effects arising from increases in cell concentrations or from formation of biofilm on the inner surface of the solar collector. In the absence of sufficient light energy, the cellular metabolism mode will switch, and thus both the productivity and biochemical composition of the microalgal cells are affected by the availability of the light (Chen *et al*., 2010). To ensure maximum productivity the distance of

light to solar array was decreased with an increase in cell density. The subsequent chapter will focus on investigating conditions within the designed TPBR in an attempt to increase biomass and enhance lipid concentrations.

Chapter Five: Optimisation of Nutritional Parameters for Maximal Biomass and Lipid Yield of *Chlorella vulgaris* within a Tubular Photobioreactor

5.1 Introduction

Biodiesel, which comprises alkyl esters of long-chain FAs derived from TAGs, has become more appealing recently due to its environmental benefits and the fact that it is made entirely from renewable resources. Due to their many advantages over conventional crops, microalgae are regarded as the feedstock of the future for sustainable biodiesel production (Chisti 2007; Li *et al*., 2008; Liu *et al*., 2008 a and b). Biomass productivity, lipid cell content, and overall lipid productivity are some of the key factors affecting the economic feasibility of microalgal oil for biodiesel production. Process optimisation is, therefore, an important aspect of technology development which could reduce the relatively high costs (Li *et al*., 2008). An ideal process would entail producing lipid at the highest productivity with the highest lipid cell content. However, this is not always attainable due to the fact that high lipid cell contents are usually produced by cells under 'stress' (typically nutrient limitation) which is linked to low biomass productivity and, consequently, low overall lipid productivity (Li *et al*., 2008; Liu *et al*., 2008 b).

The growth kinetics of microalgae is known to have an impact on biomass productivity as well as lipid accumulation in microalgal cells: microalgal growth rates affect lipid accumulation rate, and the nutrient condition determines the biomass and lipid productivity in addition to the lipid content of the microalgal biomass (Goldberg and Cohen, 2006; Rodolfi *et al*., 2009). Research on oil production from photosynthetic microalgae has largely focused on the search for species with high oil content. Species, however, with the highest oil contents grew most slowly, resulting in low rates of oil production (Lv *et al*., 2010). On the contrary, *Chlorella* strains are now been considered as promising candidates for commercial lipid production due to their rapid growth and easier cultivation (Lv *et al*., 2010). Significant increases in lipid content of 40% could also be attained in *C. vulgaris* by nutrient deprivation (Illman *et al*., 2000).

All organisms are known to possess a minimum, optimal and maximum requirement with regards to their growth variables. Growing a microalga at its optimal temperature, light intensity, nutrient concentrations and CO_2 levels will lead to significant increases in the biomass yield. Microalgae react differently to nutrient supply concentrations based on their allowance flexibility. To ensure high growth rates the optimal supply of nutrients like N, P and C is essential (Grobbelaar, 2009). Microalgae require a carbon source which is usually either dissolved CO_2 or HCO_3. An energy source is required to stimulate microalgal growth. Light intensity plays an important role in both mass culture and lipid content of microalgae. (Pulz, 2001; Grobbelaar, 2009; Lv *et al*., 2010). For example, a growth rate of 0.04 h^{-1} and lipid content of 44 to 47% were achieved for *Skeletonema costatum* under 50 and 100 µmol photons m^{-2} s^{-1} whereas 0.01 h^{-1} and 35–40% were obtained under 20 or 400 µmol photons m^{-2} s^{-1} due to the light inhibition (Blanchemain and Grizeau, 1996).

Growth in a PBR generally entails autotrophic growth together with plant growth nutrients, especially the macro and micronutrients, and in some cases vitamins. Temperature and pH should be within the toleration range of the cultured microalga (Grobbelaar, 2009). The pH regimes affect the physiology of cells and hence growth rates and biomass production (Ogbonda *et al*., 2007). Temperatures should generally range between 20 and 30 °C to support the growth of *Chlorella* sp. (Chisti, 2007).

Microalgae normally contain three kinds of organic substance: protein, carbohydrate and natural lipid. The cessation of microalgal cell division can be observed under environmental pressure and the synthesis of CO_2 is switched to lipid as storage of energy. The lipid content of the microalgal biomass therefore increases (Goldberg and Cohen, 2006; Rodolfi *et al*., 2009). Nutrient limitation (more specifically nitrate limitation) can be an efficient environmental pressure to increase lipid accumulation (Goldberg and Cohen, 2006; Rodolfi *et al*., 2009). Nitrogen limitation, for example, would cause three changes (Goldberg and Cohen, 2006; Rodolfi *et al*., 2009):

(1) Decreasing the cellular content of the thylakoid membrane,
(2) Activation of acyl hydrolase and,
(3) Stimulation of phospholipid hydrolysis.

An increase in the intracellular content of FA acyl-CoA is often linked to these changes. Meanwhile, nitrogen limitation could also activate diacylglycerol acyltransferase, which converts acyl-CoA to TAG. As a result, nitrogen limitation could increase both the lipid and TAG content in microalgal cells.

The optimisation study was carried out by batch culture of the selected *C. vulgaris* strain within a TPBR. Harvesting of biomass was done when maximum lipid yields were obtained. The effects of different nutritional conditions on biomass production and lipid yield of this particular *Chlorella* sp. was studied to ascertain whether this strain could serve as a promising source of microalgal oil for biodiesel production.

5.2 Materials and Methods

5.2.1 Chemicals and reagents

Nile Red (99% pure) was purchased from Sigma. All other solvents (analytical grade) where purchased from either Merck (SA), Polychem supplies (SA) or Lasec (SA).

5.2.2 Microscopy

Microalgal cultures were viewed using the Nikon eclipse 80*i* microscope under 1000X magnification. Images were taken with a Nikon digital sight ds-ui camera (Nikon incorporation Japan).

5.2.3 Biomass and lipid optimisation

Experiments were carried out in a TPBR (as described in chapter four), operating in semi-continuous mode, that was fed with 40 L synthetic BG11 medium at each trial run. To investigate the effect of $NaNO_3$ concentration on cell growth and lipid accumulation of *C.*

vulgaris within a closed system, various $NaNO_3$ cycles were evaluated. Modified BG11 media containing 3.8, 5, 6.3, 7.5 and 8.8 g l^{-1} $NaNO_3$, represented as run 1, 2, 3, 4 and 5 respectively were tested to maximise biomass production. These nitrate concentrations were selected based on preliminary results (Chapter three), were, the most favorable biomass production at a shake flask level occurred at a nitrate concentration of 5 g l^{-1}.

For lipid accumulation experiments BG11 media was modified with the following $NaNO_3$ concentrations: 7.5, 3.8, 1.8, 1.5, 0.9, 0.5, 0.2 and 0 g l^{-1}, represented as run 6, 7, 8, 9, 10, 11, 12 and 13 respectively.

The experimental conditions were as follows: initial cell concentration of 0.1 g l^{-1}, reactor operating at a temperature of ± 25 °C, photon flux density of 250 µmol$m^{-2}s^{-1}$, a pH of 6 to 8, and a daily injection of 4% CO_2. Cell concentration was routinely monitored and tests were carried out in triplicate. Experimentation was carried out in triplicate and the data were statistically analysed using the SPSS version 15.0 software.

5.2.4 Analytical methods

5.2.4.1 Determination of biomass yield

The microalgal density was routinely determined by measuring the OD of samples at 686 nm (OD_{686}) using a Spectrophotometer (SpectroquantR Pharo 300, Merck USA). Biomass concentration was then calculated by multiplying OD_{686} values with 0.8, which is a predetermined conversion factor converting the OD_{686} value to DCW. The conversion factor was established by plotting OD_{686} versus DCW of a series of samples of different biomass concentrations (Li *et al*., 2008). Spectrophotometric determinations of biomass were periodically verified by DCW measurements. A 50 ml sample was centrifuged (Heraeus multifuge centrifuge 4KR, USA) at 1509 x g for 15 min at 4 °C. The supernatant was discarded and the pellet was washed with distilled water and 0.05 M HCL to remove non-biological adhering materials such as mineral precipitates, and then dried at 60 °C for 24 h. Growth kinetics of the selected microalgal strain was determined using spectrophotometeric data and biomass yields.

5.2.4.2 Monitoring of operational parameters

Operational parameters within the TPBR such as pH, TDS, temperature and DO were monitored daily during the biomass optimisation experiments using the YSI 556 multi probe system (YSI Incorporated, Yellow Springs, USA).

5.2.5 Lipid analysis

5.2.5.1 NR staining and fluorescent microscopy

Nile Red is prepared by dissolving the NR dye in acetone to give a final concentration of 250 mg l^{-1} (Lee *et al*., 1998). The solution was stored in dark amber glassware and stored away from light.

Qualitative estimation of lipids was done using NR staining as per the protocol described by Greenspan *et al.* (1985). A 3 ml sample of microalgal culture was stained with 30 µL of NR solution. The cells were incubated for 20 to 45 min (Gao *et al*., 2008) to get maximum penetration and to disperse the cells uniformly. Slides were viewed under the oil immersion objective (1000X magnification) using the fluorescent microscope (Zeiss microscope; Ziess, Germany) under blue light (450 to 500 nm wavelengths) as excitation light. The microscope was equipped with an image capturing device and analysis software (AxioCam MRC, Ziess, Germany). Fluorescent microscopy was conducted to determine intracellular lipid content semi-qualitatively. The Olympus image software, version 5.0, was used to determine the lipid area (yellow) relative to the whole cell area and qualitatively determine the lipid % present within the microalgal cells. Total fluorescence for all NR staining droplets within a region was calculated as the product of area multiplied by mean fluorescence. The lipid content was expressed as the % lipid per cell, as this was determined by microscopic area measurements (Elsey *et al*., 2007; Huang *et al*., 2009).

5.2.5.2 Lipid extraction

Microalgal cells were harvested from culture suspension at the end of the stationary phase by centrifugation at 3000 rpm for 15 min at 4 ^{o}C. Supernatant was decanted and cell pellets were washed with distilled water and then freeze-dried at -80 ^{o}C. Thereafter, cells were subjected to Soxhlet extraction, for lipid cell content measurement using the procedure from a modified method of Bligh and Dyer (1959). Fifty milligrams of lyophilized microalgal biomass was placed into a test tube and 1.6 ml distilled water, 4.0 ml methanol and 2.0 ml chloroform were added. The solution was vortexed for 30 s. Subsequently, an additional 2.0 ml of chloroform and 2.0 ml distilled water were added and the content of the test tube was further vortexed for 30 s. The test tubes were centrifuged at 3000 rpm for 15 min at 4 ^{o}C. The upper layer was withdrawn using a pipette and the lower chloroform phase containing the extracted lipids was transferred into a clean culture tube. The solid material which remained at the bottom of the extraction tube was extracted with the same procedure two more times and the chloroform phases were mixed together and then evaporated to obtain dry lipid. Thereafter, the total lipids were measured gravimetrically, and the lipid content and lipid yields determined. Lipid productivity was calculated according to the equation described by Li *et al.*, 2008:

$$\textit{Lipid Productivity (g } l^{-1} \textit{ day } ^{-1}\textit{) = lipid (g/g) x DCW (g/l) / Time (day)} \quad (5)$$

The final phase of the research entailed the semi-quantitative analysis of the lipids using GC. A free FA phase column was used (ZPFFAP). Operating conditions for the GC HP5890 were as follows: temperature programme at 200 °C (held for 2 min), ramp rate of 5 °C/min, and a final temperature of 240 °C (held for 5 min). The external standard method was used to quantify the lipids present in the samples. All samples were run under the same conditions.

5.3 Results

5.3.1 Biomass optimisation study

Figure 14 shows representative growth curves for the *C. vulgaris* strain under elevated $NaNO_3$ concentrations. From this figure, five well defined growth phases can be recognised: (A) lag phase; (B) exponential growth phase; (C) linear growth phase; (D) stationary growth phase; and (E) death phase. As can be seen in Figure 14, growth occurred at all $NaNO_3$ cycles. A steady increase in growth was observed between days 1 to 11. For all $NaNO_3$ concentrations, after a maximum residence time of 11 days, the growth curves indicated characteristics of the stationary phase. Maximum cell densities were obtained during this period. Day 18 was followed by a considerable reduction in growth, eventually leading to the decline or death phase of the culture.

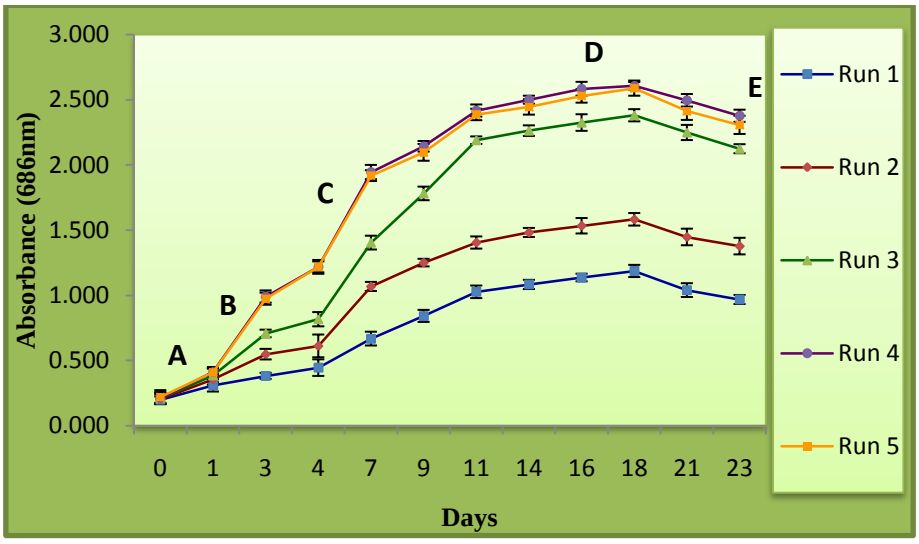

Figure 14: Time-course profiles of cell growth acquired with elevated $NaNO_3$ concentrations. (A) lag phase; (B) exponential growth phase; (C) linear growth phase; (D) stationary growth phase; and (E) death phase.

Table 6: Time-course profiles of dry cell weight readings (in g l^{-1}) at elevated $NaNO_3$ concentrations.

Days	Run 1	Run 2	Run 3	Run 4	Run 5
0	0.16	0.16	0.17	0.17	0.18
1	0.25	0.28	0.31	0.33	0.33
3	0.31	0.44	0.57	0.79	0.78
4	0.36	0.49	0.65	0.97	0.97
7	0.53	0.85	1.12	1.56	1.53
9	0.67	1.00	1.43	1.71	1.68
11	0.82	1.12	1.75	1.93	1.91
14	0.87	1.19	1.81	2.00	1.96
16	0.91	1.23	1.86	2.07	2.02
18	0.95	1.27	1.90	2.09	2.04

Table 6 shows DCW values at the various elevated $NaNO_3$ concentrations over a period of 18 days. Biomass increased uniformly for all trial runs, with the highest reading been obtained on day 18. Results suggest that the optimal $NaNO_3$ concentration for cell growth was around 7.5 g l^{-1}(trial run 4), yielding maximum biomass of 2.09 g l^{-1} on day 18 (shown in Table 6). Trial run 4 was closely followed by trial run 5 (which contained 8.8 g l^{-1} $NaNO_3$) which yielded a biomass of 2.04 g l^{-1} on day 18. The lowest $NaNO_3$ cycle (of 3.8 g l^{-1}) yielded a biomass value of 0.95 g l^{-1} at an OD of 1.178.

Table 7: Operational parameters within Tubular Photobioreactor during biomass optimisation studies.

Day	Run 1			Run 2			Run 3			Run 4			Run 5		
	DO	**TDS**	**PH**	**DO**	**TDS**	**PH**	**DO**	**TDS**	**PH**	**DO**	**TDS**	**PH**	**DO**	**TDS**	**PH**
0	4.867	6.300	6.240	4.913	6.907	6.637	5.073	8.790	6.693	5.210	10.873	7.800	5.013	12.893	6.283
1	4.913	6.423	6.500	5.073	7.138	6.477	5.187	9.090	6.887	5.553	11.240	7.607	5.457	13.023	6.687
4	5.057	6.493	6.447	5.437	7.390	6.170	6.380	9.657	6.690	6.617	11.910	7.310	6.847	13.503	7.150
7	5.103	6.927	6.847	4.833	7.867	6.310	5.940	10.120	7.150	7.827	12.643	7.680	7.393	13.840	7.437
10	4.930	7.040	6.623	5.627	8.417	6.613	6.720	11.097	7.273	6.860	13.083	6.787	6.827	13.943	6.763
13	4.810	7.148	7.143	4.417	8.650	6.450	5.620	11.483	7.327	7.580	13.583	6.323	7.323	14.230	7.673
16	5.627	7.193	6.130	5.323	8.817	6.695	5.420	11.740	6.153	6.417	13.840	6.627	7.057	14.657	6.527
19	4.447	7.230	6.890	5.263	8.990	6.857	6.377	11.943	6.613	7.267	14.040	7.393	6.837	14.930	7.840

The amount of DO present gradually increases during the first 7 days of growth in Runs 1, 4 and 5. For Runs 2 and 3, increases in DO were observed during the first 4 days of growth, thereafter, fluctuations were observed. During this period the amount of DO present was approximately 6.22 mg l^{-1} (average of trial runs 1-5). Dissolved oxygen values present across the various trial runs peaked at various periods. Throughout all runs the value of TDS constantly increased with time. pH levels was maintained between 6.2 and 7.8 although fluctuations occurred throughout the study period.

5.3.2 Lipid optimisation

Figure 15 shows the growth kinetics of *C. vulgaris* at $NaNO_3$ concentrations below its optimal requirement of 7.5 g l^{-1}. At $NaNO_3$ concentrations below 7.5 g l^{-1}, OD (Figure 14) and biomass (Table 7) values were drastically reduced. Even though the cells were in nitrate-free medium in trial run 13, a slow biomass growth of 0.33 g l^{-1} was observed on day 18.

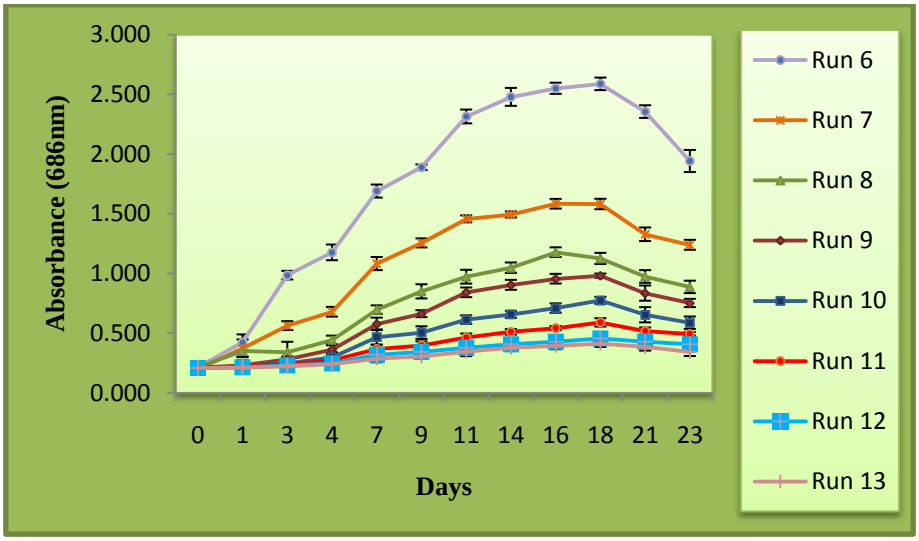

Figure 15: Time-course profiles of cell growth acquired under conditions of $NaNO_3$ limitation.

Table 8: Time-course profiles of dry cell weight values (in g l^{-1}) under conditions of $NaNO_3$ limitation.

Days	Run 6	Run 7	Run 8	Run 9	Run 10	Run 11	Run 12	Run 13
0	0.17	0.16	0.17	0.17	0.16	0.17	0.17	0.17
1	0.34	0.30	0.28	0.18	0.17	0.17	0.17	0.17
3	0.79	0.45	0.27	0.23	0.20	0.19	0.19	0.18
4	0.94	0.54	0.35	0.29	0.24	0.22	0.20	0.19
7	1.35	0.87	0.56	0.46	0.37	0.29	0.25	0.23
9	1.51	1.00	0.68	0.53	0.40	0.32	0.27	0.24
11	1.85	1.16	0.78	0.67	0.49	0.37	0.30	0.28
14	1.98	1.19	0.84	0.72	0.53	0.41	0.33	0.30
16	2.04	1.27	0.94	0.76	0.57	0.43	0.34	0.32
18	2.07	1.26	0.90	0.78	0.62	0.47	0.37	0.33
21	1.88	1.06	0.78	0.67	0.52	0.41	0.34	0.31
23	1.55	0.99	0.71	0.60	0.47	0.39	0.33	0.27

The lipid content analysis as shown in Figure 16, revealed that the microalga did not accumulate significant amounts of lipids at $NaNO_3$ concentrations beyond 1.5 g l^{-1}(trial run 6 to 9), and the largest lipid fraction occurred when $NaNO_3$ concentration in the medium was 0.5 g l^{-1}(trial run 11). In the absence of $NaNO_3$, 36.36% lipid was produced. This was a 3.75% difference in results when compared to trial run 11 which yielded 40.11% lipid. Lipid productivity was calculated using equation (4), and it was shown that trial run 6 gave a slightly higher value of 0.024 g l^{-1} day^{-1} when compared to trial run 10 which yielded a productivity of 0.011 g l^{-1} day^{-1}. Trial run 10 however, yielded 12.69 % more lipid when compared to trial run 6.

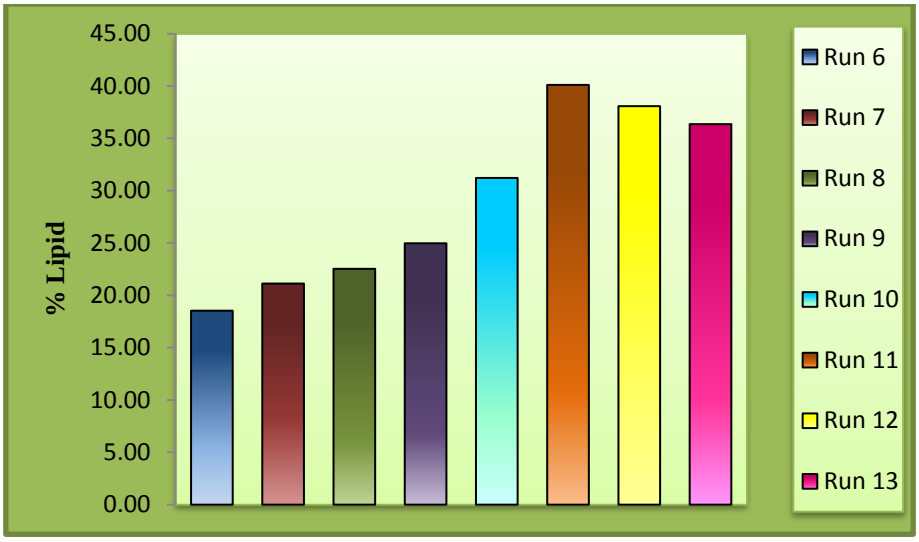

Figure 16: Lipid content obtained at the end of the stationary phase during conditions of $NaNO_3$ starvation.

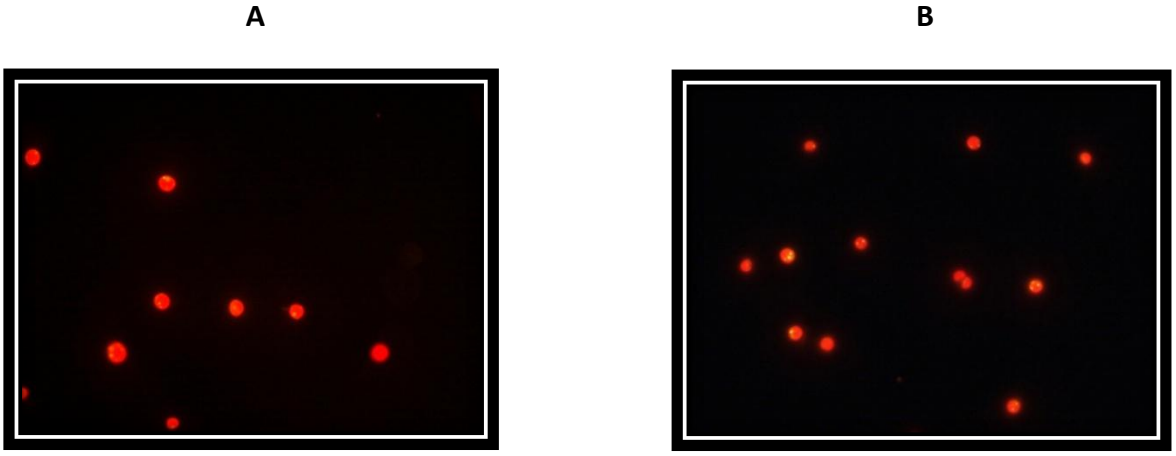

Figure 17: Micrographs of *C. vulgaris* during trial run 6 which contained 7.5 g l^{-1} $NaNO_3$ viewed at 1000X using a fluorescence microscope at 490 nm excitation and 585 nm emission filters.

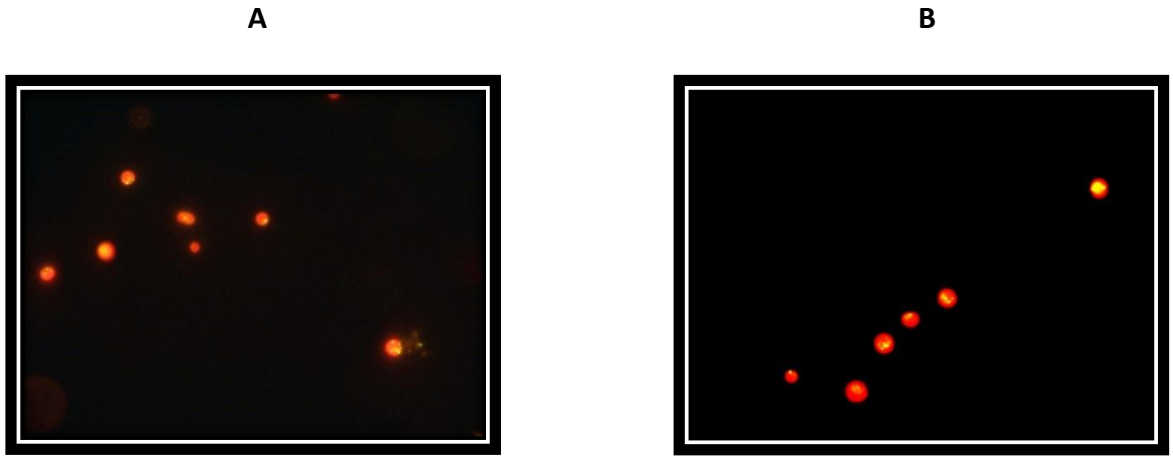

Figure 18: Micrographs of *C. vulgaris* during trial run 7 which contained 3.8 g l^{-1} $NaNO_3$ viewed at 1000X using a fluorescence microscope. Small neutral lipid globules are present in the cytosol and are stained yellow.

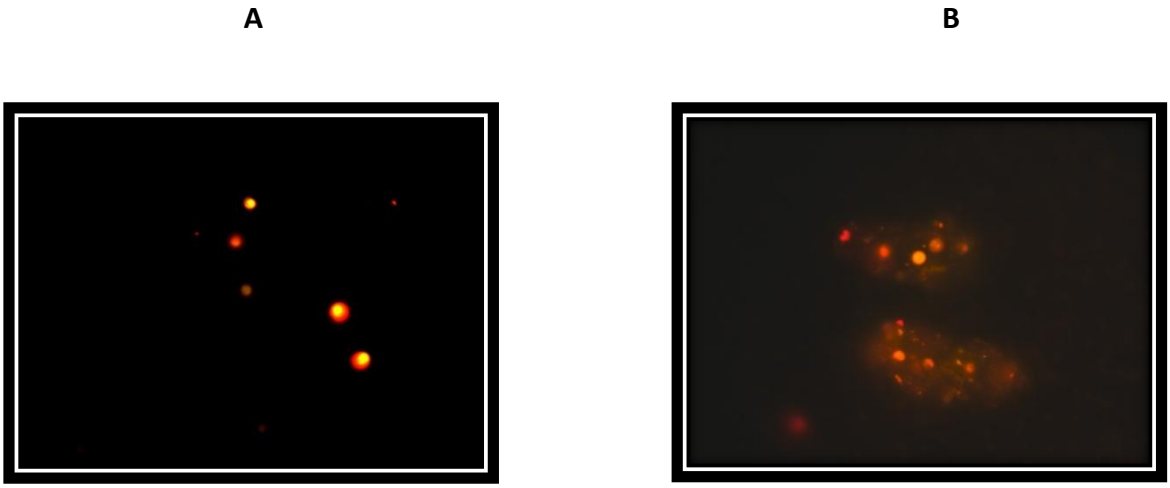

Figure 19: Micrographs of *C. vulgaris* during trial run 8 which contained 1.8 g l^{-1} $NaNO_3$ (1000X).

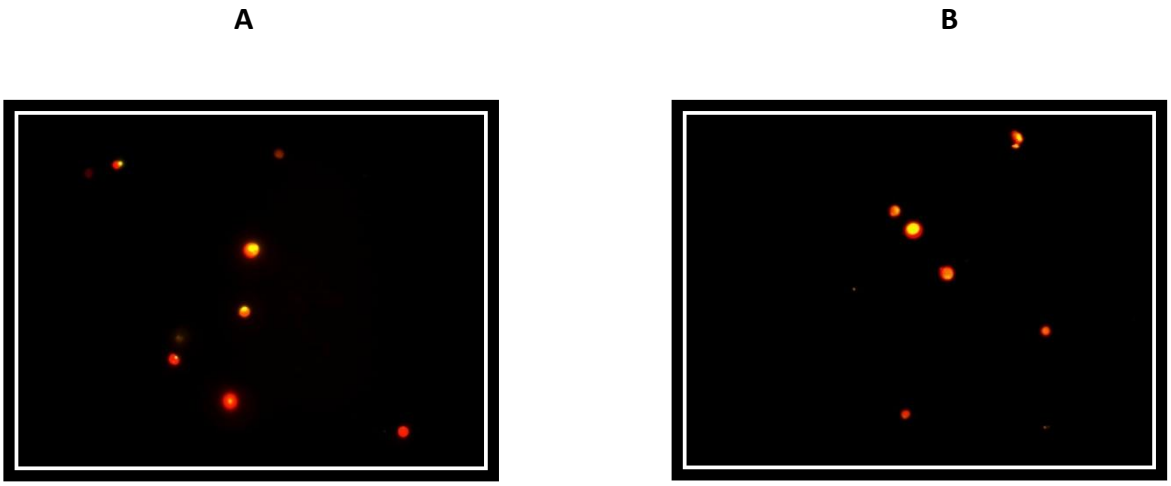

Figure 20: Micrographs of *C. vulgaris* during trial run 9, containing 1.5 g l^{-1} $NaNO_3$ (1000X).

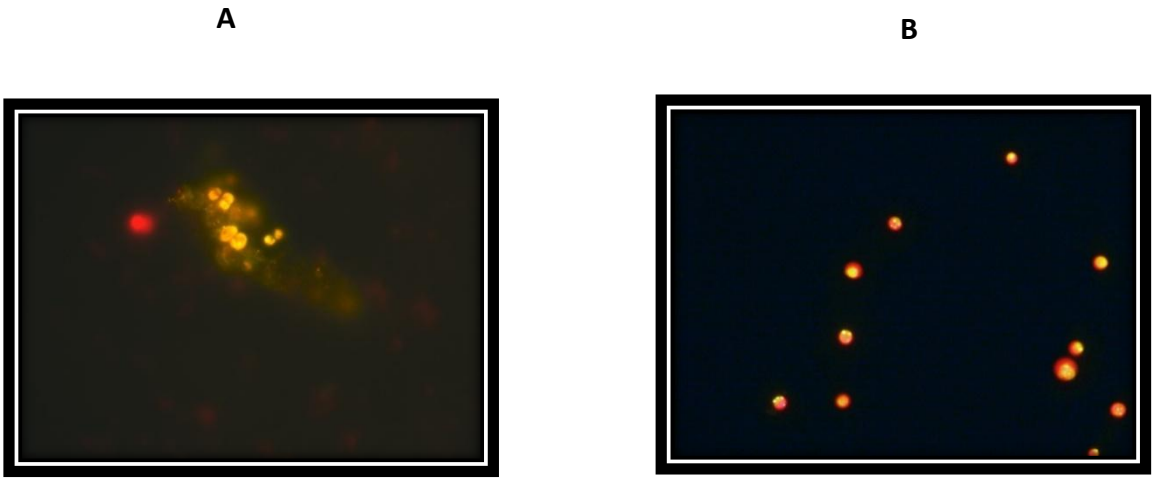

Figure 21: Micrographs of *C. vulgaris* during a $NaNO_3$ cycle of 0.9 g l^{-1} during trial run 10 (1000X). Neutral lipid globules present in the cytosol are stained yellow.

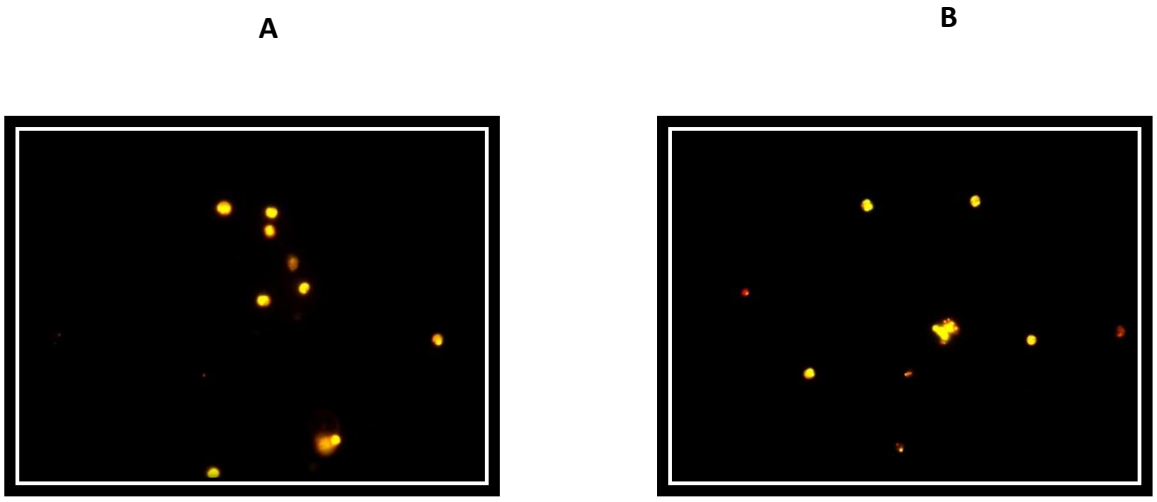

Figure 22: Micrographs of *C. vulgaris* during a $NaNO_3$ cycle of 0.5 g l^{-1} during trial run 11, viewed at 1000X magnification using a fluorescence microscope at 490 nm excitation and 585 nm emission filters. An increase in neutral lipid globules can be seen in the cytosol. These are stained yellow.

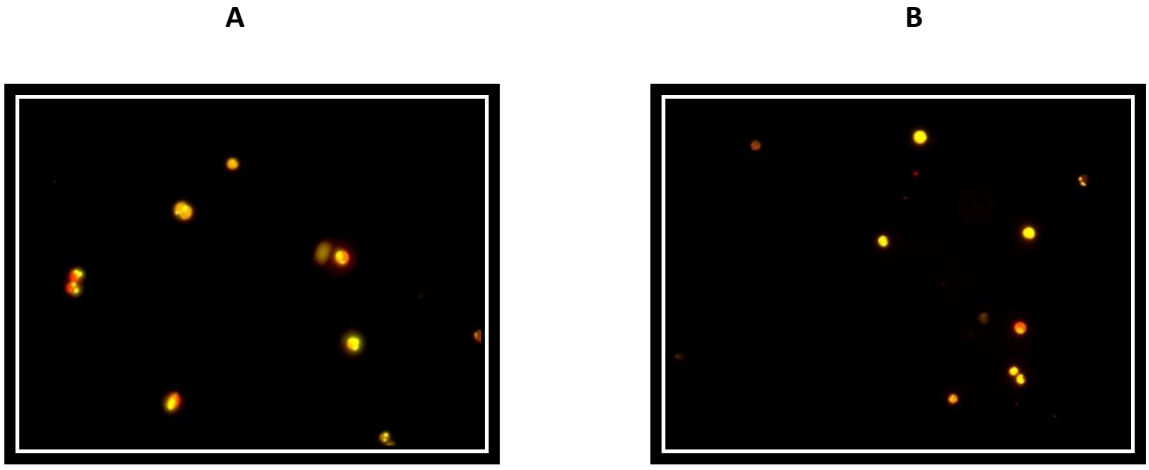

Figure 23: Micrographs of *C. vulgaris* during trial run 12 which contained 0.2 g l^{-1} $NaNO_3$ viewed using a fluorescence microscope at 1000X magnification.

A B

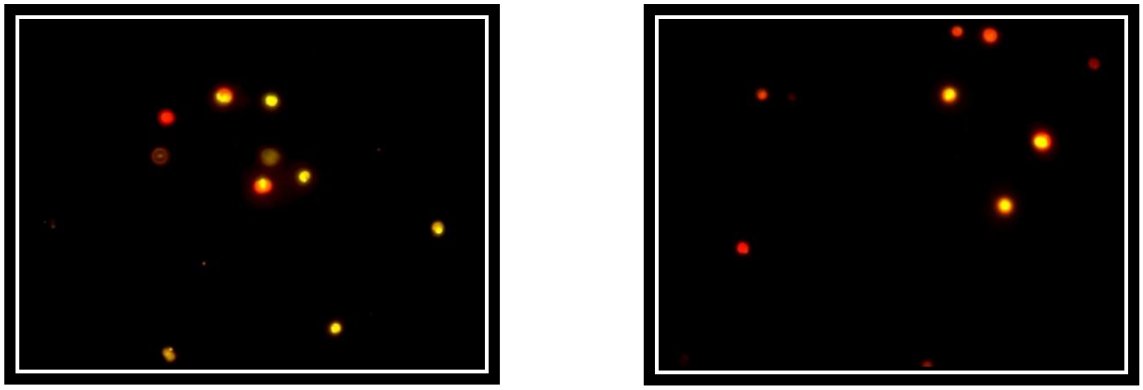

Figure 24: Micrographs of *C. vulgaris* during trial run 13 which contained no $NaNO_3$, viewed at 1000X using a fluorescence microscope at 490 nm excitation and 585 nm emission filters.

Table 9: Lipid percentages per cell area.

$NaNO_3$ cycles	Lipid content, % (A)	Lipid content, % (B)
Run 6	20.76	19.41
Run 7	23.67	22.17
Run 8	27.57	26.83
Run 9	30.37	29.61
Run 10	37.22	36.31
Run 11	55.66	59.62
Run 12	52.74	51.05
Run 13	39.71	42.12

Polar lipids (i.e., phospholipids) which are mostly present in membranes are stained in red, whereas neutral lipids (triglycerides) which are present in lipid droplets are stained in yellow.

The reduction of nitrate concentration in BG11 medium increased the lipid fraction as can be observed from the micrographs above (Figures 17 to 24 and Table 9). Micrographs of *C. vulgaris* revealed that a greater amount of neutral lipid per cell volume was present in trial runs 10 to 13, when compared to trial runs 6 to 9. Trial run 11 possessed the highest neutral lipid per cell volume, giving a lipid percentage of 57.64 (average of pictures A and B).

5.3.3 Gas chromatogram analysis

Different types of saturated FAs were detected in the investigated *C. vulgaris* strain, with butyric and palmitic acid making up most of the FA composition. Undecanoic, lauric and tridecanoic acids were also identified. Figure 26 shows that none of the known standards (Figure 25) could be identified in trial run 6 (Appendix C) which contained 7.5 g l^{-1} $NaNO_3$. Two known lipids were identified in trial run 7 (Appendix D), namely: butyric and palmitic acid which gave a total lipid % of 2.8. Trial run 8 (Appendix E) which had a $NaNO_3$ concentration of 1.8 g l^{-1} yielded the highest number of lipids. However, even though a greater number of known lipids were produced in trial run 8, the total lipid % (10.488%) was much lower when compared to trial runs 9 to 13 (Appendix F-J). Trial run 10 (Appendix K) produced 3 lipids (butyric, lauric and palmitic acid), which gave a total lipid % of 20.2. The highest lipid % was obtained in trial run 11 (Appendix H) (37.586%), even though a lower number of lipids were produced (butyric and lauric acid). Both trial runs 12 and 13 (Appendix I and J respectively) which contained considerably lower $NaNO_3$ concentrations (of 0.2 and 0 g l^{-1} respectively) showed evidence of butyric, lauric and palmitic acid.

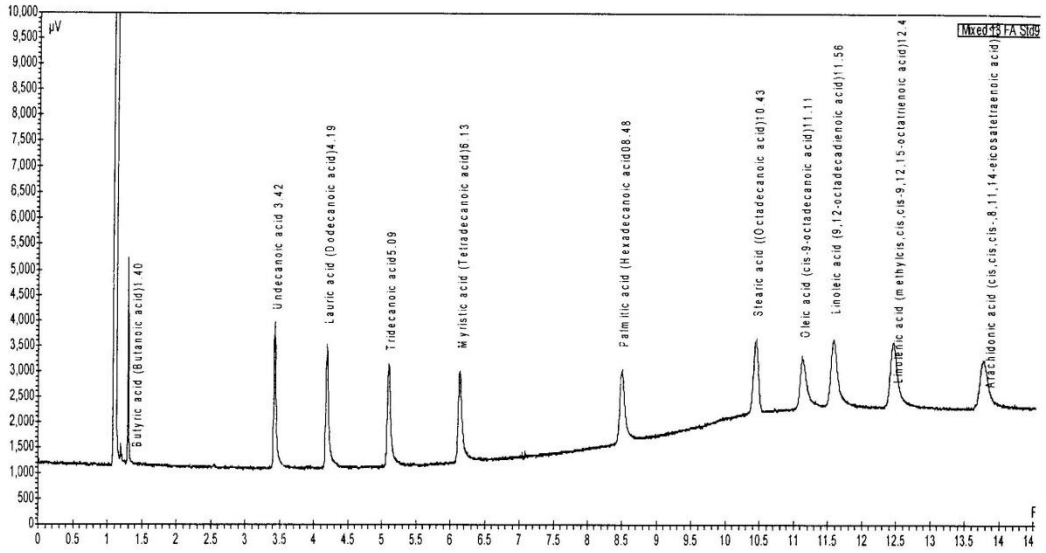

Figure 25: Gas chromatogram showing mixed standard which comprised 11 known fatty acids.

Figure 26: Lipid percentages obtained from gas chromatograms during different $NaNO_3$ concentrations.

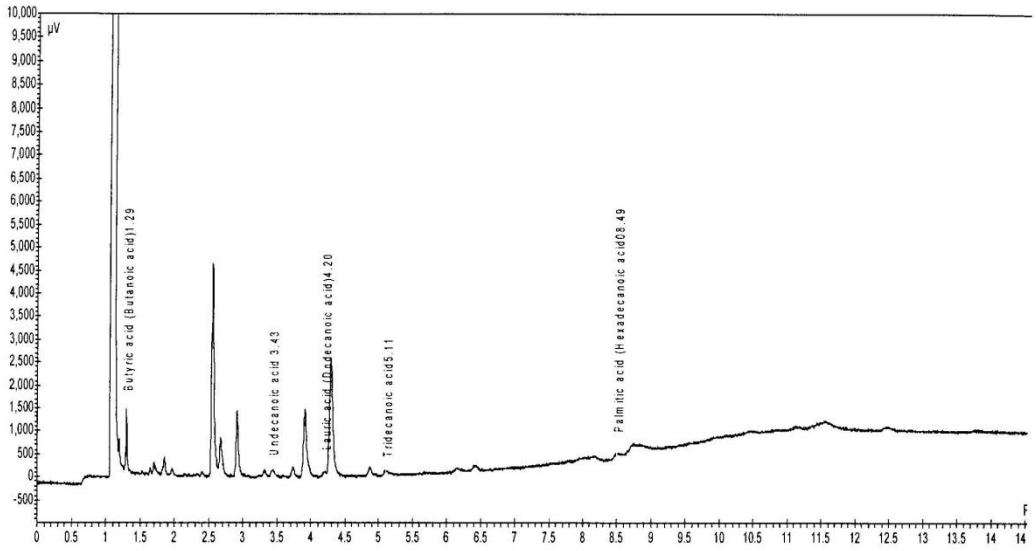

Figure 27: Gas chromatogram of trial run 8 which produced the most known lipids.

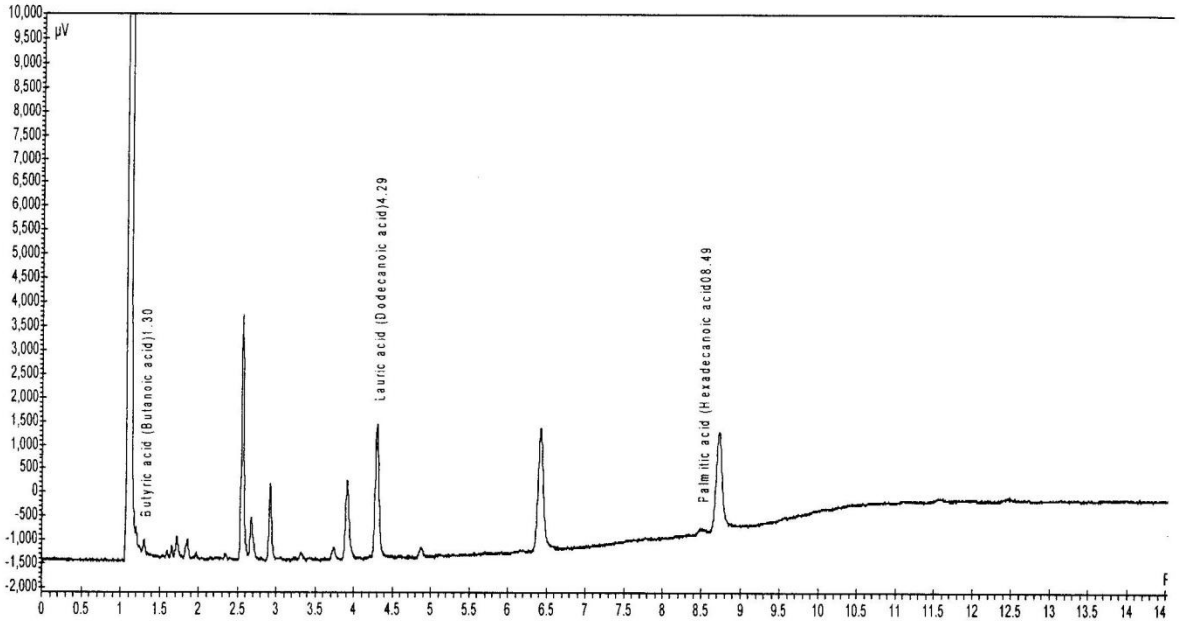

Figure 28: Gas chromatogram of trial run 10, the likely candidate for the optimal trade-off between maximising biomass and lipid yield.

5.4 Discussion

Microalgal growth rate and lipid content are the two most important parameters of microalgae. Growth rate and lipid content conflict with each other as lipid accumulation is likely to occur with nutrient depletion which happens when the growth rate slows (Goldberg and Cohen, 2006). Thus a trade-off must be established between growth rate and lipid content (Goldberg and Cohen, 2006).

Growth of *C. vulgaris* improved notably when the $NaNO_3$ concentration increased from 3.8 to 7.5 g l^{-1} (Figure 14 and Table 6). Statistic analysis (Pearson's correlation) revealed that a almost perfect correlation was observed between the physiochemical parameters and cell growth (R square = 0.87). In order to obtain maximal biomass productivity, there is an optimal duration for biomass harvesting (Pruvost *et al*., 2009). For all the conditions investigated in the present study, biomass appeared to be at a maximum on day 18. Run 4 showed a significant 2.2 fold increase in biomass ($p < 0.005$) when compared to results achieved at the lowest $NaNO_3$ cycle (of 3.8 g l^{-1}). Li *et al*. (2008) showed that the optimal $NaNO_3$ concentration for cell growth of the microalga *N. oleoabundans* was around 0.85 g l^{-1}. Although trial run 5, which contained the highest $NaNO_3$ concentration (of 8.8 g l^{-1}), did not produce the highest DCW value, the value obtained was very close to that of trial run 4. Li *et al.* (2008) recognized that a $NaNO_3$ concentration of 0.85 g l^{-1} or higher seemed to be inhibitive to cell growth of *N. oleoabundans*. Goleuke *et al*. (1967) established that an excess of nitrate could prove toxic, leading to a decline in microalgal population.

Quantity of DO present closely relates to biomass growth within microalgal PBRs. This factor coupled with light dynamics, are one of the most critical factors which affect microalgal growth processes. Photosynthetic production of microalgae is always accompanied by evolution of O_2 and consumption of CO_2 (Rubio *et al*., 1999). Dissolved O_2 as well as TDS present within the TPBR were measured so that a correlation could be established between these levels and biomass growth. Total Dissolved Solids within the TPBR comprised of the microalgal biomass as well as substrate.

Dissolved oxygen values for all the trial runs peaked around day 10 (Table 7). This could be attributed to the rapid growth that occurred due to high occurrences of photosynthetic processes. The level of DO decreases due to the respiratory processes that can be approximately considered as an inverse process to photosynthesis - releasing CO_2 while taking up O_2 and consuming energy rich storage compounds to support growth of the organism (Weissman *et al.*, 1988). Hence there is indication that high levels of DO seems to inhibit biomass growth processes. This observation can be attributed to the fact that high DO concentration in combination with high light exposure can be toxic to cells, because O_2 radicals can be generated which promote photo inhibition (Rubio *et al*., 1999). According to Molina *et al*. (2001) DO needs to be maintained at levels below 10 mg l^{-1} within closed PBRs as levels exceeding this value are reported to lead to photosynthetic inhibition. During the experiment, it was observed that the DO of the medium varied from 5.800 to 7.050 mg l^{-1} (<110% air saturation). This demonstrates the effectiveness of the O_2 release valve which is responsible for limiting the accumulation of O_2 within the retention tank. Total Dissolved Solid measurements corresponded to the DO responsive growth pattern with peaks being achieved around day 13 for all runs. These increases in TDS were due to rapid growth of biomass which occurred. Similarly as was observed from the biomass readings, these peaks were preceded by lower levels of DO which provided conditions that were conducive for cellular growth.

The final objective of the research was to maximise the lipid content of the microalgae by subjecting it to conditions of $NaNO_3$ limitation. As shown in Figure 15 and Table 8, $NaNO_3$ limitation resulted in biomass growth been progressively reduced, and lipid accumulation was triggered (Figure 16 to 24; Table 9). This corresponds to work done by Pruvost *et al*. (2009), who explained that nitrogen starvation induces several physiological changes in microalgae, which leads to an alteration in the intracellular composition and growth kinetics. A reduction in biomass growth (shown in Figure 15 and Table 8) under conditions of $NaNO_3$ limitation could be attributed to the fact that nitrate plays a central role in cell physiology and growth (Sorensen *et al*., 1996; Changdong and Azevedo, 2005;). Under nitrate limitation, biomass growth is partly supported by an intracellular storage of nitrogen which is progressively remobilised for growth (Pruvost *et al*., 2009).

Even though nitrate deficiency clearly inhibits the cell cycle as shown in Figure 15 and Table 8, the rate of lipid synthesis remains higher, which leads to the accumulation of oil in starved cells (as shown in Figure 15) (Rosenberg *et al*., 2008). Results presented suggest that the optimal trade-off between maximising biomass and lipid content occurs at 0.9 g l^{-1} $NaNO_3$ (trial run 10) among the tested conditions. However, total lipid productivity was calculated as it is a more accurate measurement being the global result of total cell lipid content, biomass growth, and time of cultivation (Pruvost *et al*., 2009). Trial run 6 gave a slightly higher lipid productivity value when compared to trial run 10. This could be attributed to the fact that on day 16, trial run 6 produced the highest biomass (2.04 g l^{-1}) but the lowest lipid (18.53%). On the contrary, trial run 10 produced 0.57 g l^{-1} of biomass on day 16, but a significantly higher lipid content of 31.22 % when compared to trial run 6 ($p < 0.005$). A lipid productivity of 0.013 g l^{-1} day^{-1} was obtained from a *C. vulgaris* strain on day 20 of incubation during a nitrate depletion study by Widjaja *et al*. (2009). They suggested that higher lipid productivity could be obtained by varying not only the normal nutrition concentrations, but also the length of nutrient starvation (Widjaja *et al*., 2009). The trend of lower $NaNO_3$concentrations leading to higher lipid cell content could be explained as follows: the initial low nitrogen concentration in the medium would have been exhausted early on at low cell density, and individual cells were exposed to a large quantity of light energy when light penetration was good, which resulted in more metabolic flux been generated from photosynthesis, which was then channelled to lipid accumulation on a unit biomass basis (Li *et al*., 2008). When sufficient nutrients are available, proteins are synthesised. However, under nitrogen deficiency, the synthetic rate of essential cellular structures including proteins and nucleic acids become low which suppresses cell division, and a greater amount of carbon is available for lipid storage (McGinnis *et al*., 1997; Meng *et al*., 2009; Huang *et al*., 2010; Feng *et al*., 2011).

Measurements of lipid per unit cell area (shown in Figures 17 to 24 and Table 9), required a calibration curve that correlated fluorescence to lipid content (Mutanda *et al*., 2010). It should be noted that when referring to Figure 22, it appears that the neutral lipid concentration is much higher than 57.64% (Table 9). The image analysis software readings presented in Table 9 provided a more accurate determination of the lipid concentration. Micrographs of cellular

lipid globules correlate with results obtained above: $NaNO_3$ deprivation stimulated lipid storage in *C. vulgaris*.

Samples with limited $NaNO_3$ concentrations (7.5, 3.8, 1.8, 1.5, 0.9, 0.5, 0.2 and 0 g l^{-1}) were further tested to determine the impact of diverse concentrations on the lipid profile of the microalgal strain under study. Accurate FA measurement is imperative for biofuel production, as clean burn properties can be influenced by FA structures, such as chain length and degree of unsaturation (Amini *et al*., 2011). The aim of this aspect of the study was to determine which concentration of $NaNO_3$ would produce the optimum amount of lipids, as well as whether the type of lipids produced could be conducive for biodiesel production. A mixed standard was analysed (shown in Figure 25), which consisted of 11 known FAs.

Biodiesel quality is dependent on the composition of FAMEs. Properties of FAMEs are determined by carbon chain length, degree of unsaturation and the alcohol content of composed FAs (Amini *et al*., 2011). Cetane number, cold-flow properties, oxidative stability and iodine values are also important properties of biofuel which can be derived from its FAME structure. According to the results shown in Appendix C-J, only saturated FAs were detected in the *C. vulgaris* strain. Saturated FAs are known to give an excellent cetane number and oxidative stability to biodiesel (Chinnasamy *et al*., 2010; Amini *et al*., 2011). Biodiesel quality can be directly related to the cetane number as it shows ignition quality in engines. Palmitic and stearic acid are recognised as the most common FAs contained in biodiesel (Amini *et al*., 2011). Stearic acid was not present in any of the trial runs. Palmitic acid however, was present in most of the trial runs. Results obtained from this study suggest that a limitation of $NaNO_3$ enhances the production of certain lipids in the selected *C. vulgaris* strain, while suppressing the production of others. From the chromatograms it can be seen that some unknowns make up a high % peak area. These can also be classified as FAs, however, it is not certain as to what group they belong to, and whether their presence will be beneficial in biodiesel production. Future studies could focus on the identification of these unknown FAs and their role in biodiesel production.

Chapter Six: Conclusion and Recommendations

6.1 Conclusion

Based on the research conducted, the following can be concluded:

- The optimised conditions at a shake flask level for higher biomass yield of the selected strain were at 4% CO_2, 0.5 g l^{-1} $NaNO_3$ and 0.04 g l^{-1} PO_4, respectively.

- The optimal pyrolytic reaction range for *C. vulgaris* was found to be close to that required for flash pyrolysis. Flash pyrolysis has shown promising results for the commercial production of liquid fuel from biomass.

- The photosynthetic rate of the organism under study was recorded at 150-350 µmol photons $m^{-2}s^{-1}$. Sunlight provides a light intensity of ± 5027 µmol photons $m^{-2}s^{-1}$. A closed reactor with artificial lighting therefore, provided the ideal set up for cultivation of this organism.

- The design of the TPBR system proved to be durable during the long periods required for the optimisation studies, as it endured various chemical substances and high volumes of liquids moving at high velocities.

- Results suggest that the selected *C. vulgaris* strain has some features that make this strain ideal for biodiesel production. These characteristics are as follows:

    - This strain was easily cultivated in a TPBR with good biomass and lipid productivity. The highest biomass yield of 2.09 g l^{-1} was produced at a $NaNO_3$ concentration of 7.5g l^{-1}, and the largest lipid fraction occurred when $NaNO_3$ concentration in the medium was 0.5 g l^{-1}

- All of the FAs identified by GC analyses during the $NaNO_3$ limitation study are saturated. Saturated FAs give good cetane number and oxidative stability to biodiesel.

- Palmitic acid, which is one of the most common FAs contained in biodiesel, was produced by the *C. vulgaris* strain.

- With the exception of butyric acid, the hydrocarbon chain length of FAs identified was between C11 and C16.

6.2 Recommendations

- The selected *C. vulgaris* strain is a promising candidate for biodiesel production, owing to its high lipid content under optimised conditions and its resilient nature. Further research could focus on the genetic manipulation of this strain in an attempt to further increase lipid and biomass yields.

- Traditional extraction processes pose challenges in terms of time and resources. Therefore, future research could investigate pyrolytic routes for production of biofuels as it is a ‘zero waste’ process.

- Closed systems for microalgal cultivation require substantial amounts of capital for their sustained operation. Thus more efforts are required to improve PBR technologies to increase their cost effectiveness and efficiency.

- Photobioreactors can also be investigated for the propagation of microalgae that produce other high value added compounds.

References

Altschul, S. F., Gish, W., Miller, W., Myers, E. W., and Lipman, D. J. 1990. Basic local alignment search tool. *Journal of Molecular Biology.* **215**: 403–410.

Amigun, B., Sigamoney, R., and Blottnitz, H. V. 2006. Commercialisation of biofuel industry in Africa: A review. *Renewable and Sustainable Energy Reviews*. **12**: 690-711.

Amini, S. R., Najafabady, N. M., Mobasher, M. M., Alhashemi, S. H., and Ghasemi, Y. 2011. *Chlorella* sp.: A new strain with highly saturated fatty acids for biodiesel production in bubble-column photobioreactor. *Applied Energy*. doi:10.1016.

Anonymous. 2009. BP Statistical review of world energy. BP plc London.

Antolin, G., Tinaut, F. V., and Briceno, Y. 2002. Optimisation of biodiesel production by sunflower oil transesterification. *Bioresource Technology*. **83**: 111-114.

Bahng, M. K., Mukarakate, C., Robichaud, D. J., and Nimlos, M. R. 2010. Current technologies for analysis of biomass thermochemical processing: A review. *Analytica Chimica Acta*. **662**: 117–138.

Balat, M., and Balat, H. 2010. Progress in biodiesel processing. *Applied Energy*. **87**: 1815-1835.

Batidzirai, B., Faaij, A. P. C., and Smeets, E. 2006. Biomass and bioenergy supply from Mozambique. *Energy for Sustainable Development*. **10**: 54-81.

Biagini, E., Barontini, F., and Tognotti, L. 2006. Devolatilization of biomass fuels and biomass components studied by tg/ftir technique. *Industrial and Engineering Chemistry*. **45**: 4486–4493.

Blanchemain, A., and Grizeau, D. 1996. Eicosapentaenoic acid content of *Skeletonema costatum* as a function of growth and irradiance; relation with chlorophyll *a* content and

photosynthetic capacity. *Journal of Experimental Marine Biology and Ecology*. **196**: 177-188.

Bligh, E. G., and Dyer, W. J. 1959. A rapid method for total lipid extraction and purification. *Journal of Physiology and Biochemistry*. **37**: 911-913.

Borowitzka, M. A. 1997. Microalgae for aquaculture: opportunities and constraints. *Journal of Applied Phycology*. **9**: 393-401.

Borowitzka, M. A. 1999. Commercial production of microalgae: ponds, tanks, tubes and fermenters. *Journal of Biotechnology*. **70**: 313-321.

Brennan, L., and Owende, P. 2010. Biofuels from microalgae-A review of technologies for production, processing, and extractions of biofuels and co-products. *Renewable and Sustainable Energy Reviews*. **14:** 557-577.

Camacho, F. G., Gomez, A. C., Fernandez, F. G. A., Sevilla, J. F., and Grima, E. M. 1999. Use of concentric-tube airlift photobioreactors for microalgal outdoor mass cultures. *Enzyme Microbial Technologies*. **24**: 164–172.

Celekli, A., Yavuzatmaca, M., and Bozkurt, H. 2009. Modeling of biomass production by *Spirulina platensis* as function of phosphate concentrations and pH regimes. *Bioresource Technology*. **100**: 3625-3629.

Changdong, S., and Azevedo, J. L. T. 2005. Estimating the higher heating value of biomass fuels from basic analysis data. *Biomass Bioenergy*. **28**: 499-507.

Chen, C. Y., Yeh, K. L., Aisyah, R., Lee, D. J., and Chang, J. S. 2010. Cultivation, photobioreactor design and harvesting of microalgae for biodiesel production: A critical review. *Bioresource Technology*. **102**: 71-81.

Chinnasamy, S., Ramakrishnan, B., Bhatnagar, A., and Das, K. C. 2009. Biomass production potential of wastewater alga *Chlorella vulgaris ARC 1* under elevated levels of CO_2 and temperature. *International Journal of Molecular Sciences.* **10**: 518-532.

Chinnasamy, S., Bhatnagar, A., Hunt, R. W., and Das, K. C. 2010. Microalgae cultivation in a wastewater dominated by carpet mill effluents for biofuel applications. *Bioresource Technology.* **101**: 3097–105.

Chisti, Y. 2007. Biodiesel from microalgae. *Biotechnology Advances.* **25**: 294-306.

Chisti, Y. 2008. Biodiesel from microalgae beats bioethanol. *Trends in Biotechnology.* **26**: 126-131.

Cohen, E., and Arad, S. 1989. A closed system for outdoor cultivation of *Porphyridium. Biomass.* **18**: 59-67.

Coleman, A. W. 2003. ITS2 is a double-edged tool for eukaryote evolutionary comparisons. *Trends in Genetics.* **19**: 370-375.

Del Campo, J. A., Garcia-Gonzalez, M., and Guerrero, M. G. 2007. Outdoor cultivation of microalgae for carotenoid production: current state and perspectives. *Applied Microbiology and Biotechnology.* **74**: 1163–1174.

Demirbas, A. 2008. Biodiesel production via rapid transesterification. *Energy Source Part A.* **30**: 1830-1834.

Desmorieux, H., and Decaen, N. 2006. Convective drying of *spirulina* in thin layer. *Journal of Food Engineering.* **66**: 497-503.

Elsey, D., Jameson, D., Raleigh, B., and Cooney, J. M. 2007. Fluorescent measurement of microalgal neutral lipids. *Journal of Microbiological Methods.* **68**: 639-642.

Eriksen, N. 2008. The technology of microalgal culturing. *Biotechnology Letters*. **30**: 1525-1536.

Feliner, G. N., and Rossello, J. A. 2007. Better the devil you know? Guidelines for insightful utilization of nrDNA ITS in species-level evolutionary studies in plants. *Molecular Phylogenetics and Evolution.* **44**: 911-919.

Feng, Y., Li, C., and Zhang, D. 2011. Lipid production of *Chlorella vulgaris* cultured in artificial wastewater medium. *Bioresource Technology.* **102**: 101-105.

Gao, C., Xiong, W., Zhang, Y., Yuan, W., and Wu, Q. 2008. Rapid quantitation of lipid in microalgae by time-domain nuclear magnetic resonance. *Journal of Microbiological Methods.* **75**: 437-440.

Genty, B., Briantais, J. M., and Baker, N. R. 1989. The relationship between the quantum yield of photosynthetic electron transport and quenching of chlorophyll fluorescence. *Biochimica et Biophysica Acta.* **90**: 87–92.

Godhe, A., Anderson, D. M., and Rehnstam-Holm, A. S. 2001. PCR amplification of microalgal DNA for sequencing and species identification: studies on fixatives and algal growth stages. *Harmful Algae.* **1**: 375-382.

Goldberg, I., and Cohen Z., 2006. The effect of phosphate starvation on the lipid and fatty acid composition of the fresh water eustigmatophyte *Monodus subterraneus*. *Phytochemistry* **67**: 696-701.

Goleuke, C. G., Oswald, W. J., and Gee, H. K. 1967. Effect of nitrogen additives on algal yield. *Water Environment Federation*. **39**: 823-834.

Goyal, H. B., Seal, D., and Saxena, R. C. 2008. Bio-fuels from thermochemical conversion of renewable resources: a review. *Renewable and Sustainable Energy Reviews*. **12**: 504–517.

Greenspan, P., and Fowler, S. D. 1985. Spectrofluorometric studies of the lipid probe, Nile Red. *Journal of Lipid Research*. **26**: 781-788.

Greenwell, H. C., Laurens, M. L., Shields, R. J., Lovitt, R. W., and Flynn, K. J. 2009. Placing microalgae on the biofuels priority list: a review of the technological challenges. *Journal of Royal Society Interface*. **7**: 703-726.

Grierson, S., Stezov, V., Ellem, G., Mcgregor, R., and Herbetson, J. 2008. Thermal characterisation of microalgae under slow pyrolysis conditions. *Journal of Analytical and Applied Pyrolysis.* **8**: 118-123.

Grima, E. M., Belarbi, E. H., Ferna´ndez, F. G. A. N., Medina, A. R., and Chisti, Y. 2003. Recovery of microalgal biomass and metabolites: process options and economics. *Biotechnology Advances*. **20**: 491–515.

Grobbelaar, J. U. 2009. Factors governing algal growth in photobioreactors: the "open" versus "closed" debate. *Journal of Applied Phycology*. **21**: 489-492.

Guy, A. T. 1996. Lipids and membrane function in green algae. *Biochemical and Biophysical.* **1302**: 17-45.

Hu, Q., Sommerfeld, M., Jarvis, E., Ghirardi, M., Posewitz, M., Seibert, M., and Darzins, A. 2008. Microalgal triacylglycerols as feedstocks for biofuel production: perspectives and advances. *The Plant Journal.* **54**: 621-639.

Huang, G., Chen, G., and Chen, F. 2009. Rapid screening method for lipid production in alga based on Nile red fluorescence. *Biomass and Bioenergy*. **68**: 639-642.

Huang, G., Chen, F., Wei, D., Zhang, W., and Chen, C. 2010. Biodiesel production by microalgal biotechnology. *Applied Energy*. **87**: 38-46.

Illman, A. M., Scragg, A. H., and Shales, S. W. 2000. Increase in *Chlorella* strains calorific values when grown in low nitrogen medium. *Enzyme and Microbial Technology.* **27**: 631-635.

Kajiwara, S., Yamada, H., and Narumasa, O. 1997. Design of the bioreactor for carbon dioxide fixation by S*ynechococcus PCC7942*. *Energy Conversion Management.* **38**: 529–532.

Kemka, H., Ogbonda, Rebecca, E., Aminigo, and Gideon, O. A. 2007. Influence of aeration and lighting on biomass production and protein biosynthesis in a *Spirulina sp*. isolated from an oil-polluted brackish water marsh in the Niger Delta, Nigeria. *African Journal of Biotechnology* **6**: 2596-2600.

Khan, S. A., Rashmi, Hussain, M. Z., Prasad, S., and Banerjee, U. C. 2009. Prospects of biodiesel production from microalgae in India. *Renewable and Sustainable Energy Reviews*. **13**: 2361-2372.

Kobayashi, K., and Fujita, K. 1997. Tube diameter on tubular photobioreactor for microalgal culture and its biomass productivity. *Journal of Chemical Engineering of Japan*. **30**: 339–341.

Kodama, M., Ikemoto, H., and Miyachi, S. 1993. A new species of highly CO_2-tolerant fast growing marine microalga suitable for high density culture. *Journal of Marine Biotechnology.* **1**: 21-25.

Lee, S. J., Yoon, B. D., and Oh, H. M. 1998. Rapid method for the determination of lipid from the green alga *Botryococcus braunii. Biotechnology Techniques.* **12**: 553-556.

Lehr, F., and Posten, C. 2009. Closed photo-bioreactors as tools for biofuel production. *Current Opinion in Biotechnology*. **20**: 280–285.

Lenaers, G., Maroteaux, L., Michot, B., and Herzog, M. 1989. Dinoflagellates in evolution: a molecular phylogenetic analysis of large-subunit ribosomal RNA. *Journal of Molecular Evolution*. **29**: 40– 51.

Li, Y., Horsman, M., Wang, B., Wu, N., and Lan, C. Q. 2008. Effects of nitrogen sources on cell growth and lipid accumulation of green alga *Neochloris oleoabundans*. *Applied Microbiology and Biotechnol*ogy. **81**: 629-636.

Liu, Z. Y., Wang, G. C., and Zhou, B. U. 2008 a. Effect of iron on growth and lipid accumulation in *Chlorella vulgaris*. *Bioresource Technology*. **99**: 4717-4722.

Liu, Z. W., Zong, M., and Wu, H. 2008 b. Efficient lipid production with *Trichosporon fermentans* and its use for biodiesel preparation. *Bioresource Technology*. **99**: 7881-7885.

Lopes, E. J., Lacerda, L. M. C. F., and Franco, T. X. 2007. Biomass production and carbon dioxide fixation by Aphanothece microscopica *N¨ageli* in a bubble column photobioreactor. *Biochemical Engineering Journal*. **40**: 27-34.

Lv, J. M., Cheng, L. H., Xu, X. H., Zhang, L., and Chen, H. L. 2010. Enhanced lipid production of *Chlorella vulgaris* by adjustment of cultivation conditions. *Bioresource Technology*. **101**: 6797-6804.

Maiti, S., Purakayastha, S., and Ghosh, B. 2007. Thermal characterization of mustard straw and stalk in nitrogen at different heating rates. *Fuel*. **86**: 1513– 1518.

Marchetti, J. M., Miguel, V. U., and Errazu, A. F. 2007. Possible methods for biodiesel production. *Renewable and Sustainable Energy Reviews.* **11**: 1300-1131.

Martin-Jezequel, V., Hildebrand, M., and Brzezinski, M. A. 2000. Silicon metabolism in diatoms: implications for growth. *Journal of Phycology*. **36**: 821-840.

Mata, T. M., Martins, A. A., and Caetano, N. S. 2010. Microalgae for biodiesel production and other applications: A review. *Renewable and Sustainable Energy Reviews.* **14**: 217-232.

McGinnis, K. M., Dempster, T. A., and Sommerfeld, M. R. 1997. Characterization of the growth and lipid content of the diatom *Chaetoceros muelleri*. *Journal of Applied Phycology*. **9**: 19–24.

Meng, X., Yang, J., Xu, X., Zhang, L., Nie, Q., and Xian, M. 2009. Biodiesel production from oleaginous microorganisms. *Renewable Energy*. **34**: 1-5.

Miao, X., and Wu, Q. 2006. Biodiesel production from heterotrophic microalgal oil. *Bioresource Technology*. **97**: 841-846.

Milner, H. W. 1953. Algal culture from laboratory to pilot plant, pp. 102-110 **In:** Burlew, J.S. Rocking tray. (ed). Carnegie Institution. Washington, DC.

Molina, G. E., Belarbi, E. H., Fernandez, F. G., Medina, A. R., and Chisti, Y. 2001. Tubular photobioreactor design for algal cultures. *Journal of Biotechnology*. **92**: 113-131.

Morgan-Kiss, R. M., Ivanov, A. G., Modla, S., Czymmek, K., Huner, N. P. A., Priscu, J. C., Lisle, J. T., and Hanson, T. E. 2008. Identity and physiology of a new psychrophilic eukaryotic green alga, *Chlorella sp.*, strain BI, isolated from a transitory pond near Bratina Island, Antarctica. *Extremophiles*. **12**: 701–711.

Murugesan, A., Umarani, C., Chinnusamy, T. R., Krishan, M., Subramanian, R., and Neduzchezhain, N. 2008. Production and analysis of bio-diesel from non-edible oils - A review. *Renewable and Sustainable Energy Reviews*. **111**: 800-813.

Mutanda, T., Ramesh, D., Karthikeyan, S., Kumari, S., Anandraj, A., and Bux, F. 2010. Bioprospecting for hyper-lipid producing microalgal strains for sustainable biofuel production. *Bioresource Technology*. **102**: 4744-4753.

Namasivayam, A. M., Korakianitis, T., Crookes, R. J., Bob-Manuel, J. D. H., and Olsen, J. 2010. Biodiesel, emulsified biodiesel and dimethyl ether as pilot fuels for natural gas fuelled engines. *Applied Energy*. **87**: 769-778.

Ogbonda, K. H., Aminigo, R. E., and Abu, G. O. 2007. Influence of temperature and pH on biomass production and protein biosynthesis in a putative *Spirulina* sp. *Bioresource Technology*. **98**: 2207–2211.

Peng, W. M., and Wu, Q. Y. 2000. Effects of temperature and holding time on production of renewable fuels from pyrolysis of *Chlorella protothecoides*. *Journal of Applied Phycology*. **12**: 147-152.

Pirt, S. J., Lee, Y. K., Walach, M. R., Pirt, M. W., Balyuzi, H. H. M., and Bazin, M. J. 1983. A tubular bioreactor for photosynthetic production of biomass from carbon dioxide: design and performance. *Journal of Chemical Technology*. **33**: 35–58.

Pruvost, J., Van, G. V., Cogne, G., and Legrand, J. 2009. Investigation of biomass and lipids production with *Neochloris oleoabundans* in photobioreactor. *Bioresource Technology*. **100**: 5988-5995.

Pulz, O. 2001. Photobioreactors: production systems for phototrophic microorganisms. *Applied Microbiology and Biotechnology*. **57**: 287-293.

Pulz, O., and Gross, W. 2004. Valuable products from biotechnology of microalgae. *Applied Microbiology and Biotechnology*. **65**: 635-648.

Rachlin, J. W., and Grosso, A. 1991. The effects of pH on the growth of *Chlorella vulgaris* and its interactions with cadmium toxicity. *Archives of Environmental Contamination and Toxicology*. **20**: 505–508.

Ralph, P. J., and Gademann, R. 2003. Rapid light curves: A powerful tool to assess photosynthetic activity. *Aquatic Biology*. **82**: 222-237.

Richmond, A., and Wu, Z. C. 2000. Optimization of a flat plate glass reactor for mass production of *Nannochloropsis* sp. outdoors. *Journal of Biotechnology*. **85**: 259-269.

Rodolfi, L., Zittelli, G. C., Bassi, N., Padovani, G., Biondi, N., Bonin, G., and Tredici, M. R. 2009. Microalgae for oil: strain selection, induction of lipid synthesis and outdoor mass cultivation in a low-cost photobioreactor. *Biotechnology and Bioengineering*. **102**: 100–112.

Rosenberg, J. N., Oyler, G. A., Wilkinson, L., and Betenbaugh, M. J. 2008. A green light for engineered algae: redirecting metabolism to fuel a biotechnology revolution. *Current Opinion in Biotechnology*. **19**: 430–436.

Ross, A. B., Biller, P., Kubacki, M. L., Li, H., Lea-Langton, A. and Jones, J. M. 2010. Hydrothermal processing of microalgae using alkali and organic acids. *Fuel*. **89**: 234–2243.

Rubio, C. F., Acién Fernández, F. G., Sánchez Pérez, J. A., García Camacho, F., and Grima, M. E. 1999. Prediction of dissolved oxygen and carbon dioxide concentration profiles in tubular photobioreactors for microalgal culture. *Biotechnology Bioenergy*. **62**: 71–86.

Schenk, P., Thomas-Hall, S., Stephens, E., Marx, U., Mussgnug, J., and Posten, C. 2008. Second generation biofuels: high-efficiency microalgae for biodiesel production. *BioEnergy Research*. **1**: 20-43.

Scragg, A. H., Illman, A. M., Carden, A., and Shales, S. W. 2002. Growth of microalgae with increased calorific values in a tubular bioreactor. *Biomass Bioenergy*. **23**: 67-73.

Sepp, R., Szabo, I., Uda, H., and Sakamoto, H. 1994. Rapid techniques for DNA extraction from routinely processed archival tissue for use in PCR. *Journal of Clinical Pathology*. **47**: 318-323.

Shafizadeh, F. 1982. Introduction to pyrolysis of biomass. *Journal of Analytical and Applied Pyrolysis*. **3**: 283-305.

Sheehan, J., Dunahay, T., Benemann, J., and Roessler, P. 1998. "A Look Back at the U.S. Department of Energy's Aquatic Species Program- Biodiesel from Algae." National Renewable Energy Laboratory. NREL/TP-580-24190.

Shuping, Z., Yulong, W., Mingde, Y., Chun, Li., and Junmao, T. 2010. Pyrolysis characteristics and kinetics of the marine microalgae *Dunaliella tertiolecta* using thermogravimetric analyzer. *Bioresource Technology*. **101**: 359–365.

Smeets, E. M. W., Faaij, A. P. C., Lewandowski, I. M., and Turkenburg, W. C. 2007. A bottom-up assessment and review of global bio-energy potentials to 2050. *Progress in Energy and Combustion Science.* **33**: 56-106.

Sorensen, B. H., Nyholm, N., and Baun, A. 1996. Algal toxicity tests with volatile and hazardous compounds in air-tight test flasks with CO_2 enriched headspace. *Chemosphere.* **32**: 1513-1521.

Spolaore, P., Joannis-Cassan, C., Duran, E., and Isambert, A. 2006. Commercial applications of microalgae. *Journal of Bioscience and Bioengineering.* **101**: 87-96.

Suh, I. S., and Lee, C. G. 2003. Photobioreactor engineering: design and performance. *Biotechnology and Bioprocess Engineering*. **8**: 313-321.

Ugwu, C. U., Aoyagi, H., and Uchiyama, H. 2008. Photobioreactors for mass cultivation of algae. *Bioresource Technology.* **99**: 4021-4028.

Vamvuka, D., Kakaras, E., Kastanaki, E., and Grammelis, P. 2003. Pyrolysis characteristics and kinetics of biomass residuals mixtures with lignite. *Fuel*. **82**: 1949-1960.

Vasudevan, P. T., and Briggs, M. 2008. Biodiesel production-current state of the art and challenges. *Journal of Industrial Microbial Biotechnology*. **35**: 421-430.

Vicente, G., Martinez, M., and Aracil, J. 2004. Integrated biodiesel production: a comparison of different homogeneous catalysts systems. *Bioresource Technoogy.* **92**: 297-305.

Wang, B., Li, Y., Wu, N., and Lan, C. 2008. CO_2 bio-mitigation using microalgae. *Applied Microbiology and Biotechnology.* **79**: 707-718.

Watanabe, M. M., Kawachi, M., Hiroki, M., and Kasai, F. 2000. NIES-Collection list of strains, microalgae and protozoa. Microbial Culture Collections. (ed). National Institute for Environmental Studies, Tsukuba, Japan.

Weissman, J. C., Goebel, R. P. and Benemann, J. R. 1988. Photobioreactor design: mixing, carbon utilization, and oxygen accumulation. *Biotechnology Bioenergy.* **31**: 336–344.

Widjaja, A., Chien, C. C., and Ju, Y. H. 2009. Study of increasing lipid production from fresh water microalgae *Chlorella vulgaris. Journal of the Taiwan Institute of Chemical Engineers*. **40**: 13-20.

Wu, X., and Merchuk, J. C. 2004. Simulation of algae growth in a bench scale internal loop airlift reactor. *Chemical Engineering Science.* **59**: 2899 - 2912.

Zhang, K., Kurano, N., and Miyachi, S. 2002. Optimized aeration by carbon dioxide gas for microalgal production and mass transfer characterization in a vertical flat-plate photobioreactor. *Biotechnology and Bioengineering*. **25**: 97–101.

Appendix A- Recipe for BG 11 Media (Watanabe *et al*., 2000)

Compound	g l^{-1}
1) NaNO3	1.5
2) $K_2HPO_4.3H_2O$	0.04
3) $MgSO_4$.7H2O	0.075
4) $CaCl_2.2H_2O$	0.036
5) Citric acid	0.006
6) $FeCl_3$. $6H_2O$	0.006
7) EDTA	0.001
8) Na_2CO_3	0.2
9) Trace metal mix	1 ml

9) Trace metal mix

Compound	g l^{-1}
H_3BO_3	2.86
$MnCl_2.4H_2O$	1.81
FeCl3.6H2O	97.0
$Na_2MoO_4.2H_2O$	0.390
$CuSO_4$. $5H_2O$	0.079
$CO(NO_3)_2.6H_2O$	0.049

Add the indicated quantity of compounds and bring the final volume to 1 L using distilled water. Autoclave for 15 min at 121 °C at 1 atm. pH should be 7.5 at room temperature after autoclaving.

Appendix B- Gas Chromatogram of Mixed Standard

System : GC3
Method : ZB-FFAP01(TP3a)
User : Administrator

Acquired : 2010/07/23 09:44:26 AM
Processed : 2010/07/23 09:59:31 AM
Printed : 2010/09/15 11:58:03 AM

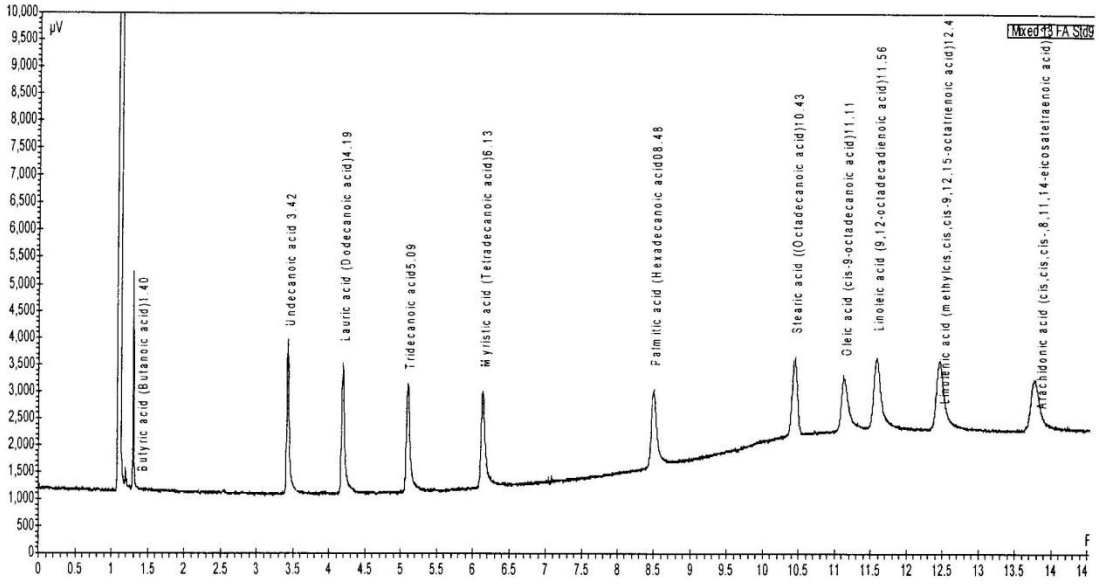

Peak results :

Index	Name	Time [Min]	Area [µV.Min]	Area % [%]	Quantity [Mass %]
1	unknown	0.06	0.7	0.056	0.00
2	unknown	1.19	5.0	0.415	0.00
3	Butyric acid (Butanoic acid)	1.40	0.5	0.045	0.00
4	unknown	1.47	0.8	0.065	0.00
5	Undecanoic acid	3.42	118.4	9.808	0.00
6	Lauric acid (Dodecanoic acid)	4.19	119.1	9.858	0.00
7	unknown	5.01	1.3	0.109	0.00
8	Tridecanoic acid	5.09	122.6	10.153	0.00
9	unknown	5.24	1.0	0.084	0.00
10	Myristic acid (Tetradecanoic acid)	6.13	117.2	9.706	0.00
11	unknown	7.08	0.8	0.070	0.00
12	Palmitic acid (Hexadecanoic acid0	8.48	112.4	9.304	0.00
13	Stearic acid ((Octadecanoic acid)	10.43	119.8	9.924	0.00
14	Oleic acid (cis-9-octadecanoic acid)	11.11	97.0	8.032	0.00
15	Linoleic acid (9,12-octadecadienoic acid)	11.56	137.7	11.403	0.00
16	Linolenic acid (methylcis,cis,cis-9,12,15-octatrienoic acid)	12.44	137.2	11.363	0.00
17	Arachidonic acid (cis,cis,cis-,8,11,14-eicosatetraenoic acid)	13.75	116.0	9.606	0.00
Total			1207.6	100.000	0.00

Appendix C- Gas Chromatogram of Run 6

System : GC3
Method : ZB-FFAP01(TP3a)rev
User : Administrator(Shanr)

Acquired : 2010/07/23 12:14:23 PM
Processed : 2010/09/15 12:12:00 PM
Printed : 2010/09/15 12:36:40 PM

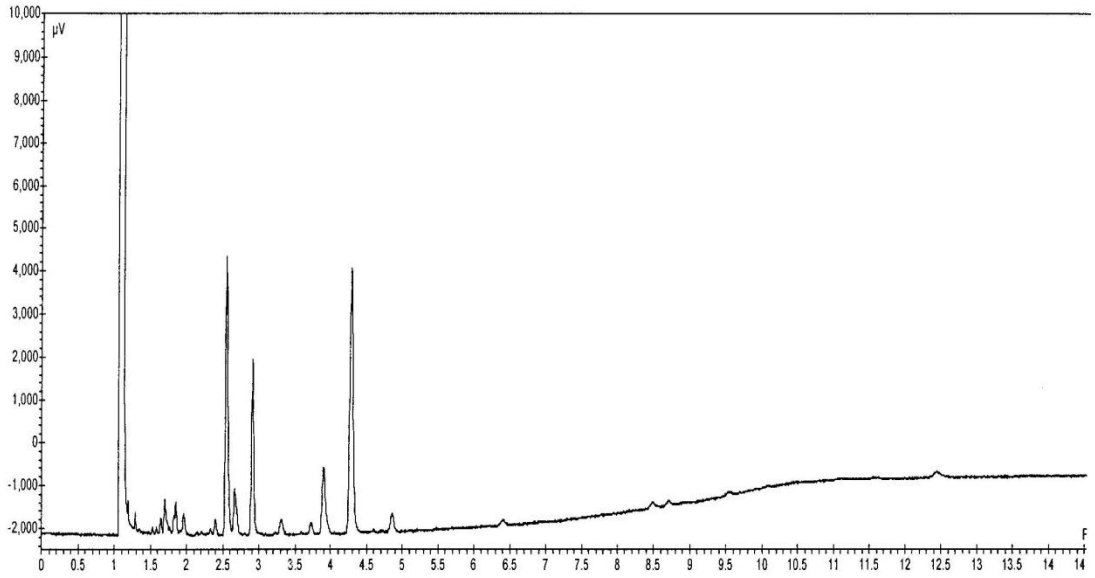

Peak results :

Index	Name	Time [Min]	Area [µV.Min]	Area % [%]	Quantity [Mass %]
1	unknown	1.19	4.7	2.179	0.00
2	unknown	1.64	8.9	4.177	0.00
3	unknown	1.70	26.3	12.301	0.00
4	unknown	1.85	25.9	12.081	0.00
5	unknown	1.96	15.6	7.310	0.00
6	unknown	2.40	12.0	5.625	0.00
7	unknown	2.66	45.3	21.185	0.00
8	unknown	3.90	75.2	35.142	0.00
Total			214.0	100.000	0.00

Page 1/1

Appendix D- Gas Chromatogram of Run 7

System : GC3
Method : ZB-FFAP01(TP3a)
User : Administrator

Acquired : 2010/07/23 12:32:35 PM
Processed : 2010/07/23 12:47:39 PM
Printed : 2010/10/19 11:19:23 AM

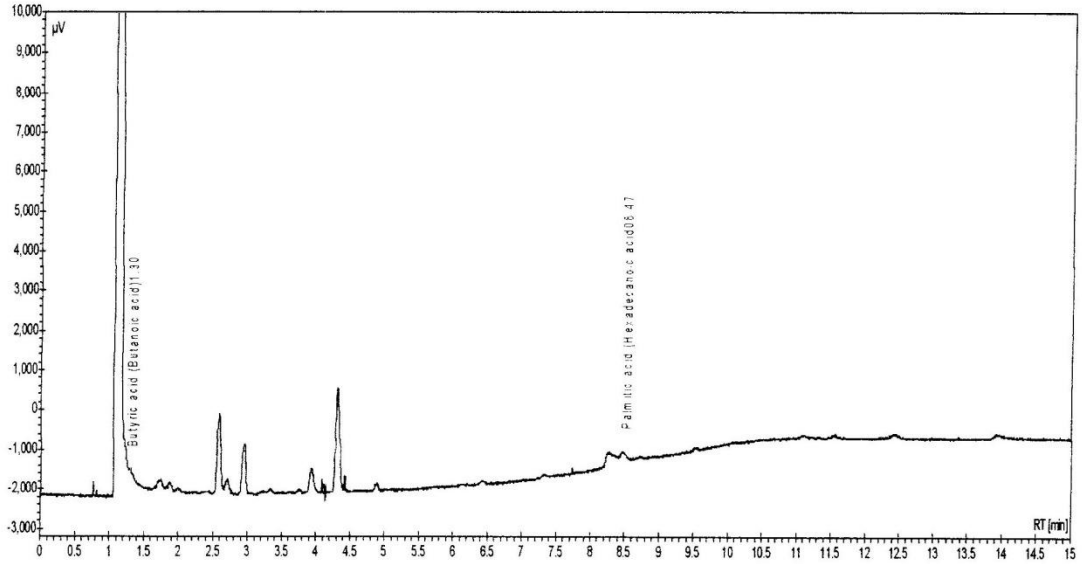

Peak results :

Index	Name	Time [Min]	Area [µV.Min]	Area % [%]	Quantity [Mass %]
1	unknown	0.06	0.3	0.057	0.00
2	unknown	0.12	0.8	0.139	0.00
3	unknown	0.82	1.3	0.223	0.00
4	Butyric acid (Butanoic acid)	1.30	4.7	0.816	0.00
5	unknown	1.73	22.6	3.970	0.00
6	unknown	1.87	13.7	2.397	0.00
7	unknown	1.98	5.0	0.879	0.00
8	unknown	2.59	128.6	22.562	0.00
9	unknown	2.70	28.5	4.992	0.00
10	unknown	2.95	80.6	14.144	0.00
11	unknown	3.76	7.5	1.323	0.00
12	unknown	3.93	52.1	9.129	0.00
13	unknown	4.08	7.3	1.281	0.00
14	unknown	4.31	170.0	29.819	0.00
15	unknown	4.41	8.9	1.568	0.00
16	unknown	4.47	0.8	0.141	0.00
17	unknown	4.88	11.6	2.037	0.00
18	unknown	8.23	14.6	2.564	0.00
19	Palmitic acid (Hexadecanoic acid0	8.47	11.2	1.956	0.00
Total			570.2	100.000	0.00

Page 1/1

Appendix E- Gas Chromatogram of Run 8

System : GC3
Method : ZB-FFAP01(TP3a)
User : Administrator

Acquired : 2010/07/23 10:21:51 AM
Processed : 2010/07/23 10:36:55 AM
Printed : 2010/10/19 11:25:20 AM

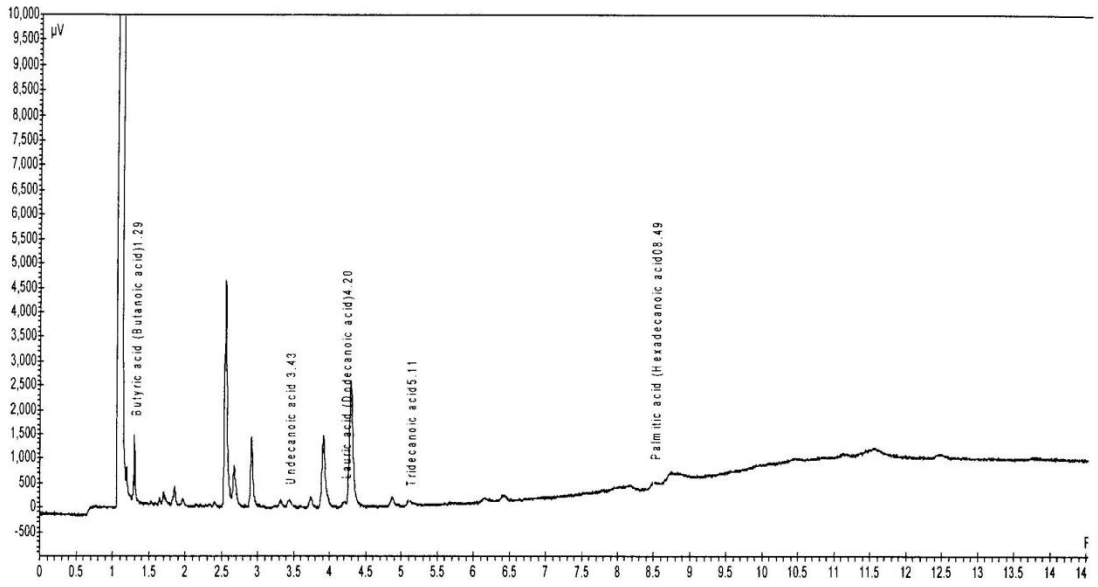

Peak results :

Index	Name	Time [Min]	Area [µV.Min]	Area % [%]	Quantity [Mass %]
1	unknown	0.71	7.8	1.610	0.00
2	unknown	0.95	0.3	0.070	0.00
3	unknown	1.19	5.4	1.107	0.00
4	unknown	1.23	0.7	0.141	0.00
5	Butyric acid (Butanoic acid)	1.29	26.6	5.480	0.00
6	unknown	1.34	1.1	0.221	0.00
7	unknown	1.39	0.4	0.089	0.00
8	unknown	1.41	0.1	0.028	0.00
9	unknown	1.53	1.5	0.308	0.00
10	unknown	1.58	1.0	0.205	0.00
11	unknown	1.64	3.7	0.752	0.00
12	unknown	1.70	11.6	2.395	0.00
13	unknown	1.76	1.4	0.287	0.00
14	unknown	1.85	14.5	2.974	0.00
15	unknown	1.91	0.8	0.172	0.00
16	unknown	1.96	6.1	1.249	0.00
17	unknown	2.14	1.6	0.338	0.00
18	unknown	2.40	3.7	0.756	0.00
19	unknown	2.45	0.4	0.086	0.00
20	unknown	2.67	32.2	6.616	0.00
21	unknown	2.91	59.7	12.287	0.00
22	unknown	3.00	1.1	0.224	0.00
23	unknown	3.32	5.4	1.101	0.00
24	Undecanoic acid	3.43	8.6	1.773	0.00
25	unknown	3.74	11.5	2.373	0.00
26	unknown	3.91	83.7	17.213	0.00
27	unknown	4.04	0.7	0.145	0.00
28	Lauric acid (Dodecanoic acid)	4.20	6.1	1.251	0.00
29	unknown	4.29	152.0	31.271	0.00

Chromatogram :

System : GC3
Method : ZB-FFAP01(TP3a)
User : Administrator

Acquired : 2010/07/23 10:21:51 AM
Processed : 2010/07/23 10:36:55 AM
Printed : 2010/10/19 11:25:20 AM

Index	Name	Time [Min]	Area [µV.Min]	Area % [%]	Quantity [Mass %]
30	unknown	4.87	8.8	1.802	0.00
31	Tridecanoic acid	5.11	2.7	0.550	0.00
32	unknown	6.41	8.0	1.651	0.00
33	Palmitic acid (Hexadecanoic acid0	8.49	7.0	1.434	0.00
34	unknown	8.72	9.9	2.040	0.00
Total			486.1	100.000	0.00

APPENDIX F- Gas Chromatogram of Run 9

System : GC3
Method : ZB-FFAP01(TP3a)
User : Administrator

Acquired : 2010/07/23 12:32:35 PM
Processed : 2010/07/23 12:47:39 PM
Printed : 2010/10/19 11:19:23 AM

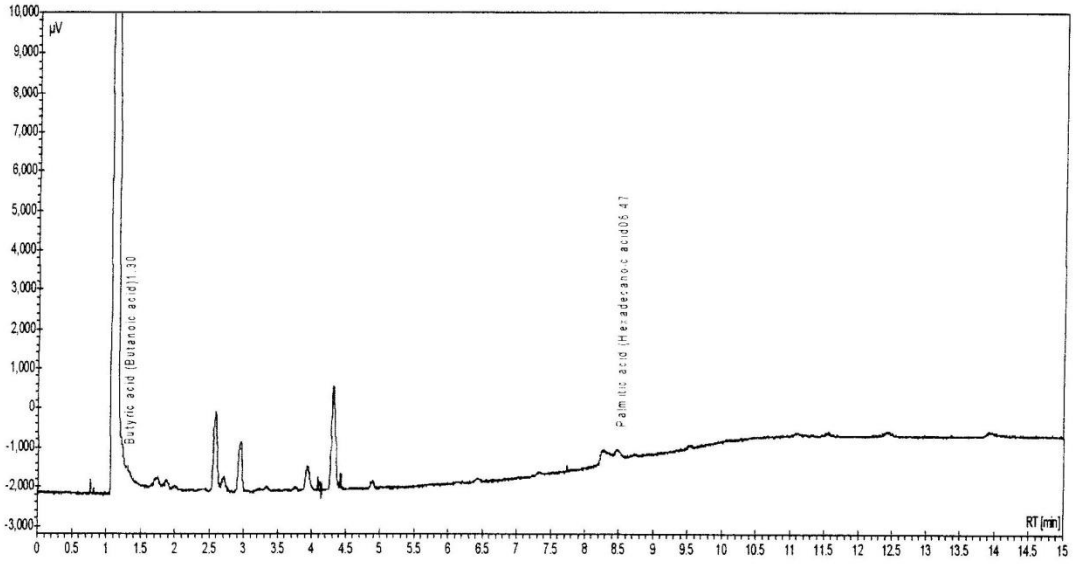

Peak results :

Index	Name	Time [Min]	Area [µV.Min]	Area % [%]	Quantity [Mass %]
1	unknown	0.06	0.3	0.057	0.00
2	unknown	0.12	0.8	0.139	0.00
3	unknown	0.82	1.3	0.223	0.00
4	Butyric acid (Butanoic acid)	1.30	4.7	0.816	0.00
5	unknown	1.73	22.6	3.970	0.00
6	unknown	1.87	13.7	2.397	0.00
7	unknown	1.98	5.0	0.879	0.00
8	unknown	2.59	128.6	22.562	0.00
9	unknown	2.70	28.5	4.992	0.00
10	unknown	2.95	80.6	14.144	0.00
11	unknown	3.76	7.5	1.323	0.00
12	unknown	3.93	52.1	9.129	0.00
13	unknown	4.08	7.3	1.281	0.00
14	unknown	4.31	170.0	29.819	0.00
15	unknown	4.41	8.9	1.568	0.00
16	unknown	4.47	0.8	0.141	0.00
17	unknown	4.88	11.6	2.037	0.00
18	unknown	8.23	14.6	2.564	0.00
19	Palmitic acid (Hexadecanoic acid0	8.47	11.2	1.956	0.00
Total			570.2	100.000	0.00

Page 1/1

Appendix G- Gas Chromatogram of Run 10

System : GC3
Method : ZB-FFAP01(TP3a)
User : Administrator

Acquired : 2010/07/23 11:19:06 AM
Processed : 2010/07/23 11:34:10 AM
Printed : 2010/10/19 11:24:07 AM

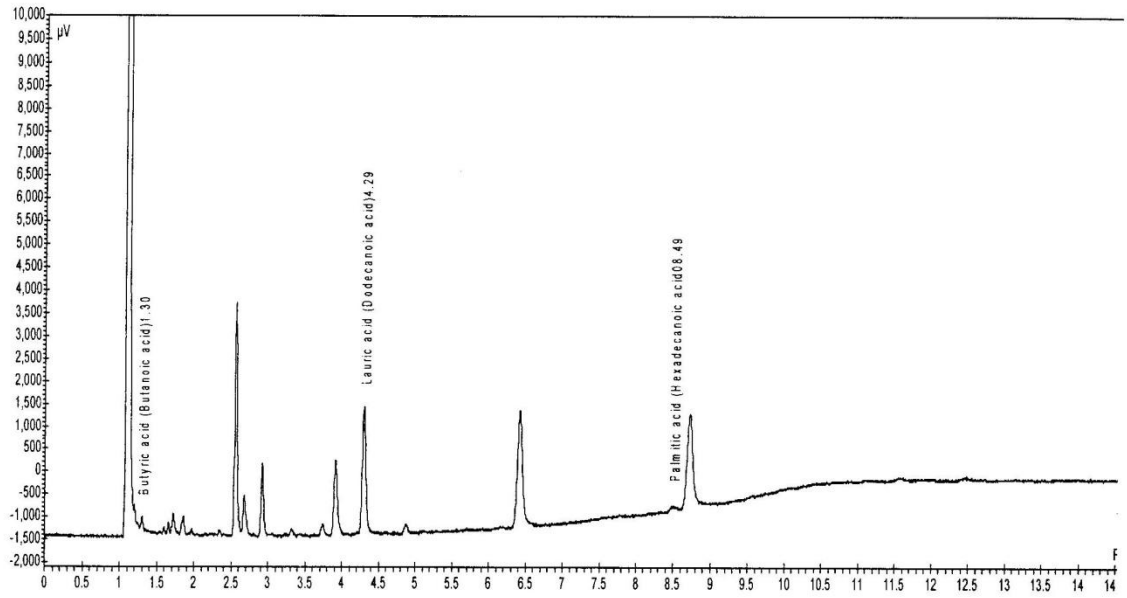

Peak results :

Index	Name	Time [Min]	Area [µV.Min]	Area % [%]	Quantity [Mass %]
1	unknown	0.02	1.5	0.174	0.00
2	unknown	1.20	3.3	0.395	0.00
3	Butyric acid (Butanoic acid)	1.30	7.2	0.849	0.00
4	unknown	1.35	0.6	0.069	0.00
5	unknown	1.54	1.9	0.220	0.00
6	unknown	1.59	3.3	0.392	0.00
7	unknown	1.66	6.6	0.777	0.00
8	unknown	1.72	20.4	2.408	0.00
9	unknown	1.86	17.9	2.114	0.00
10	unknown	1.97	5.7	0.669	0.00
11	unknown	2.03	0.7	0.085	0.00
12	unknown	2.28	2.2	0.258	0.00
13	unknown	2.35	4.5	0.528	0.00
14	unknown	2.39	1.0	0.114	0.00
15	unknown	2.67	37.9	4.479	0.00
16	unknown	2.92	61.1	7.235	0.00
17	unknown	3.24	2.5	0.297	0.00
18	unknown	3.32	7.4	0.874	0.00
19	unknown	3.74	13.1	1.547	0.00
20	unknown	3.91	91.1	10.780	0.00
21	Lauric acid (Dodecanoic acid)	4.29	154.8	18.320	0.00
22	unknown	4.87	10.3	1.213	0.00
23	unknown	6.42	199.9	23.649	0.00
24	Palmitic acid (Hexadecanoic acid	8.49	8.5	1.002	0.00
25	unknown	8.72	182.1	21.551	0.00
Total			845.1	100.000	0.00

Page 1/1

Appendix H- Gas Chromatogram of Run 11

System : GC3
Method : ZB-FFAP01(TP3a)
User : Administrator

Acquired : 2010/07/23 10:40:12 AM
Processed : 2010/07/23 10:55:16 AM
Printed : 2010/09/15 12:26:42 PM

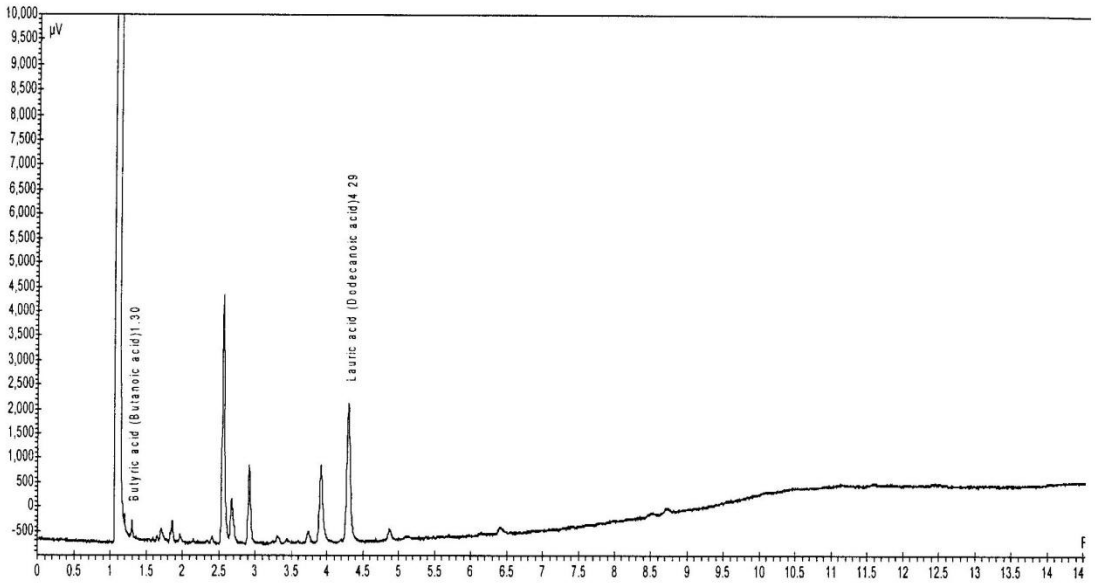

Peak results :

Index	Name	Time [Min]	Area [µV.Min]	Area % [%]	Quantity [Mass %]
1	unknown	0.03	0.8	0.172	0.00
2	unknown	0.06	0.5	0.111	0.00
3	unknown	1.20	3.4	0.756	0.00
4	Butyric acid (Butanoic acid)	1.30	7.6	1.696	0.00
5	unknown	1.53	1.5	0.334	0.00
6	unknown	1.59	1.6	0.359	0.00
7	unknown	1.65	2.8	0.626	0.00
8	unknown	1.71	10.0	2.235	0.00
9	unknown	1.86	14.9	3.340	0.00
10	unknown	1.93	0.9	0.209	0.00
11	unknown	1.97	6.1	1.376	0.00
12	unknown	2.15	1.6	0.369	0.00
13	unknown	2.41	3.9	0.874	0.00
14	unknown	2.67	38.8	8.696	0.00
15	unknown	2.92	62.5	14.000	0.00
16	unknown	3.32	5.9	1.326	0.00
17	unknown	3.74	12.2	2.724	0.00
18	unknown	3.91	91.4	20.471	0.00
19	unknown	4.04	0.6	0.126	0.00
20	Lauric acid (Dodecanoic acid)	4.29	160.3	35.890	0.00
21	unknown	4.87	10.6	2.372	0.00
22	unknown	6.41	8.6	1.936	0.00
Total			446.6	100.000	0.00

Page 1/1

Appendix I- Gas Chromatogram of Run 12

System : GC3
Method : ZB-FFAP01(TP3a)
User : Administrator

Acquired : 2010/07/23 12:32:35 PM
Processed : 2010/07/23 12:47:39 PM
Printed : 2010/10/19 11:19:23 AM

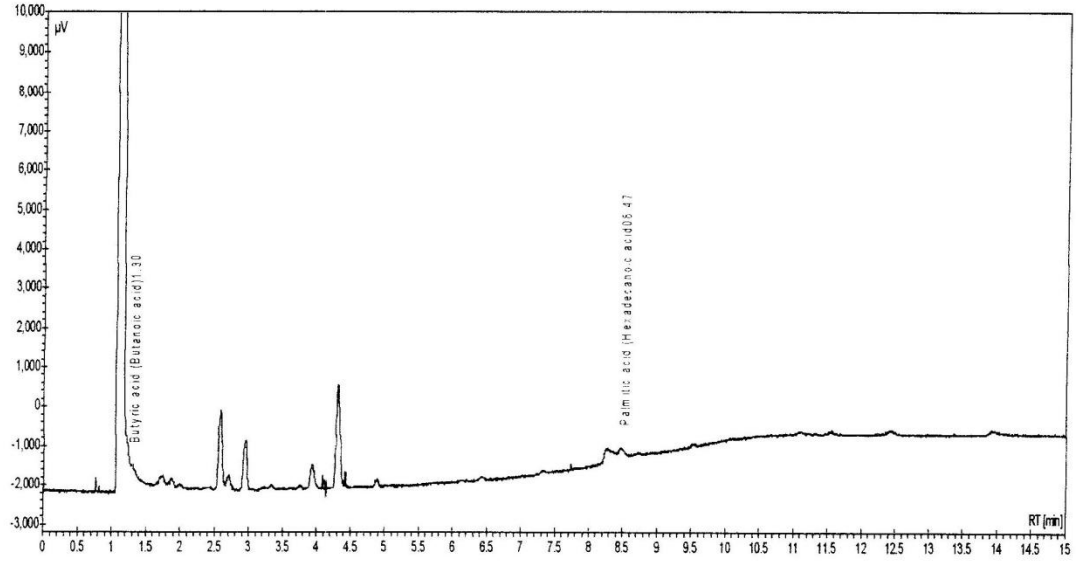

Peak results :

Index	Name	Time [Min]	Area [µV.Min]	Area % [%]	Quantity [Mass %]
1	unknown	0.06	0.3	0.057	0.00
2	unknown	0.12	0.8	0.139	0.00
3	unknown	0.82	1.3	0.223	0.00
4	Butyric acid (Butanoic acid)	1.30	4.7	0.816	0.00
5	unknown	1.73	22.6	3.970	0.00
6	unknown	1.87	13.7	2.397	0.00
7	unknown	1.98	5.0	0.879	0.00
8	unknown	2.59	128.6	22.562	0.00
9	unknown	2.70	28.5	4.992	0.00
10	unknown	2.95	80.6	14.144	0.00
11	unknown	3.76	7.5	1.323	0.00
12	unknown	3.93	52.1	9.129	0.00
13	unknown	4.08	7.3	1.281	0.00
14	unknown	4.31	170.0	29.819	0.00
15	unknown	4.41	8.9	1.568	0.00
16	unknown	4.47	0.8	0.141	0.00
17	unknown	4.88	11.6	2.037	0.00
18	unknown	8.23	14.6	2.564	0.00
19	Palmitic acid (Hexadecanoic acid0	8.47	11.2	1.956	0.00
Total			570.2	100.000	0.00

Page 1/1

Appendix J- Gas Chromatogram of Run 13

System : GC3
Method : ZB-FFAP01(TP3a)
User : Administrator

Acquired : 2010/07/22 12:19:33 PM
Processed : 2010/07/22 12:32:44 PM
Printed : 2010/10/19 11:25:58 AM

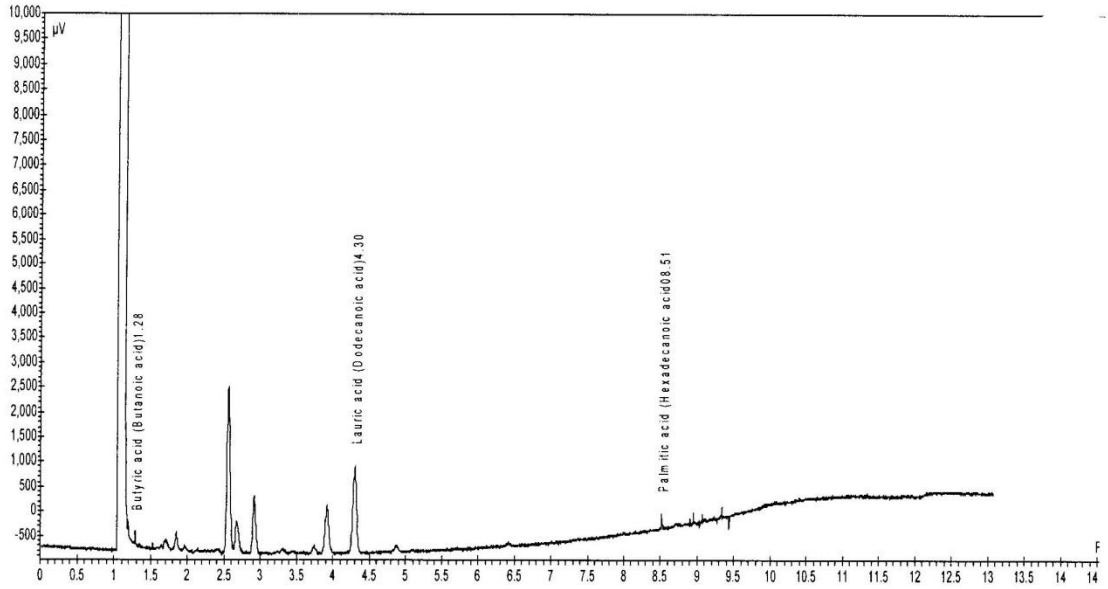

Peak results :

Index	Name	Time [Min]	Area [µV.Min]	Area % [%]	Quantity [Mass %]
1	unknown	1.19	3.4	0.684	0.00
2	Butyric acid (Butanoic acid)	1.28	3.7	0.732	0.00
3	unknown	1.35	0.9	0.182	0.00
4	unknown	1.53	2.4	0.478	0.00
5	unknown	1.59	1.8	0.361	0.00
6	unknown	1.64	4.2	0.827	0.00
7	unknown	1.70	13.9	2.757	0.00
8	unknown	1.85	16.8	3.324	0.00
9	unknown	1.96	5.2	1.025	0.00
10	unknown	2.55	162.6	32.226	0.00
11	unknown	2.67	38.8	7.690	0.00
12	unknown	2.91	56.2	11.134	0.00
13	unknown	3.30	3.9	0.765	0.00
14	unknown	3.74	9.3	1.851	0.00
15	unknown	3.92	59.3	11.748	0.00
16	Lauric acid (Dodecanoic acid)	4.30	100.9	19.988	0.00
17	unknown	4.87	6.6	1.317	0.00
18	Palmitic acid (Hexadecanoic acid0	8.51	6.5	1.279	0.00
19	unknown	8.58	1.1	0.211	0.00
20	unknown	8.94	2.0	0.394	0.00
21	unknown	9.07	2.1	0.422	0.00
22	unknown	9.33	2.1	0.408	0.00
23	unknown	13.04	1.0	0.197	0.00
Total			504.6	100.000	0.00

Page 1/1